Structural Characterisation and Seismic Evaluation of Steel

Antonio Di Carluccio

Università degli Studi di Napoli "Federico II"

Polo delle Scienze e delle Tecnologie

Structural Characterisation and Seismic Evaluation of Steel Equipments in Industrial Plants

Antonio Di Carluccio

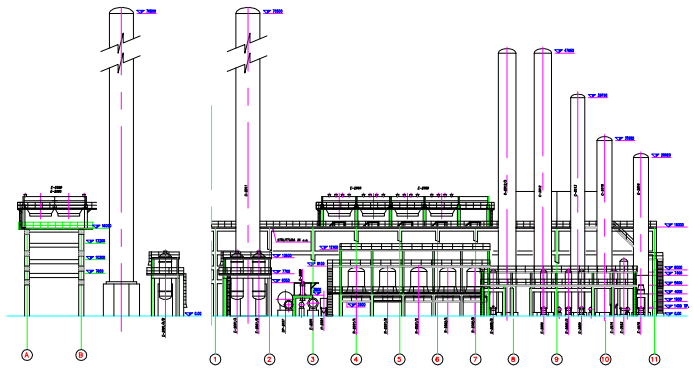

Dottorato di Ricerca in Rischio Sismico

UNIVERSITY OF NAPLES "FEDERICO II"

Structural Characterisation and Seismic Evaluation of Steel Equipments in Industrial Plants

DISSERTATION
Submitted for the degree of
DOCTOR OF PHILOSOPHY
In SEISMIC RISK

By

Eng. Antonio Di Carluccio

Tutor: Prof. Eng. Giovanni Fabbrocino

Coordinator: Prof. P. Gasparini

2007

"....ricett' o pappc vicin a noc
ramm tiemp che t' sprtos...."

Doctor of Philosophy Antonio Di Carluccio

DEDICATION

This dissertation is dedicated to my future wife,
Gabriella,
and my to parents, Mario and Rosa.
Their constant love and caring are every reason for where I am and what I am. My gratitude and my love for them are beyond words.

Contents

List of Figures

List of Tables

Pubblications

Fabbrocino, G., Iervolino, I, Di Carluccio, A., Dynamic Analysis of Steel Tanks Subjected To Three-Dimensional Ground Motion, Proceedings of The Tenth International Conference on Civil, Structural and Environmental Engineering Computing, CC2005 & AI2005, Rome, 2005.

Fabbrocino, G., Iervolino, I, Di Carluccio, A., Simplified Models of Unanchored Steel Tanks for Seismic Fragilità Analysis, XX Congresso CTA, First International Workshop On Advances In Steel Construction, Ischia, 2005.

Di Carluccio, A., Iervolino, I, Manfredi, G., Fabbrocino, G., Salzano, E., Quantitative Probabilistic Seismic Risk Analysis of Storage Facilities, CISAP-2, Second International Conference on Safety & Environmental in Process Industry, Napoli, 2006.

Fabbrocino, G., Di Carluccio, A., Iervolino, I., Dynamic Analysis of Liquid Storage Steel Tanks for seismic reliability assessments, ISEC-4, The fourth Internaltional Structural Engineering & Construction Conference, Melbourne, 2007.

Salzano, E., Fabbrocino, G., Di Carluccio, A., Manfredi, G., The Interaction of Earthquakes with Process Equipment in the Framework of Risk Assessment, 41st Annual Loss Prevention Symposium, Houston (TX), 2007.

Salzano, E., Di Carluccio, A., Agreda, A.G., Fabbrocino, G., Risk Assessment and Early Warning Systems for Industrial Facilities in Seismic Zones, 12th International Symposium Loss Prevention and Safety Promotion in the Process Industries., 2007.

Fabbrocino, G., Di Carluccio, A., Salzano, E., Manfredi, G., Iervolino, I., Structural Characterization of Equipment and Systems of Critical Industrial Plants, LessLoss Final Workshop, Risk Mitigation for Earthquakes and Landslides Integrated Project.

Fabbrocino, G., Di Carluccio, A., Salzano, E., Manfredi, G., Design and Assessment of Storage Steel Tanks in Hazardous Industrial Plants, LessLoss Final Workshop, Risk Mitigation for Earthquakes and Landslides Integrated Project.

Fabbrocino, G., Di Carluccio, A., Salzano, E., Manfredi, G., Risk Assessment for Industrial Facilities in Seismic Zones LessLoss Final Workshop, Risk Mitigation for Earthquakes and Landslides Integrated Project.

Fabbrocino, G., Di Carluccio, A., Manfredi, G., Iervolino, I, Salzano, E., Structural Characterization of Industrial Facilities in the Framework of Seismic Risk Analysis, XXI Congresso CTA, Catania, 2007.

Fabbrocino, G., Di Carluccio, A., Manfredi, G., I, Salzano, E., Seismic Behaviour or Industrial Steel Components in Industrial Plants, XXI Congresso CTA, Catania, 2007.

Salzano, E., Agreda, A.G., Di Carluccio, A., Fabbrocino, G., Risk Assessment and Early Warning Systems for Industrial Facilities in Seismic Zones, Resliability Engineering & System Safety, (Submitted).

Di Carluccio, A., Fabbrocino., G., Iervolino, I., Seismic Demand Analysis of Steel Storage Tanks Under Generalised Ground Motion, Engineering Structures, (Submitted).

Acknowledgements

I would like to express my deep gratitude to Professor Giovanni Fabbrocino, my tutor, for his guidance, encouragement and gracious support throughout the course of my graduate study, for his expertise in the field of earthquake engineering, which motivated me to work on this subject, and for his faith in me during the most difficult stages of the research; I am very thankful. Particular thanks go to Mrs. Maria, Raffele and Anna Paola, for their patience; I apologize for having taken their precious time to spend with their loved Giovanni.

Also, I am very grateful to Dott. Ernesto Salzano, a friend and scientist, for his contribution to my scientific growth.

I thank the friends of UNART Group and the friends of scientific group StreGa whose activities have helped to stimulate my desire for knowledge.

I thank friends of 4th floor, Raf, Concy and Ale and Cristiano for having shared with me both good and bad moments of these last years of my life.

Special acknowledgement is also due to my girlfriend Gabriella for her love, support, and untiring encouragement. No words can express my appreciation and gratitude to her.

The last, but not for importance, a special thank to my sister Carmela and her husband Francesco: give me a nephew soon, please!!

Abstract

The present study investigates the risk analysis of industrial plant. The work done during the doctorate activity is inserted within a research activity very broad and interdisciplinary which seeks to quantify the industrial seismic risk.

The main objective is the definition of a clear classification of industrial constructions from the structural engineering perspective. The study represents a useful support for QRA analysts in seismic areas, because it ensures a simulated design of constructions and processes even when data are not available.

After an introduction on the methodology for a quantitative seismic risk analysis a large study of typical industrial equipment has been conducted both in terms of industrial process, to know the service condition, and in terms of geometric and structural characteristic.

Among the various structural equipment presents in a industrial plant has decided to focus attention on the atmospheric storage steel tanks. This choice was determined by

different factors. First of all, they are components that are intrinsic hazard due to the fact that very often contain hazardous materials. Moreover, a large database of post earthquake damage exists and finally are present in many industrial plants. For this reasons a seismic fragility analysis of this structure has been made in terms of limit states relevant for industrial risk analysis (Elephant Foot Buckling and base-sliding). An MatLab algorithms to integrate equations of motions have been formulated.

Advanced FEM analysis have been carried out and a comparison between simplified procedures proposed by Eurocode 8 and used to develop seismic fragility of tanks has been discussed.

CHAPTER 1:

INTRODUCTION

Natural catastrophic events may affect the integrity of industrial structures (equipment, auxiliary system, instrumentation, structural support, utilities). As a consequence, loss of energy or mass or, more generally, both mass and energy from the containment system is likely to occur. If industrial facilities store large amount of hazardous materials, accidental scenarios as fire, explosion, or toxic dispersion may be triggered, thus possibly involving working people within the installation and/or population living in the close surrounding or in the urban area where the industrial installation is located.

Despite these considerations a recent literature analysis has showed that none of the European countries have specific risk and emergency management programs in place which contemplate explicitly the occurrence of natural disaster interacting with industrial installations. Eventually, the development of tool for the analysis of mutual interaction of earthquake and industrial installation is necessary for the risk management practice [1-2], for budget-oriented decision-making analysis, emergency or prevention plan, on either industrial side or public-governmental-civil protection side, for

structural safety priorities, and more generally for the Quantitative Risk Assessment (QRA) of industrial areas or single facilities (also known as Probabilistic Risk Assessment (PRA) or Probabilistic Safety Assessment (PSA)).

All risk applications and procedures cited deal with the occurrence of individual failure events and their possible consequences on the analysed system. Moreover, any is based on integrated procedures to quantify human, environmental and economical losses related to relevant accidents. However, as for any risk assessment, a deterministic or a probabilistic approach, or a mix of them can be used (as in the case of the choice of cut-off value for consequence-based analysis).

When the seismic risk is of concern, deterministic approach can use the "Maximum Credible Accident" analysis or "Worst Case Analysis", both starting form worst case earthquake scenarios, for the evaluation of risks and consequences.

These approaches are largely used in European regulations [3] for emergency planning outside industrial installation (as in the Seveso II application in France and Italy) but often lead to great overestimation of the total risk, often providing a risk grade which is both economically and politically not applicable, e.g. in the case of civil protection action. Moreover, the uncertainties on the initial conditions for either the seismic scenario or the evolution of the industrial accident scenario related to the earthquake itself are often too large. This circumstance leads analysts to use a probabilistic approach (i.e.

QRA), where uncertainties are explicitly taken into account and described through random variables, by their probability distributions. As a first conclusion, risk assessment tools have then to be developed for both the approaches, keeping into account the main purposes of risk assessment.

As cited above, any integrated risk assessment procedure can quantify human, environmental or economical losses. It's worth noting that the three goals are not consistent and cannot be simply overlapped.

The well known – and relatively recent - accidents of Seveso in Italy (which addressed few strict European Directives), or Bhopal, in India, both resulting in tenths of thousands of people affected or deaths, were triggered by almost insignificant failure of small reactor, with virtually no direct economical losses (bankrupting of companies occurred for later governmental and insurance action). Besides, catastrophic accidents with large economical losses, as huge refinery fires or river or see environmental pollution, for instance, are typically characterised by a very small number of injured, often with no casualties.

Furthermore, with specific reference to earthquakes, it's important noting that very low intensity seismic waves can however trigger catastrophic industrial accidents starting from relatively small release of energy (as a jet fire towards toxic of flammable storage tanks), as escalation effects are among the main factor affecting industrial safety.

As a conclusion, either deterministic or probabilistic goals have to be clearly addressed, since the beginning: human effects, environmental effects, economic effects, or their combination.

In the most common probabilistic methodology, the human effects of industrial accident are the primary concern. To this regard, common measures for industrial quantitative risk assessment include individual risk and societal risk. The individual risk for a point-location around a hazardous activity is defined as the probability that an average unprotected person permanently present at that point location, would get killed due to an accident at the hazardous activity.

The societal risk for a hazardous activity is defined as the probability that a group of more than N persons would get killed due to an accident at the hazardous activity. The societal risk is often described as FN curve (frequency number curve), i.e. the exceedance curve of the annual probability of the event and the consequences of that event in terms of the number of casualties [4].

The practical evaluation of both individual and societal risk is a complex task which requires first the identification of all credible equipment failures, i.e. the "top event". The latest has to be coupled with related probabilities of occurrence, based on historical analysis or process related analysis (e.g. fault tree analysis). At this point, the physical phenomena which are able to produce damages to people, e.g. fire or explosion or

dispersion of toxic substance, and equipment (aiming at domino effect evaluation) and the related probability (e.g. through event tree analysis), for each of the possible top events, has to be modelled, in order to produce the temporal and spatial distribution of overpressure, heat radiation and concentration. Moreover, the relationship of these variables with human being has to be assessed.

When deterministic approaches are required or mandatory, probabilistic evaluation for credibility of accidents (in terms of annual probability of occurrence) has still to be used for the simplification of analysis, either for WCA or MCA. Hence, consequence analysis is performed by classical methodologies, coherently with the most accepted risk assessment procedure presented in literature.

Economical losses and environmental consequences are the other main purposes of risk assessment. In the first case, the analysis should be addressed by the structural damage caused by the earthquake effect. To this regard, it should be noted that the assessment of damage is the starting point of the QRA, even if, as already explained, large structural damage do not mean necessarily higher risks for human lives. However, the development of tools for economical risk assessment is parallel. The only main difference is the quantification of cost for recovering-restoring the facilities.

Finally, regarding environmental risks, it is important to noting that large risks occur typically when large amount of

polluting substances are available in the industrial installation. In this case, it's mandatory to assume that the same installation is provided with the active strategies to avoid polluting and that these strategies are positively activated when the spatial and temporal development of industrial incidents is predictable for the relatively slow time-history of loss of containment.

Quite clearly, the emergency procedure can fail, and pollution may occur. However, some main points can be sketched in dependence of the physic state of released substance. If the released substance is a toxic or flammable liquid or gas, then the environmental analysis is just analogous to the QRA previously described if fire, explosion or toxic dispersion in the atmosphere is of concern.

If the release is a noxious or toxic liquid, then it's likely that passive strategies (e.g. catch basin) will possibly collect the substance. If pollution of river or land or see pollution is of concern and passive actions are unable to produce beneficial effects, than large-scale release of substance should be analysed in terms of land or water dispersion with respect to consequence assessment, and risk assessment is reduced to specific assessment of probability of failing for both passive and active strategies.

In this framework, the efforts of this thesis has been addressed to increase of knowledge and to the production of simplified "engineering" tools for the analysis of industrial accidental scenarios produced by interaction of seismic wave

with industrial equipment containing relevant amounts of hazardous materials, either toxic or flammable or both.

CHAPTER 2:

RISK ANALYSIS OF INDUSTRIAL PLANT

2.1 INTRODUCTION

It is only in recent years that the discipline of seismic probabilistic risk analysis to assess industrial plants experienced a large scale use and development. In fact the sub-discipline of seismic-QRA analysis in past years both because it's a young discipline and because it suffers the technical problems that lead to significant numerical uncertainties in the "bottom-line" core damage and risk results. Besides seismic-QRA analysis was seriously approached only during 1980's, more than a half-decade after the first internal-initiators analysis of WASH-1400. Also, compared to internal-initiator analysis the number of practitioners is fewer, so there is less opportunity for a broader community to have digested and re-digested the methods, models, data, and results. This is true for both the fragility analysis methods and the hazard-analysis methods. The fact is that the seismic-QRA analysis, like analyses involving other external initiators such as high winds and external flooding, have developed a "bad reputation" in some quarters – they are

still considered too uncertain, or too conservative, or supported by too little solid data to be of important use. Fortunately, this picture has begun to change recently.

2.2 SELECTION OF EXTERNAL EVENTS

The external events, as demonstrated by world-wide experience with probabilistic risk analysis (QRA) of industrial plants, can be a significant contributor to core damage frequency in some instance. The "external" events are those events whose cause is external to all systems used in normal operation, as earthquakes, floods, and wind storms [5]. As a consequence, the need of a procedure to consider all possible external events exists together with variability of more flexible tools able to prove a screening of significant ones to include in detailed PRAs. The screening procedure, quite obviously, is a basic step in the QRA and can strongly affect the results of the total risk analysis of the plant.

To consider all possible external events a diligent study of geologic, seismologic, hydrologic, and meteorological characteristics of the site region as well as present and designed industrial activities in the vicinity of the plant should be conducted. The screening technique is meant to identify the significant external events to be included in the detailed risk assessment. The starting point is a list of hazards compiled according to section 2 of NUREG-1407 [6], from

NUREG/CR-5042 [7-8] and NUREG/CR-2300 [9]. An example of list of natural and man-made external events is shown in the Table 2.1. After the individuation of all possible external events screening criteria are established and each external event is reviewed to judge whether it deserves further study.

The knowledge of the plant and its design basis are used to screen out from the list all the hazards that, reasonably, have a negligible contribution to risk of the plant.

Events	
Aircraft impact	Low winter temperature
Avalanche	Meteorite
Coastal erosion	Pipeline accident
External flooding	Intense precipitation
External winds and tornadoes	River diversion
Fire	Sandstorm
Fog	Seiche
Forest Fire	Seismic activity
Frost	Snow
Hail	Soil shrink-swell consolidation
High summer temperature	Storm surge
Hurricane	Transportation accidents
Ice cover	Tsunami
Internal flooding	Toxic gas
Landslide	Turbine-generated missile
Lightning	Volcanic activity
Low lake or river water level	Waves
Release of chemicals in onsite storage	Industrial or military facility accident
High tide, high lake level, or high river stage	

Table 2.1. Natural and man-made external events.

According to NUREG/CR-4839 [10] and NUREG/CR-2300 [9], a particular hazard can be screened out if:

- The event has a damage potential equal or lower than the specific events for which the plan has been designed. This required an evaluation of plant design bases in order to estimate performance against a specific external event. This screening criterion is not applicable to events like earthquakes, floods, and extreme winds since their hazard intensities could conceivably exceed the plant design bases.
- The event has a significantly lower mean frequency of occurrence than other events with similar uncertainties and could not result in worse consequences than those events.
- The hazard can not take place close enough to the plant.
- The event is included in the definition or consequences of other events. For example, storm surge is included in external flooding.

The general methodology to identify each external event as potentially significant hazard is suggested by NUREG-1407. This methodology is based upon the concept of "progressive screening", and it can be described as a sequence of steps described as following:

Review plant-specific hazard data and licensing bases. In this step hazard data specific to the plant are gathered. The data airways and aircraft traffic in the vicinity of the plant, surface

transportation routers and traffic on them, wind speed series at the plant's meteorological tower or nearby station, river flow records, etc. In this step the design basis hazards are also gathered. They will be used as a point of reference for the assessment.

Identify significant changes since operating license issuance. Significant changes include military and industrial facilities within 5 miles to the site, onsite storage or other activities involving hazardous materials, transportation or developments that could affect the original design conditions.

Determine if the plant design meets Standard Review Plan (SRP) criteria. If the information obtained from the review in previous steps, shows conformance to SRP regarding to a particular hazard, it can be judged that the contribution from that hazard to core damage frequency is less than 10^{-6} per year and, very likely, that it has a negligible influence in the plant's vulnerability to severe accidents. Consequently, the hazard can be carried out to confirm the absence of vulnerabilities not included in the original design basis analysis.

Determine if the hazard frequency is acceptably low. If the original design basis does not meet current regulatory requirements, the approach could be to demonstrate that the design basis hazard frequency is sufficiently low (less than 10^{-5} per year) and the conditional core damage frequency is judged to be less than 10^{-1}. If the design basis hazard frequency combined with the conditional core damage frequency is not sufficiently low (less

than the screening criterion of 10^{-6} per year), additional analysis may be needed.

Bounding analysis. This step is intended to provide a conservative calculation showing that either the hazard would not result in core damage or the core damage frequency is below the reporting criterion.

Probabilistic safety assessment. This is last step, which is reached in those rare cases where the particular event could not be screened out in one of the previous steps. If the core damage frequency resulting from QRA is less than 10^{-6} per year, the event need not be considered further. Otherwise, vulnerabilities have to be found and reported.

2.3 RISK ASSESSMENT: METHODOLOGY

The seismic probabilistic risk analysis for industrial plant [11] can be subdivided in four steps, which are combined together. The four sub-methodologies to be evaluated here are:

- The seismic hazard analysis for calculating the frequency of earthquakes of various "size" at given site and characterising the motion parametrically.
- The seismic failure mode and fragility methodology for calculating the capacity of individual components and structures, and from that capacity the seismic fragility curve for each item and correlations among these.
- The seismic-QRA systems analysis.

- The seismic QRA methodology for analysing plant response and off-site release and consequences.

The outputs of QRA are damage-state probabilities. In each steps the uncertainties (e.g., uncertainty in the frequencies of exceeding different levels of hazard intensity, uncertainty in component fragilities) must be considered, and appropriately propagated through the entire analysis. The evaluation of seismic risk requires information on the seismologic and geologic characteristics of the region, the capacities of structure and equipment to withstand earthquakes beyond the design bases, and on the interaction between the failures of various components and systems of an industrial plant. Empirical data available on these aspects are generally limited; the use of sophisticated analytical tools to calculate the real capacities of equipments and structures is generally assumed to be expensive and has to be done on a selective basis commensurate with the uncertainties of overall seismic risk problem.

2.4 SEISMIC HAZARD ANALYSIS

The base in the probabilistic seismic risk analysis (and in probabilistic risk analysis for generically external event) is the hazard analysis. In hazard analysis are calculated the frequencies of occurrence of different intensities of an external event. It may be performed by developing a phenomenological model of the event, with parameter values estimated from available data

and expert opinion. Typically, the output of hazard analysis is a so called hazard curve that represents the exceedance frequency versus hazard intensity for a given time window. Typical hazard curves are shown in Figure 2.1. They are given in terms of PGA (Peak Ground Acceleration) for three sites in Campania Region (Southern Italy):Sant'Angelo dei Lombardi (AV-southern Italy), Pomigliano d'Arco (NA-southern Italy) and Altavilla Irpinia (AV-southern Italy). Two are the methodologies for the determination of seismic hazard analysis for a site of interest:

- DSHA: Deterministic Seismic Hazard Analysis
- PSHA: Probabilistic Seismic Hazard Analysis

2.4.1 Deterministic Seismic Hazard Analysis (DSHA)

The basis of DSHA is to develop earthquake scenarios, defined by location and magnitude, which could affect the site under consideration. The resulting ground motions at the site, from which the controlling event is determined, are then calculated using attenuation relations; in some cases, there may be more than one controlling event to be considered in design.
To perform a deterministic analysis, the following information is needed:

- Definition of an earthquake source and its location relative to the site.
- Definition of a design earthquake magnitude that the source is capable of producing.

- A relationship which describes the attenuation, or decay with distance, of ground motion.

A site may have several known active faults in its proximity. A maximum magnitude is defined for each fault. The maximum magnitude is a function of the fault length and historical knowledge of past earthquakes on that particular source. The attenuation relationships are developed based on statistical analyses motion records from earthquakes occurring in similar geologic and tectonic conditions.

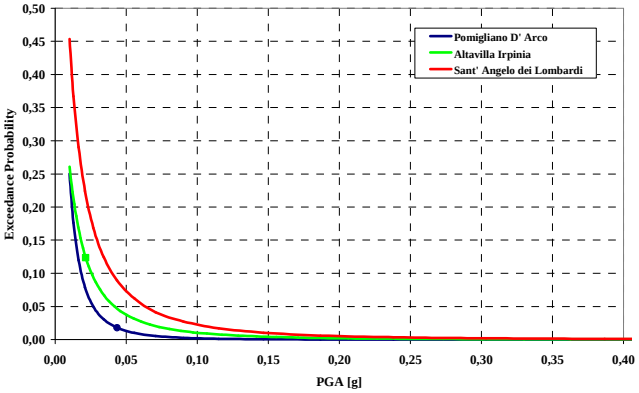

Figure 2.1: Seismic hazard curve for Sant'Angelo dei Lombardi, Altavilla Irpinia, Pomigliano D'Arco. Time interval: 1 year.

2.4.2 Probabilistic Seismic Hazard Analysis (PSHA)

In the following the basic principles for the seismic hazard analysis for the site of interest is presented; more details for the seismic hazard analysis may be elsewhere. In hazard analysis are calculated the frequencies of occurrence of different intensities

of earthquakes. This analysis is based on the data of past earthquakes for every region. Generally the seismic hazard analysis can be subdivided in four as follows:

- Identification of sources
- Earthquake recurrence relationship
- Ground motion attenuation relationship
- Hazard Curves

Common to both approaches is the very fundamental, and highly problematic, issue of identifying potential sources of earthquakes. Another common feature is the modelling of the ground motion through the use of attenuation relationships. The principle difference in the two procedures resides in those steps of PSHA that are related to characterising the rate at which earthquakes and particular levels of ground motion occur.

In a DSHA the hazard will be defined as the ground motion at the site resulting from the controlling earthquake, whereas in PSHA the hazard is defined as the mean rate of exceedance of some chosen ground-motion amplitude. Another important difference between the two approaches is related to the treatment of hazard due to different sources of earthquakes. In PSHA, the hazard contributions of different seismogenic sources are combined into a single frequency of exceedance of the ground-motion parameter; in DSHA, each seismogenic

source is combined separately, the design motions corresponding to a single scenario in a single source.

2.4.3 Identification of Sources

The individuation of the sources consists of the characterisation of the sources near the site of interest for the seismic analysis of the plant. First of all the sources must be identified (Figure 2.2).

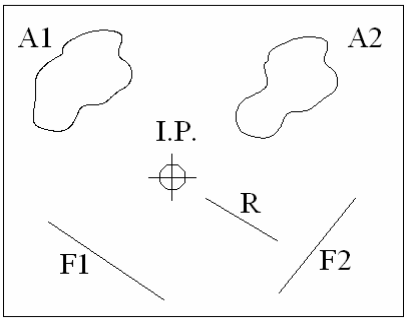

Figure 2.2: Identification of Sources.

Faults, points and area can be as earthquake sources. Whenever an area is concerned, the occurrence of earthquake is generally assumed to be spatially uniform. If this assumption does not apply, the single source zone can be divided into smaller areas characterized by different uniform seismicity. However, it is worth noting that only in highly active seismic regions faults are well characterised and allow to easily set seismic sources.

These models can then be applied to the set of seismic source for use in the subsequent analysis. Models range from the simple to the complex, and can incorporate factors such as possible interactions among sources, time dependence or independence of earthquake occurrence due stress build-up, and so on. A typical site-specific model might be founded on a continent-sized tectonic model, coupled with other regional and local features. Usually, unless specific knowledge indicates otherwise, the different zones are assumed to be independent of each other, in the sense that seismicity in one zone is uncorrelated with seismicity in adjacent zones.

2.4.4 Earthquake recurrence relationship

After the individuation of sources, the earthquake recurrence relationship, to characterize the activity of each source is necessary. This relationship is typically expressed in terms of annual frequency as a function of magnitude, for each source or source zone. Models for the recurrence relationship can be characterised by different levels of complexity, on the analogy with the assessment of seismic sources. Much judgment is necessary even in cases where the historical earthquake record is extensive. Controversial can be the case where historical records are poor or a few relevant earthquakes occurred. For most areas where this is not the case, and because except for very recent events the few important earthquakes usually have not been properly measured by good instruments, the

judgement can be controversial. Part of the problem of understanding large earthquakes in the distant past is that the knowledge is often limited to spatial distribution of the damage that they caused. This is not easily transformed into a more scientific parameter like magnitude (which, itself, is only a rough scheme for categorising earthquake "size").

Typical earthquake recurrence relationship is the well known Gutenberg-Richter relationship:

$$N(m) = \alpha \left(\frac{e^{-\beta m} - e^{-\beta m_u}}{e^{-\beta m_l} - e^{-\beta m_u}} \right) \tag{2.1}$$

Where $N(m)$ is the mean number of earthquakes in a given time period with magnitude equal to or greater than m for a given source, α is the mean number of events of any magnitude in the interval $[m_l, m_u]$. In other words α is representative of the seismic activity of the source in the time period of interest, while the term in the brackets represents the probability $Pr\{M>m\}$, i.e. the probability that an event has a magnitude $M>m$.

2.4.5 Ground motion attenuation relationship

The third step is working out the ground-motion attenuation relationship (Figure 2.3), which means associating a motion vs. distance relationship with each magnitude. The form of a typical attenuation relationship is:

$$\log I = b + g_M(m) + g_R(r) + \varepsilon \qquad (2.2)$$

Where I is the ground motion parameter, m is the magnitude of the earthquake, r is the distance to energy centre or the causative fault and ε is a random error term with mean of zero and (typically) a Gaussian probability distribution describing the variability in ground motion. It has long been recognized that the prediction of I is dependent on local and regional site conditions. These site effects can be modelled in different ways, depending on the degree of sophistication required. Attenuation relationships are typically developed using statistical regression analyses to data recorded by a strong-motion instrument, or derived from such records, such as acceleration, velocity and displacement time series.

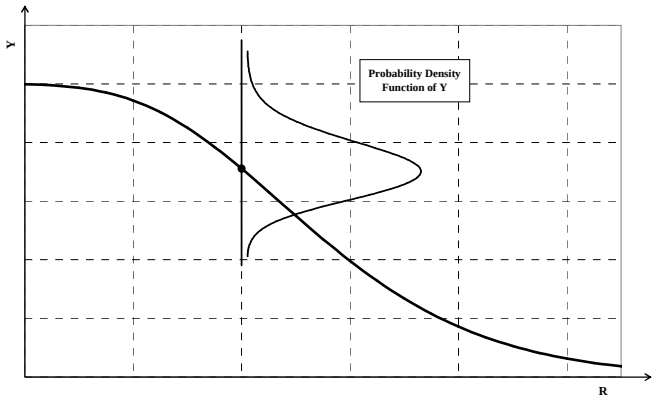

Figure 2.3 Ground motion attenuation relationship.

Several relationships of this type have been developed in the past; excellent summaries have been published by Campbell [12] and Joyner and Boore [13]. Besides Cornell et al. have discussed the variability introduced in the predicted response by different attenuation approaches.

The fourth and final step of the hazard assessment is producing the "hazard curve" themselves. These curves are usually expressed in terms of the annual frequency of exceedance vs. a ground-motion parameter like peak ground acceleration or a spectral acceleration (Figure 2.1).

2.5 STRUCTURAL ANALYSIS AND FRAGILITY OF COMPONENTS

Behaviour of structures and components under load induced by external hazard event, like earthquakes, is relevant and must be assessed to evaluate probabilities of faults and malfunctioning. This process is based generally on structural analysis and relates intensity measures of a given loads to effects on the structures. Comparison between strength (Capacity) and induced actions (Demand) leads to recognise if a given limit state of the structure is fulfilled or not.

The hazard input could be a set of earthquake time histories. For each hazard intensity, the output of the response analysis would be a frequency distribution of the responses. The specific

responses calculated depend on the failure modes of the components.

In order to define failure frequencies for structure, equipment, and piping, it is needed to know the responses of these structures under the action of earthquake; in special way it is necessary to known the seismic responses to various levels of the ground-motion parameter. Measured earthquakes signals refer to seismic waves radiating from the seism epicentre to the gauge location and can be related to global characteristics of the earthquakes: Magnitude, distance and soil type; these quantities are mainly reflected in the frequency content of the motion. Despite this simplification, earthquake signals carry several uncertainties and it is not even a trivial task to define a univocally determined intensity of earthquake, thus allowing comparison of records. However, geophysicists and structural engineers use to classify earthquakes on the basis of two classes of parameters such as "ground parameters" and "structural dynamic affecting factors". The choice of these intensity parameters is important since they summaries all the random features of earthquakes, including energy and frequency contents, which meaningfully affect the structural response of components. Ground parameters refer to the intensity measures (IM) characterizing the ground motion: PGA or alternatively peak ground velocity (PGV) and response spectra (RS) at the site location of the component. Structural affecting factors usually refer to the dynamic amplification induced on a

single degree of freedom system with the same period of the analysed structure (first mode spectral acceleration); although experimental investigations have showed that different parameters are needed if the effects of the earthquake on the structures would be accurately reproduced by structural analysis. For instance, in seismic analysis of piping system PGV is commonly used, whereas PGA is more useful when steel storage tanks are under investigation.

For existing industrial plants, seismic design procedures and criteria would have been much different from the current ones, and not all of the seismic design information (e.g., structural and piping analyses models, stress reports, and equipment-qualification reports) may be available. For such plants, it may be necessary to develop structural and piping analysis models and to calculate the responses for critical components. Some amount of iteration and interaction between the structures analyst and systems analyst would reduce the amount of response analysis by concentrating on the critical structures and components. For a newer plant, the analyst can rely on the design-analysis information.

Design drawings and as-built conditions are reviewed to develop structural analysis models for the critical structures. In some cases, in order to obtain a good estimation of structural response, the introduction in the analysis of the soil-structure interaction is required. Such an interaction can be taken into account via simplified methods able to fit the most relevant

aspects of the response. A typical example of this issue is the analysis of unanchored storage tanks [14]. In fact, in this case soil-structure interaction cannot be neglect because same failure modes depended on this interaction; e.g. during the earthquake the unanchored tanks can slide on the ground and if this relative displacement is elevated, it produces the failure of connection piping and the loss of the liquid. The output of the response analysis is the frequency density function of the peak response (e.g., moment, stress, and deformation) of each critical component. In Figure 2.4 is showed a typical output of structural analysis.

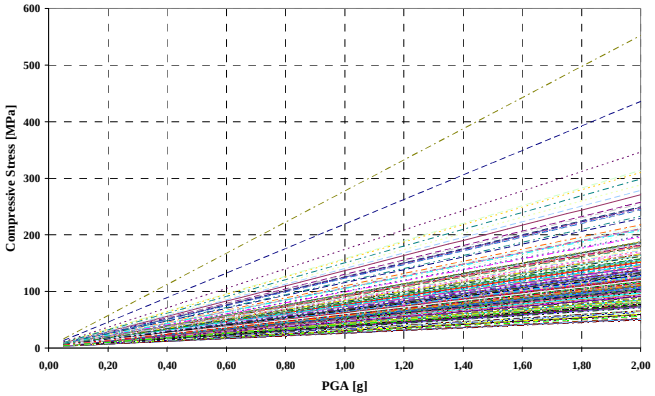

Figure 2.4 Example of median demand versus PGA.

This Figure shows the value of compressive stress for the anchored storage steel tank for each value of PGA. A time history analysis is a method of performing a dynamic analysis considered to give a realistic estimate of structural response to a

given earthquake. In a time history approach, the input is defined in terms of a time history of ground motion usually defined in terms of acceleration. A finite element or lumped mass model of the structure is a mathematical representation of the structure which properly allows for the distribution of mass and stiffness of the structure to an extent which is adequate for the calculation of the significant features of its dynamic response.

2.5.1 Analysis of Plant's Facilities

A key aspect of the risk analysis of the industrial plat is the detailed knowledge of each component and sub-system, in terms of design installation and operation mode. This step gives a contribution to the ranking of facilities depending on hazard or the individuation of critical components that can thoroughly increase the seismic risk. To this aim it is north to divide the system in a number of sub-systems that have to be analysed in detail up to component level. These are the basic information for the construction of fault-tree and sequences of events. A review of the printout of design of the plant and all information relative to the boundary conditions is fundamental; at the same time the inspection of the plant is recommended to establish the maintenance status of the facilities and upgrade models for capacity estimation.

2.5.2 Structural Systems

Industrial facilities show a large number of constructions and structural components [15]. As materials are concerned, it is easy to recognize that both reinforced concrete and steel constructions are commonly used, even in combination like composite structures. Large installation can be characterized by use of prestressed members, especially when long spans are required. However, it is worth nothing that a large variety of functions have to be accomplished by structural components so that the latter can be classified as follows:

- Building like structures
- Non-Building like structures

2.5.2.1 Building Structures

Building structures typically found in an industrial plant include administration buildings, control buildings, substations, warehouses, firehouses, maintenance buildings, and compressor shelters or buildings. They are typically single story buildings, but may have as two or three stories. Lateral force resisting systems used include shear wall, braced frames, rigid frames, and combinations. These are structures such as a pipe-ways, equipment support frames and box-type heaters which have a lateral force resisting systems similar to those of building systems, such as braced frames, moment resisting frames or shear wall systems. A flexible structure is typically defined as having a natural period of vibration (T) of 0.06 seconds or

more, which is equivalent to a frequency of about 17 Hz or less. Examples of building-like structures found in an industrial plant include:

- Moment resisting frames (steel or concrete) or braced frames (cross-braced or chevron-braced) supporting exchangers and horizontal vessels. Such structures can be up four or five levels high.
- Pipe-ways with lateral force resisting systems that are moment resisting frames (usually in the transverse direction to provide access beneath the pipe way) or braced frames (usually in the longitudinal direction).
- Rectangular furnaces.

2.5.2.2 Non-Building Structures

On the other actual buildings in an industrial plant, all structures are typically classified as non-building structures. However, their structural may resemble those of buildings, for example transverse moment frames for pipe-ways. Therefore, these structures are classified as building-like structures. Other structures, whose structural systems do not resemble those of buildings, are classified as non-building-like structures. Tanks or vessels are examples of such class of constructions. Non-building-like structures cover many industrial constructions and self supporting equipment items found in a typical industrial plant, such as vertical vessels, horizontal vessels and

exchangers, stacks and towers. Non-building-like structures found in an industrial plant fall into four categories described below:

- Rigid structures, i.e., those whose fundamental structural period is less than 0.06 seconds, such as horizontal vessel or exchanger, supported on short, stiff piers.
- Flat-bottom tanks supported at or below grade. Such structures respond very differently (compared to regular structures) during an earthquake. Special issues for unanchored tanks, such as the effects of fluid sloshing and tank uplifting must also be considered.
- Other non-building-like structures. Example of this category of structures include skirt-supported vertical vessels, spheres on brace legs, horizontal vessels or exchangers on long piers, guyed structures, and cooling towers.
- Combination structures. In petrochemical facilities, such structures generally supported flexible non-structural elements whose combined weight exceeds about 25% of the weight of the structure. A typical example is a tall vertical vessel, furnace or tank supported above grade on a brace or moment resisting frame. The analysis methods depends on whether the non-structural element is flexible or rigid, and whether

its weight exceeds or is less than about 25% of the weight of the supporting structure.

2.5.2.3 Subsystems

In addition to various structures described in the preceding sections, various equipment and components that are supported within a structure can be considered subsystems. The weight of subsystems should only be a small portion of the total weight of the supporting structures (i.e., less than about 25%). Examples of subsystems typically found in a petrochemical facility include:

- Horizontal vessels and exchangers supported on a structure, weighing less than about 25% of the weight of the supporting structure.
- Electrical and mechanical equipment supported within a structure.
- Cable tray, conduit, ductwork and/or piping supported on a pipe way or within a building.

2.5.3 Characterisation of Failure Mode

The first step in generating fragility curves like that in Figure 2.5 is the development of a clear definition of failure modes.

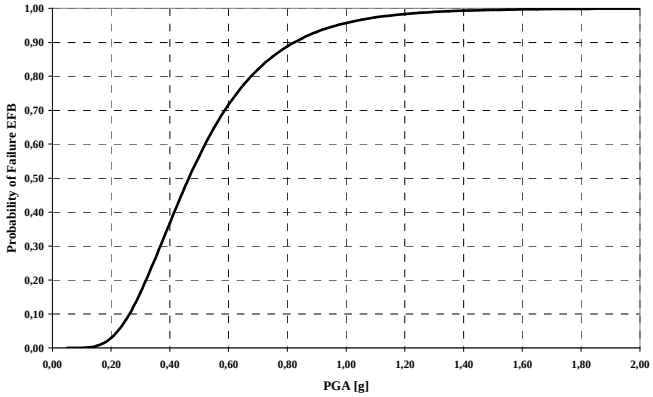

Figure 2.5 Example of fragility curve of a component versus PGA.

This definition must be acceptable to both the structural analyst, who generate the fragility curves, and the systems analyst, who must judge the consequences of a component's failure in estimating plant risk. It may be necessary to consider several failure modes (each one with a different consequence), and fragility curves are required for each mode.

For example, a storage tank can fail in any of the following modes:

- *Shell Buckling Mode.* One of the most common forms of damage in steel tanks involves outward buckling of the bottom shell courses, a phenomenon know as "Elephant Foot Buckling". Sometimes the buckling occurs over the full circumferences of the tank. Buckling of the lower courses has occasionally resulted

in the loss of tank contents due to weld or piping fracture and, in some cases, total collapse of the tank.

- *Roof and Miscellaneous Steel Damage.* A sloshing motion of the tank contents occurs during earthquake motion. The actual amplitude of motion at the tank circumference has been estimated, on the basis of scratch marks produced by floating roofs, to have exceeded several meters in some cases. For full or near full tanks, resistance of the roof the free sloshing results in an upward pressure distribution on the roof. Common design codes do not provide guidance on the seismic design of tank roof systems for slosh impact forces. Modern tanks built after 1980 and designed to resist elephant foot buckling or other failure modes may still have inadequate designs for roof slosh impact forces. In past earthquakes, damage has frequently occurred to the frangible joints between walls and cone roof, with accompanying spillage of tank contents over the top of the wall. Extensive buckling of the upper courses of the shell walls has occurred. Floating roofs have also sustained extensive damage to support guides from the sloshing of contents. Steel roofs whit curved knuckle joints appear to perform better, but these too have had supporting beams damaged from slosh impact forces. Lateral movement and torsional rotations from ground shaking have caused broken guides, ladder and

other appurtenances attached between the roof and the bottom plate. Extensive damage to roofs can cause extensive damage to upper course of a steel tank. However, roof damage or broken appurtenances, although expensive to repair, usually do lead to more than a third of total fluid contents loss.

- *Anchorage Failure.* Many steel tanks have hold-down bolts, straps or chairs. However, these anchors may be insufficient to withstand the total imposed load in large earthquake events and still can be damaged. The presence of anchors, as noted by field inspection, may not preclude anchorage failure loss of contents. Seismic overloads often result in anchor pull out, stretching or failure. However, failure of an anchor does not always lead to loss of tank contents.
- *Tank Support System Failure.* Steel and concrete storage tanks supported above grade by columns or frames have failed because of the inadequacy of the support system under lateral seismic forces. Such failure most often leads to complete loss of contents.
- *Hydrodynamic Pressure Failure.* Tensile hoop stresses can increase due to shaking-induced pressures between the fluid and the tank, and can lead to splitting and leakage. This phenomenon has occurred in riveted tanks where leakage at the riveted joints resulted from seismic

pressure-induced yielding. This happens more often in the upper courses. No known welded steel has actually rupture because of seismically induced hoop strains; however, large tensile hoop stress can contribute to the likelihood of elephant foot buckling near the tank base due to the overturning moment. Hydrostatic pressure failure may also be a cause for failure in concrete tanks, due to excessive hoop tensile forces in the steel reinforcement.

- *Connecting Pipe Failure.* One of the more common causes of loss of tank contents in earthquakes has been the fracture of piping at connections to the tank. This generally results from large vertical displacements of the tank caused by tank buckling, wall uplift or foundation failure. Failure of rigid piping that connects to adjacent tanks has also been caused by relative horizontal displacements of the tanks. Piping failure has also resulted in extensive scour in the foundation materials. Another failure mode has been the breaking of pipes that penetrate into the tank from underground, due to the relative movement of the tank and pipe.

By reviewing the equipment design, it may be possible to identify the failure mode that is most likely to be caused by the seismic event and to consider only that mode. Otherwise, in developing fragility curves it is necessary to use the premise that the component can fail in any of all potential failure modes.

The identification of credible modes of failure is based largely on the analyst's experience and judgment. In this step is can be useful analysed the historical data of damages caused by past earthquakes.

2.5.4 Fragility of Components

The fragility or vulnerability of a component [9-16] is defined as the conditional frequency of its failure for a given value of response parameter. It's calculated by developing the frequency distribution of the seismic capacity of a component and finding the frequency for this capacity being less than the response parameter value. All fragility curves should be given as a function of the same parameter of hazard curves. For example, assume the earthquake hazard is characterized by the P.G.A. (peak ground acceleration). The response (e.g. force, stress) due to this P.G.A. at a component location is R_0. The component's capacity to withstand the seismic force is a random variable, C. The fragility of the component is calculated as

$$f = frequancy\{C < R_0\} \tag{2.3}$$

Developing fragility curves can be used three general approaches:

- The empirical approach. This involves use of observed damage/non-damage from past earthquakes.

- The analytical approach. This involves the use of specific engineering characteristics of a component to assess its seismic capacity in a probabilistic way.
- The engineering judgment approach. This involves the review of available information by cognizant engineers and making an informed judgment as to the capacity of a component.

In developing fragility curves randomness and uncertainty often are characterized separately. Randomness reflects variables in the real world that current technology and understanding cannot explain. In other words, no reasonable amount of additional study of the problem will reduce randomness. Randomness exists in the level of ground motion at two nearby sites, even if they have very similar soil profiles and distance from the fault rupture. Randomness is characterized using a logarithmic dispersion parameter:

$$\beta_R \tag{2.4}$$

Uncertainty reflects the uncertainty in the predictions, given the level of simplification taken in the analysis. For example, suppose a water utility wanted to do a quick earthquake loss estimate for buried transmission pipelines without having to do a detailed effort to ascertain exactly what type of buried pipelines are in use at which locations, how old they are, what

their leak history is, which soils are most susceptible to corrosion, which soils are most susceptible to PGDs, what level of corrosion protection has been taken for a particular pipeline, and so on. In such a case, the fragility curve used should take into account that there is uncertainty in the pipeline inventory, as well as how that inventory would respond to a given level of ground motion. Uncertainty is characterized using a logarithmic dispersion parameter:

$$\beta_U \tag{2.5}$$

The total uncertainty is then expressed as:

$$\beta_T = \sqrt{\beta_R^2 + \beta_U^2} \tag{2.6}$$

In deterministic analysis, the deterministic factor of safety, F_D, is defined as the ratio of the deterministic code capacity, C_D, to the deterministic computed response, R_D, i.e.

$$F_D = \frac{C_D}{R_D} \tag{2.7}$$

In probabilistic analysis, both the capacity C and the response R are random variables. Thus, the factor of safety is given by:

$$F = \frac{C}{R} \tag{2.8}$$

This is also a random variable. A capacity factor, F_C, can be defined as the ratio of the actual capacity, C, to deterministic code capacity, C_D. Similarly, a response factor, F_R, is defined as the ratio of the deterministic computed response, R_D, to the actual response R, i.e.

$$F_C = \frac{C}{C_D} \tag{2.9}$$

$$F_R = \frac{R_D}{R} \tag{2.10}$$

Thus, the probabilistic factor of safety, F, can be defined in terms of the deterministic factor of safety, F_D, by:

$$F = F_C \bullet F_R \bullet F_D \tag{2.11}$$

The probability of failure is the probability that the factor of safety, F, is less than 1. The reliability is the probability that the factor of safety, F, is 1 or greater. Computation of the probability of failure is tractable mathematically when the capacity and the response factors, F_D and F_R, are assumed to be lognormally distributed random variables. F is a lognormal random variable if F_D and F_R are lognormal random variables. The median value, $\hat{F}$ and the logarithmic standard deviation, β_F and F are given by:

$$\hat{F} = \hat{F}_C \bullet \hat{F}_R \bullet \hat{F}_D \tag{2.12}$$

$$\beta_F^2 = \beta_C^2 + \beta_R^2 \tag{2.13}$$

Where $\hat{F}_C$ and $\hat{F}_R$ are the median values and β_C and β_R are the logarithmic standard deviations for the capacity, F_C and response, F_R, factors. The probability of failure is then given by:

$$P_f = \Phi\left(\frac{\ln\left(1/\hat{F}\right)}{\beta_F}\right) \tag{2.14}$$

Where Φ is the standard cumulative distribution function. For seismic events that have discrete hazard-parameter values (e.g. P.G.A.), the component fragility is calculated at the corresponding discrete response values. The fragility is estimated in any give failure mode. However, in estimating the capacity, uncertainties arise from several sources: an insufficient understanding of structural material properties and failure modes, errors in the calculated response due the approximations in modelling. Before the individual component fragilities can be combined in the plant-system logic it is necessary to evaluate the degree of dependence to be assumed among the failure frequencies in sets of multiple components. An incorrect assumption that the failure occur independently can lead to optimistic predictions if the multiple components appear within the same minimal cut set or to conservative predictions if they are not in the same cut set.

2.6 PLANT-SYSTEM AND ACCIDENT-SEQUENCE ANALYSIS

System analysis is a directed process for the orderly and timely acquisition and investigation of specific system information. It's necessary to acquire a lot of information about system and system's processes to perform a good analysis of events sequences. Typically the systems are subdivided in a number of sub-systems, A, B, C, etc. Observe also that in the few cases is necessary to subdivide the subsystems into its smallest sub-subsystems. This constitutes a choice of an internal boundary for the system.

The choice of the appropriate system boundaries in particular cases is a matter of vital importance, for the choice of external boundaries determines the comprehensiveness of the analysis, whereas the choice of a limit of resolution limits the detail of the analysis. There are two generic analytical methods by means of which conclusions are reached in the human sphere: induction and deduction.

2.6.1 Inductive Methods

Induction constitutes reasoning from individual cases to a general conclusion. If, in the consideration of a certain system, a particular fault or initiating condition and attempt to ascertain the effect of that fault condition on system operation are assumed, an inductive system analysis is under development.

Examples of this method are: Parts Count, Failure Mode and Effect Analysis (FMEA), Failure Mode Effect and Criticality Analysis (FMECA) and Event Tree Analysis.

Probably the simplest and most conservative assumption regarding the systems is that any single component failure will produce complete system failure. Under this assumption is based the Parts Count approach. In this case an easy list of all the components along their estimated probabilities of failure can be done. The individual components probabilities are then added and this sum provides an upper bound on the probability of system failure. This process is represented below:

Components	Failure Probability
A	f_A
B	f_B

Where F, the failure probability for the system, is equal to $f_A+f_B+\ldots$

In FMEA (Failure Mode and Effect Analysis) it is possible to identify, with reasonable certainty, those component failures having "non-critical" effects, but the number of possible component failure modes that can realistically be considered is limited. Conservative dictates that unspecified failure modes and questionable effects be deemed "critical". The objectives of the analysis are to identify single failure modes and to quantify these modes; the analysis needs be no more elaborate than the

strictly needed. FMECA (Failure Mode Effect and Criticality Analysis), is essentially similar to a Failure Mode and Effect Analysis in which the criticality of the failure is analyzed in greater detail, and assurances and controls are described for limiting the likelihood of such failures. Although FMECA is not an optimal method for detecting hazards, it is frequently used in the course of a system safety analysis. The four fundamental facets of such approach are:

- Fault identification
- Potential effects of the fault
- Existing or projected compensation and/or control
- Summary of findings.

These four facets generally appear as column headings in FMECA layout. Column 1 identified the possible hazards condition. Column 2 explains why this condition is a problem. Column 3 describes what has been done to compensate for or to control the condition. Finally the, Column 4 states whether the situation is under control or whether further steps should be taken.

2.6.2 Deductive Methods

Deduction constitutes reasoning from the general to the specific. In a deductive system analysis, it is assumed that the system itself has failed in a certain way, and modes of system/component behaviour contribute to this fault is seeking.

Fault Tree Analysis is an example of deductive system analysis. In this technique, some specific system state, which is generally a failure state, is postulated, and chains of more basic faults contributing to this undesired event are built up in a systematic way. In summary, inductive methods are applied to determine what system states (usually failed states) are possible; deductive methods are applied to determine how a given system state (usually a failed state) can occur. The plant risk is calculated by using the plant logic combined with component fragilities and seismic hazard estimates. Event and fault tree are constructed to identify the accident sequences that may lead a release of hazard material.

The first step in the plant-system and accident-sequence analysis is the identification of earthquake-induced initiating events. In the identification of initiating events caused by earthquake, the analyst may have to look beyond the single initiating events studies for internal events.

2.6.3 Fault Tree

Fault tree analysis [17] is a deductive failure analysis which focused on one particular undesired event and which provides a method for determining causes of this event. The undesired event constitutes the top event in a fault tree diagram constructed for the system, and generally consists of a complete or catastrophic failure as mentioned above. Careful choice of the top event is important to the success of the analysis. If it is

too general, the analysis become unmanageable; if it is too specific, the analysis does no provide a sufficiently broad view of the system. A fault tree analysis can be simply described as an analytical technique, whereby an undesired state of the system is specified, and the system is then analysed in the context of its environmental and operation to find all credible ways in which the undesired event can occurs. The faults tree itself is a graphic model of the various parallel and sequential combinations of the fault that will result in the occurrence of the predefined undesired event. A fault tree thus depicts the logical interrelationships of basic events that lead to the undesired event, which is the top event of the fault tree. It most important understand that a fault tree model is not a model of all possible system failures or all possible causes of system failure. In fact, a fault tree model is tailored to its top event which corresponds to some particular system failure mode, and the fault tree thus includes only those faults that contribute to this top event. It is also important to point out that a fault tree is not itself a quantitative model, but it is a qualitative model.

2.7 CONSEQUENCE ANALYSIS

This section provides an overview of consequence and effect models commonly used in industrial quantitative risk analysis [18-19-20-21]. Accidents begin with an incident, which usually results in the loss of containment of material from the process.

The material has hazardous properties, which might include toxic properties and energy content. Typical incidents might include the rupture or break of a pipeline, a hole in a tank or pipe, runway reaction, fire external to the vessel, etc. One the incident is defined, source models are selected to describe how materials are discharged from the process. The source model provides a description of the rate discharge, the total quantity discharged (or total time of discharge), and the state of the discharge, that is solid, liquid, vapour or a combination. A dispersion model is subsequently used to describe how the material is transported downwind and dispersed to some concentration levels. For flammable releases, fire and explosion model convert the source model information on the release into energy hazard potentials such as thermal radiation and explosion overpressures. Effect models convert these incident-specific results into effects on people (injury or death). More details can be found elsewhere.

2.7.1 Source models

Source models are used to quantitative define the release scenario by estimating discharge rates, total quantity release (or total time duration), extent of flash and evaporation from a liquid pool, and aerosol formation. Dispersion models convert the sources term outputs to concentration fields downwind from the source.

2.7.1.1 Discharge models

Most acute hazardous incidents start with a discharge of flammable or toxic material from its normal containment. This may be from a crack or fracture of process vessels or piping, from an open valve, or from an emergency event. Such leaks may be gas, liquid or two-phase flashing liquid-gas releases. Different models are appropriate for each of these. The underlying technology for gas and liquid discharges is well developed in chemical engineering theory and full descriptions of them can be found elsewhere. The first step in the procedure is to determine an appropriate scenario. Table 2.2 contains a partial list of typical scenario grouped according to the material discharge phase, i.e., liquid, gas, or two-phase.

Liquid Discharges

Hole in atmospheric storage tank or other atmospheric pressure vessel or pipe under liquid head.

Hole in vessel or pipe containing pressurized liquid below its normal boiling point.

Gas Discharges

Hole in equipment (pipe, vessel) containing gas under pressure.

Relief valve discharge (of vapour only).

Boiling-off evaporation from liquid pool.

Relief valve discharge from top of pressurized storage tank.
Generation of toxic combustion products as a result of fire.
Two-phase Discharges
Hole in pressurized storage tank or pipe containing a liquid above its normal boiling point.
Relief valve discharge (e.g., due to a runway reaction or foaming liquid).

Table 2.2: Typical Release Outcomes (Emergency Engineered or Emergency Unplanned Releases), and the Relationship to Material Phase.

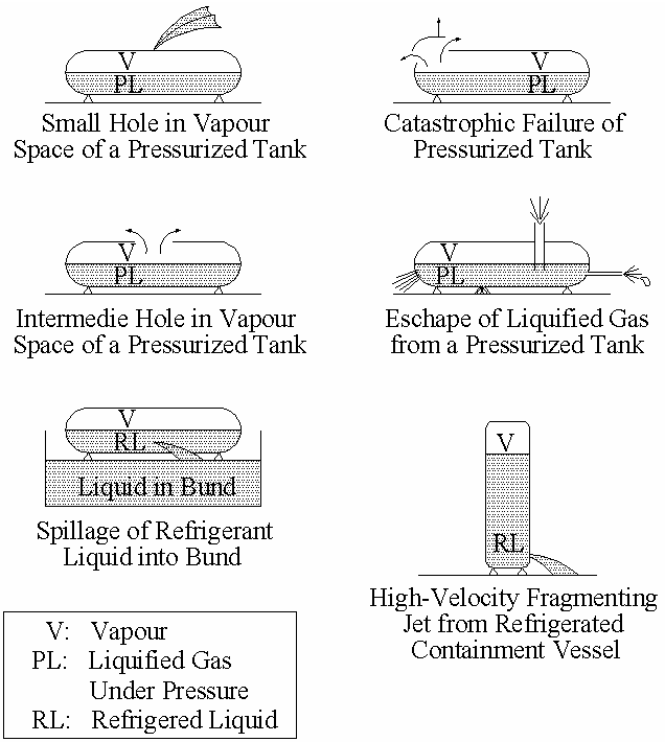

Figure 2.6: Illustration of some releases mechanisms.

Figure 2.6 shows some conceivable discharge scenarios with the resulting effect on the material's release phase. Several important issues must be considered at this point in the analysis. These include: release phase, thermodynamic path and endpoint, hole size, leak duration, and other issues. Discharge rate models require a careful consideration of the phase of the released material. The phase of the discharge is dependent on

the release process and can be determined by using thermodynamic diagrams or data, or vapour-liquid equilibrium model, and thermodynamic path during the release.

2.7.1.2 Flash and Evaporation

The purpose of flash and evaporation models is to estimate the total vapour or vapour rate that forms a cloud, for use as input to dispersion models. When a liquid is released from process equipment, several things may happen, as shown in Figure 2.7. If the liquid is stored under pressure at a temperature above its normal boiling point (superheated), it will flash partially to vapour when released to atmospheric pressure. The vapour produced may entrain a significant quantity of liquid as droplets. Some of this liquid may rainout onto the ground, and some may remain suspended as an aerosol with subsequent possible evaporation. The liquid remaining behind is likely to form a boiling pool which will continue to evaporate, resulting in additional vapour loading into the air. An example of a superheated release is a release of liquid chlorine or ammonia form pressurized container stored at ambient temperature.

If the liquid is not superheated, but has a high vapour pressure (volatile), then vapour emission will arise from surface evaporation from the resulting pools. The total emission rate may be high depending on the volatility of the liquid and the

total surface area pool. An example is a release of liquid toluene, benzene or alcohol.

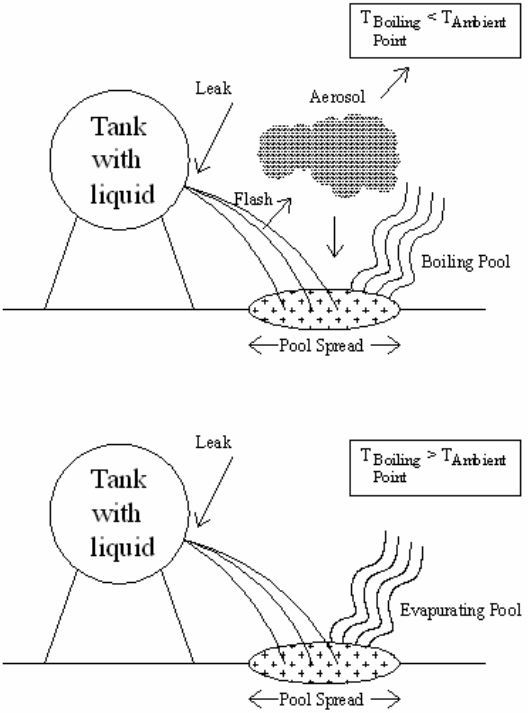

Figure 2.7: Two common liquid release situations dependent on the normal boiling point of the liquid.

2.7.2 Dispersion models

Typically, the dispersion calculations provide an estimate of the area effected and the average vapour concentrations expected. The simplest calculations require an estimate of the release rate of the gas (or the total quantity released), the

atmospheric conditions (wind speed, time of day, cloud cover), surface roughness, temperature, pressure and perhaps release diameter. More complicated models may require additional detail on the geometry, discharge mechanism, and other information on the release. Three kinds of vapour cloud behaviour and three different release-time modes can be defined:

Vapour Cloud Behaviour

- Neutrally buoyant gas
- Positively buoyant gas
- Dense (or negatively) buoyant gas

Duration of Release

- Instantaneous (puff)
- Continuous release (plumes)
- Time varying continuous

A large numbers of parameter affect the dispersion of gases. These include:

- Atmospheric stability
- Wind speed
- Local terrain effects
- Height of the release above the ground
- Release geometry
- Momentum of the material released
- Buoyancy of the material release

Whether conditions at the time of the release have a major influence on the extent of dispersion. Atmospheric stability is an estimate of the turbulent mixing; stable atmospheric condition lead to the least amount of mixing and unstable conditions to the most. The stability is commonly defined in terms of the atmospheric vertical temperature gradient. Wind speed is significant as any emitted gas will be diluted initially by passing volumes of air. As the wind speed increased, the material is carried downwind faster, but the material is also diluted faster by a larger quantity of air. Terrain characteristics affect the mechanical mixing of the air as in flows over the ground. Thus, the dispersion over a like is considerably different from the dispersion over a forest or a city of tall buildings. Most dispersion field data and tests are in flat, rural terrains. Figure 2.8 shows the effect of height on the downwind concentrations due to a release. As the release height increases, the ground concentration decreases since the resulting plume has more distance to mix with fresh air prior to contacting the ground.

2.7.3 Explosion and fires

The objective of this section is to review the types of models available for estimation of the consequences of accidental explosion and fire incident outcomes. Many types of outcomes are possible for a release. This includes:

- Vapour cloud explosions (VCE)

- Flash fire
- Physical explosions
- Boiling liquid expanding vapour explosions (BLEVE) and fireballs
- Confined explosions
- Pool fire explosions and jet fires

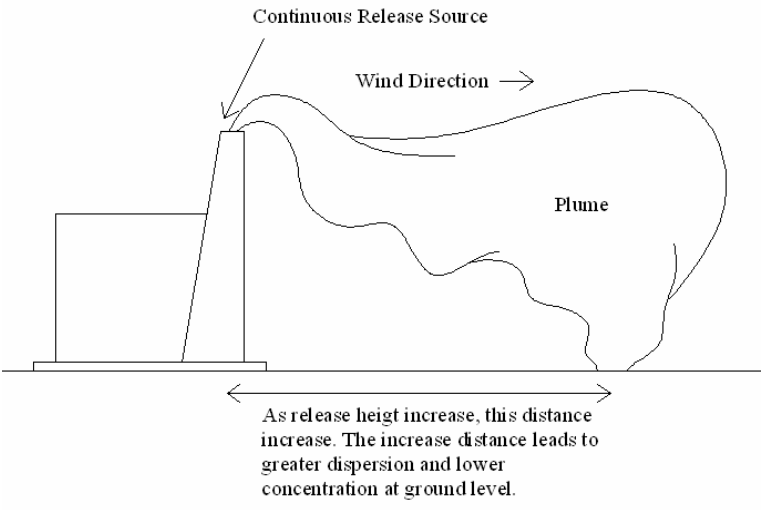

Figure 2.8: Effect of release height on ground concentration.

2.7.3.1 Vapour could explosion (VCE)

When a large amount of flammable vaporizing liquid or gas is rapidly released, a vapour cloud forms and disperses with the surrounding air. The release can occur from a storage tank, process, transport vessel, or pipeline. If this cloud is ignited

before the cloud is diluted below its lower flammability limit, a VCE or flash fire will occur. The main consequences of a VCE are an overpressure, while the main consequence of flash fire is direct flame contact and thermal radiation. Four features must be present in order for a VCE to occur:

- First, the release material must be flammable.
- Second, a cloud of sufficient size must form prior to ignition, with ignition delays of from 1 to 5 min considered the most probable for generating vapour cloud explosions.
- Third, a sufficient amount of the cloud must be within the flammable range. Fourth, sufficient confinement or turbulent mixing of a portion of the vapour cloud must be present.

The blast effects produced depend on whether a deflagration or detonation results, with deflagration being, by far, the most likely. A transition from deflagration to detonation is unlikely in the open air. A deflagration or detonation result is also dependent on the energy of the ignition source, with larger ignition sources increasing the likelihood of a direct detonation.

2.7.3.2 Flash Fire

A flash fire is non-explosive combustion of a vapour cloud resulting from release of flammable material into the open air.

Major hazards form flash fire are from thermal radiation and direct contact.

The literature provides little information on the effects of thermal radiation from flash fire, probably because thermal radiation hazards from burning vapour clouds are considered less significant than possible blast effects. Furthermore, flash combustion of a vapour clod normally lasts non more that a few tenth of a seconds. Therefore, the total intercepted radiation by an object near a flash fire is substantially lower than in the case of a pool fire.

2.7.3.3 Physical Explosion

When a vessel containing a pressurized gas ruptures, the resulting stored energy is released. This energy can produce a shock wave and accelerate vessel fragments. If the contents are flammable it is possible that ignition of the released gas cloud result in additional consequence effects. The effects are similar to a detonation than a vapour cloud explosion (VCE). The extent of a shock wave depends on the phase of the vessel contents originally present. There is a maximum amount of energy in a bursting vessel that can be released. This energy is allocated to the following:

- Vessel stretch and tearing
- Kinetic energy of fragments
- Energy in shock wave

- "Waste" energy (heating of surrounding air)

Relative distribution of these energy terms will change over the course of the explosion.

2.7.3.4 BLEVE and Fireball

A boiling expanding vapour explosion (BLEVE) occurs when there is a sudden loss of containment of a pressure vessel containing a superheated liquid or liquefied gas. A BLEVE is a sudden release of a large mass of pressurized superheated liquid to the atmosphere. The primary cause is usually an external flame impinging on the shell of a vessel above the liquid level, weakening the container and leading to sudden shell rupture. A pressure relief valve does not protect against this mode of failure, since the shell failure is likely to occur at a pressure below the set pressure of the relief system. It should be noted, however, that a BLEVE can occur due to any mechanism that results in the sudden failure of containment, including impact by an object, corrosion, etc. The sudden containment failure allows the superheated liquid to flash, typically increasing its volume over 200 times.

This is sufficient to generate a pressure wave and fragments. If the released liquid is flammable, a fireball may result. Blast or pressure from BLEVEs are usually small, although they might be important in the near field. These effects are of interest primarily for the prediction of domino effects on adjacent vessels. Four parameters used to determine a fireball's thermal

radiation hazard are the mass of fuel involved and the fireball's diameter, duration and thermal emissive power. The problem with a fireball of a BLEVE is that the radiation will depend on the actual distribution of flame temperatures, the composition of the gases in the vicinity of the fireball, the geometry of the fireball, absorption of the radiation by fireball itself, and the geometric relationship of the receiver with respect to the fireball. All of these parameters are difficult to quantify for a BLEVE.

2.7.3.5 Confine explosion

Dust explosions and vapour explosions within low strength vessels and buildings are one major category of confined explosion. Combustion reactions, thermal decompositions, or runway reactions within process vessels and equipment are the other major category of confined explosions. In general, a deflagration occurring within a building or low strength structure such as a silo less likely to impact the surrounding community and is more of an in-plant threat because of the relatively small quantities of fuel and energy involved. Shock waves and projectiles are the major threats from confined explosions.

2.7.3.5 Pool fire and Jet fire

Pool fire tends to be localized in effect and is mainly of concern in establishing the potential for domino effects. The

primary effects of such fire are due to thermal radiation from the flame source. Issues of inter-tank and inter-plant spacing, thermal insulation, fire wall specification, etc., can be addressed on the basis on specific consequence analyses for a range of possible pool fire scenarios. A pool fire may result via a number of scenarios. It begins typically with the release of flammable material from process equipment. If the material is liquid, stored at a temperature below its normal boiling point, the liquid will collect in a pool. The geometry of the pool is dictated by the surrounding, but an unconstrained pool in an open, flat area is possible, particularly if the liquid quantity spilled is inadequate to completely fill the diked area.

If the liquid is stored under pressure above its normal boiling point, then a fraction of the liquid will flash into vapour, with unflashed liquid remaining to form a pool in the vicinity of the release. Once a liquid pool has formed, an ignition source is required. The ignition can occur via the vapour cloud, with the flame travelling upwind via the vapour to ignite the liquid pool. Once an ignition has occurred, a pool fire results and the dominant mechanism for damage is via thermal effects, primarily via irradiative heat transfer from the resulting flame. If the release of flammable material from the process equipment continues, then a jet fire is also likely; jet fire typically result from the combustion of a material as it is being released from a pressurized process unit. The main concern, similar to pool fires, is in local radiation effects.

CHAPTER 3:

CHARACTERIZATION OF INDUSTRIAL FACILITEIS

3.1 INTRODUCTION

Industrial facilities are very complex systems that may require large efforts to ensure safe operations, as they often store large amount of toxic and flammable substances. Hence, the assessment of risks associated to such plants is a key issue, and tools to design prevention and mitigation measures are required [4]. To this regard, structural performances of constructions, components and equipment are certainly relevant when natural hazards, like earthquake or wind storm, are concerned.

In recent years, Quantitative Risk Analysis (QRA) procedures, originally developed for nuclear power plants, have been extended to other typical industrial installations, i.e. petrochemical, chemical plants or facilities for storage of hazardous materials [1-2]. This circumstance is also related to the emanation of well known Seveso EU directive [3] concerning safety of facilities at relevant risks, that have been

strictly classified depending on the type of process and the amount of hazardous material present within the plant. The objectives of (QRA) of industrial facilities is to estimate the consequences derived to the external or internal events; consequences in terms of environment damages, economical loss or also the loss in terms of human life. In this framework, an effort has been devoted to increase the knowledge and to develop simplified "engineering" tools for the analysis of industrial accidental scenarios produced by interaction of earthquakes with industrial equipments containing relevant amounts of hazardous materials, either toxic or flammable or both. To this aim, principal classes of equipment have been sketched. In particular a detailed study on these defined classes of equipment has been conducted to carry out a design and construction standardization in the framework of seismic risk analysis.

3.2 INDUSTRIAL PLANTS

A large study of typical industrial equipment has been conducted both in terms of industrial process, to know the service condition, and in terms of geometric and structural characteristic. The structures and structural details studied are: supports of vertical tanks; reinforced concrete structures for vertical tank support; support for horizontal tanks; anchorages; cathedral furnaces; high pressure stream boiler; fractionating

column for hot products; fractionating column for cold products; train of exchangers; atmospheric and pressurized storage tanks; under-ground tanks for GPL; pumps; compressors.

Figure 3.1 shows a typical fractionating column that is used in many processes to separate hot product. In such component, usually installed downstream to the cathedral furnaces for thermal cracking (Figure 3.2), the hot product, in mix phase, is separated by the internal plates of the column. The resulting product (Quench Oil) is sent to the exchanger (Figure 3.3) to be filtrated. Fractionating column can be atmospheric or low pressure, and can be included in a large class (*atmospheric or low pressure equipment*) which includes a relevant number of operational units as dryers, separators, cyclones, distillation towers, extraction units, low pressure reactors, boilers, heat exchanger, ovens, and furnaces, pumping system, which are characterised by relatively small volumes with respect to the large-scale storage tanks. Hazardous substances can be gas, or dust or liquid, toxic or flammable or both.

Risk assessment is specific to the scale of unit, to the operating conditions (high temperature, low temperature), to the presence of one or more physical phases, to the specific auxiliary system installed.

Risk assessment is often poorly performed even in the design phase, and QRA often refers to approximate solution

starting from the amount and condition (Temperature, Pressure) of substances in the main section.

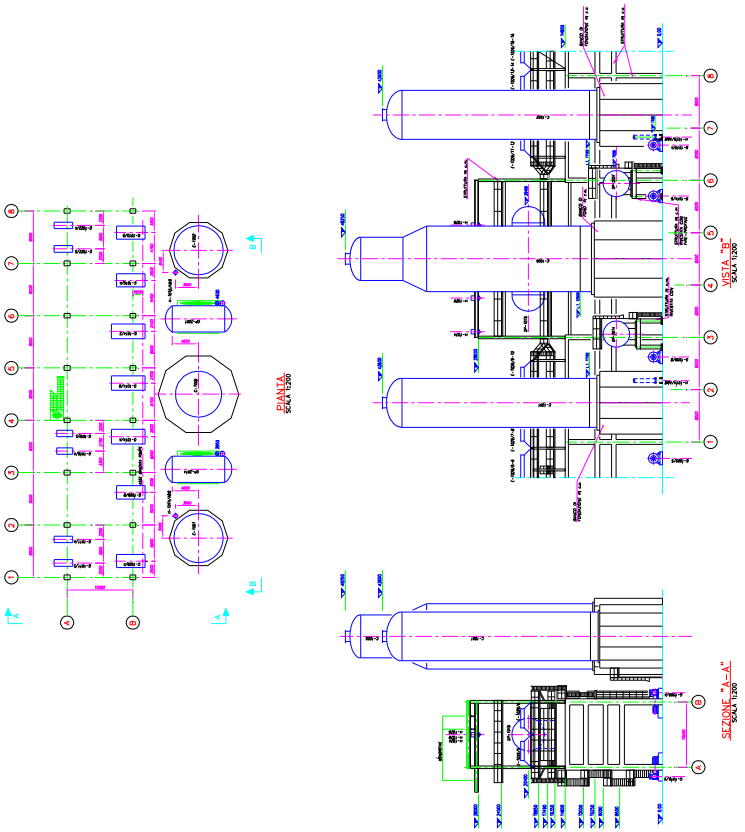

Figure. 3.1: Example of typical installation of fractionating column for hot product.

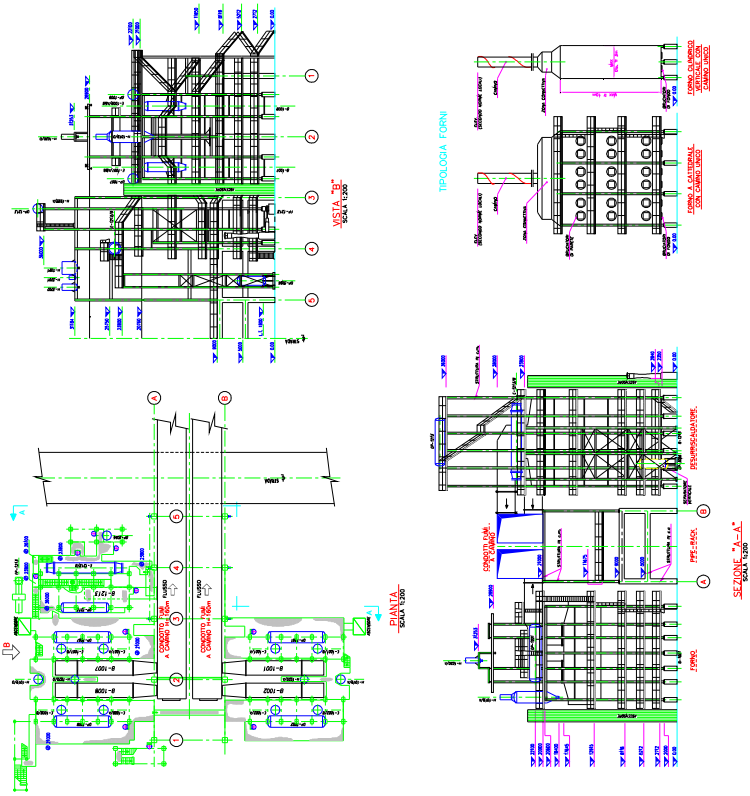

Figure. 3.2: Example of *cathedral furnaces* used to thermal cracking of liquid or gaseous hydrocarbon as Ethane, Propane, Naphtha, Gas Oil.

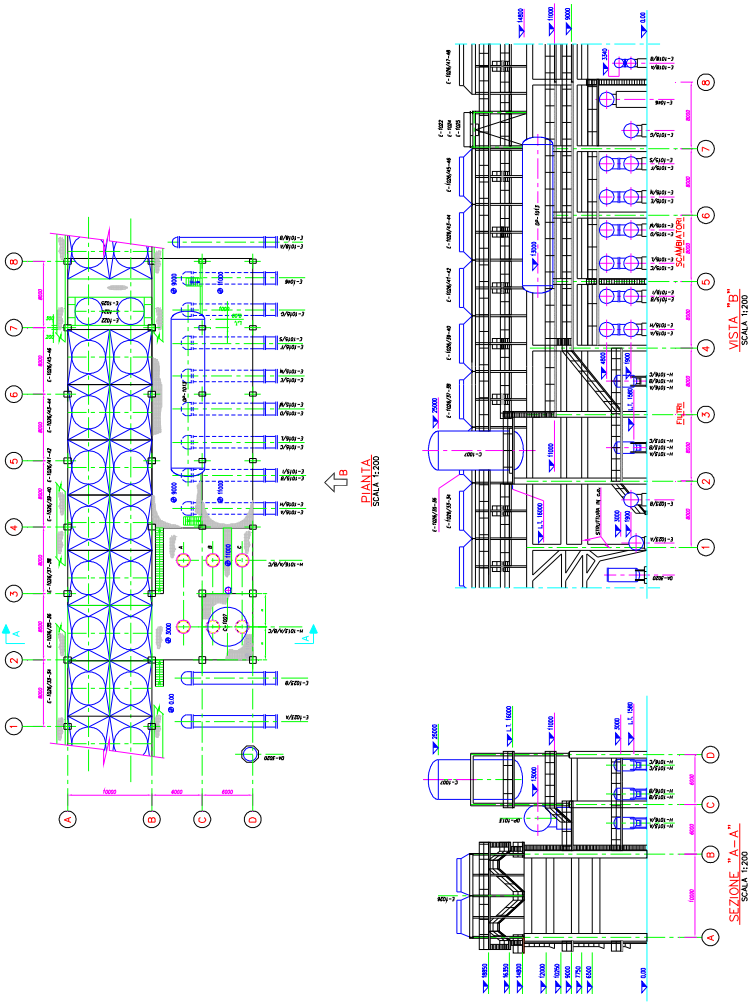

Figure. 3.3: Example of *train of exchanger* used to cool Quench Oil in industrial process.

Quite clearly, economical losses can be consistent for the complexity of system but the evaluation is completely separated from QRA.

As an example, if earthquake causes loss of control of equipment in a dust drier, an internal explosion can occur, thus destroying the entire equipment and often producing catastrophic escalation of events. This incident is not related in any point with the structural damage of equipment due to seismic load, which can be economically not relevant for the single equipment but in turns has allowed the destructive explosion of equipment (because the varied fluid-dynamic conditions of equipment.

Due to the relatively small amount of hazardous materials, environmental issues are not relevant for this class of equipment unless release of toxic dispersion in the atmosphere is considered. However, this issue is included in QRA. For the entire set of equipment, no reference is given to the risk related to the fire and to the combustion product of substances (often toxic) stored in warehouse (either liquid or solid) and ignited for the escalation of primary accidents triggered by earthquake, as it is out of the scope of this study.

The product or the feeding of industrial processes can be stored in *steel tank*s (Figure 3.4 and Figure 3.5), to use it as combustible for furnaces in the example reported above. Liquid storage tanks can be found in many configurations: elevated, ground-based, and underground. Steel ground-based tanks

consist essentially of a steel wall that resists outward liquid pressure, a thin flat bottom plate that prevents liquid from leaking out, and a thin roof plate that protects contents from the atmosphere.

It is common to classify such tanks in two categories depending on support conditions: anchored and unanchored tanks. Anchored tanks must be connected to large foundations to prevent the uplift in the event of earthquake occurrence. However, improperly detailed anchors may damage the shell under seismic loading resulting in a ripped tank bottom. Hence, it is common, particularly for large size tanks, to support the shell on a ring wall foundation with out anchor bolts and to support the bottom plate on a compacted soil though, sometimes, ring walls are omitted.

Based on the orientation of the axis of symmetry, anchored tanks are either horizontal or vertical. Circular vertical tanks made of carbon steel are more numerous than any other type because they are efficient in resisting liquid hydrostatic pressure mostly by membrane stresses, simple in design, and easy in construction.

This type of equipment (*atmospheric liquid fuel storage*) is characterised by the presence of large amount of flammable substance which can be released if seismic wave is able to cause structural damage to the shell or to the auxiliary equipment. Hence, it has to be treated separately with respect to the larger

class of equipment described above, due to its importance and diffusion in the industrial facilities.

To this regard, as it is mandatory, any hazardous substance storage has to be installed within catch basin whose volume is equivalent to the liquid volume contained in the tank.

Moreover, it is good engineering practice to provide several active strategies for prevention and mitigation of accidental releases as foaming, sprinkler, water deluge.

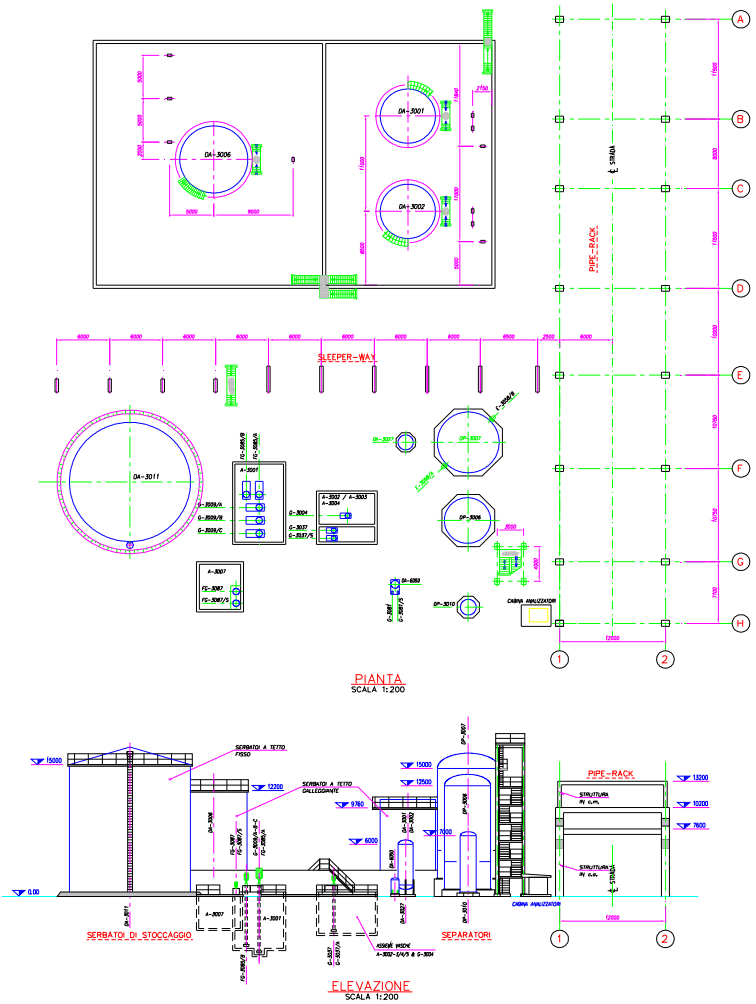

Figure. 3.4: Example of *atmospheric steel storage tank* installation.

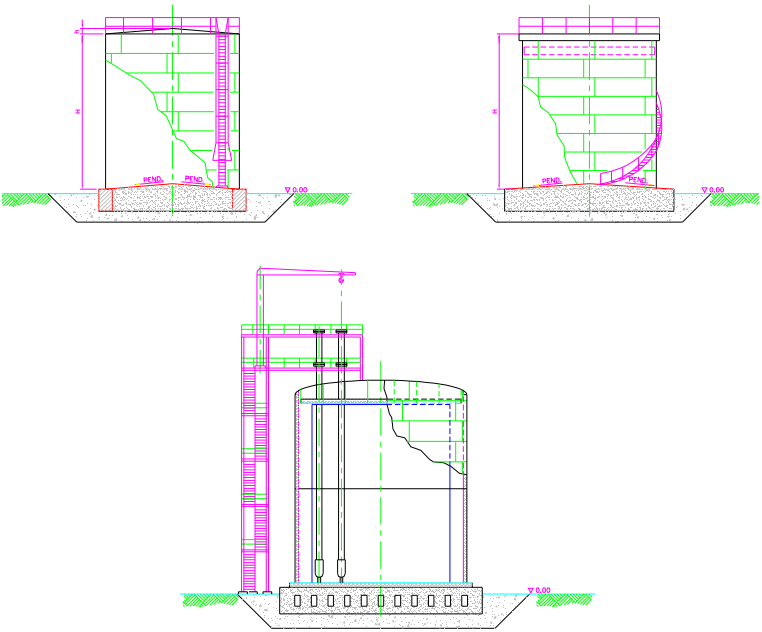

Figure. 3.5: Example of different kind of *atmospheric steel storage tank*.

The evaluation of risks due to the interaction of earthquake with equipment is mainly related to the evaluation of risks produced by structural damage of tank, which can be in turns the basis for evaluation for the economical losses, provided the cost of damage repairs is given. Environmental issues, provided that atmospheric dispersion of vapour has been previously faced, are only related to the dispersion of liquid in surrounding rivers or see. Risk assessment is then related to the evaluation of probability of occurrence of release in water due to the

failure of industrial safety system and mainly to the prediction of the flow rate if multiple tanks are affected by earthquake.

Other equipment usually present in industrial plants are *above-ground pressurised gas and vapour storage system* (Figure 3.6).

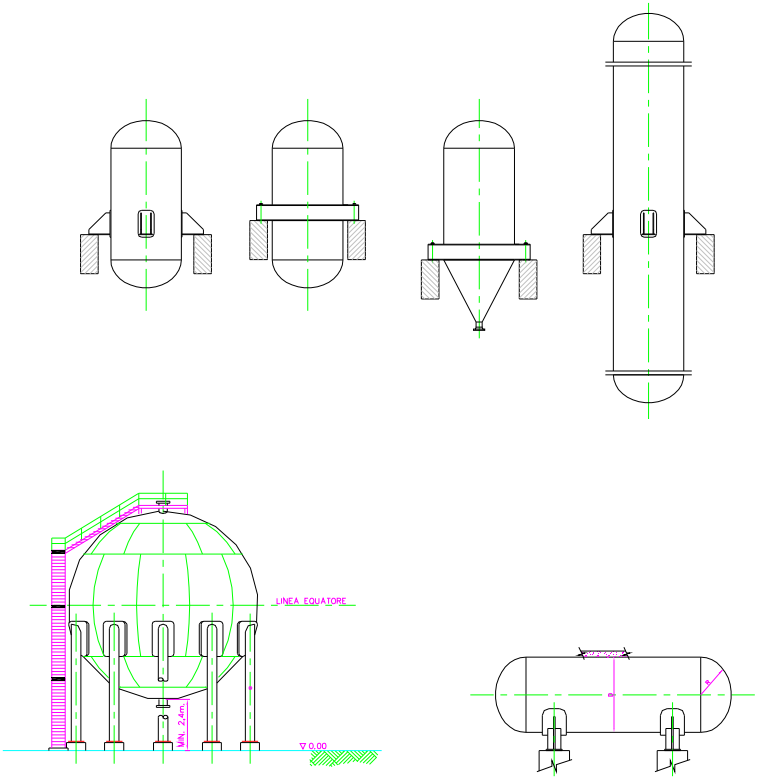

Figure. 3.6: Example of different kind of *pressurised gas and vapour storage system.*

This class of equipment is very common in industry and collects a number of typical units operating either as storage or

as operational unit in production processes. The main difference with the atmospheric tank is related to the possibility of large loss of containment even for very small crack or failure produced by earthquake, as the pressure difference with atmosphere is the main driving force. Risk assessment is related to the entire set of accidental scenario which derives from the release of toxic or flammable gas or vapour. As for atmospheric systems, structural damage is the starting point for the evaluation of release and the entire analysis allows the assessment of cost for repairs and restoring the process.

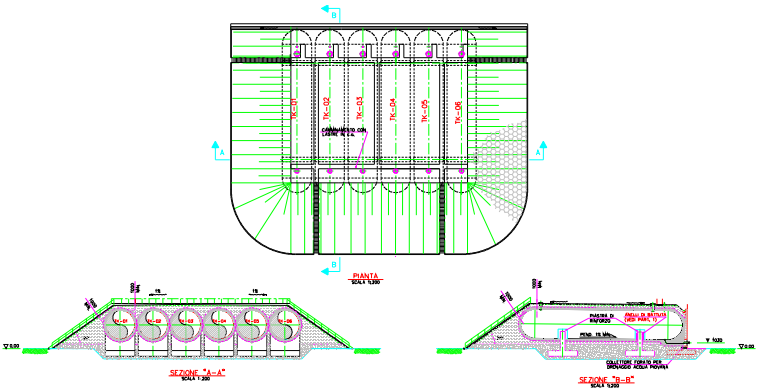

Figure. 3.7: Example of typical installation of *under-ground storage* of GPL.

Due to the hazard of storage tank or reservoir, it is common use to bury or mound storage tanks (Figure 3.7) if possible, in order to avoid any escalation effects in the case of fire, and any damage to the shell of equipment (*Under-ground gas and vapour reservoir or tank*). Moreover, any release is relatively halted by the

presence of soil. Environmental issues are practically absent, unless toxic gases are stored. In this case, however, dispersion analysis, which is necessary for QRA, covers also environmental issues. Economical issues are related to the repairs of system, if affected by earthquake.

Other typical equipment and industrial installation are showed in the following. Figure 3.8 shows an example of vertical storage with different supports configuration.

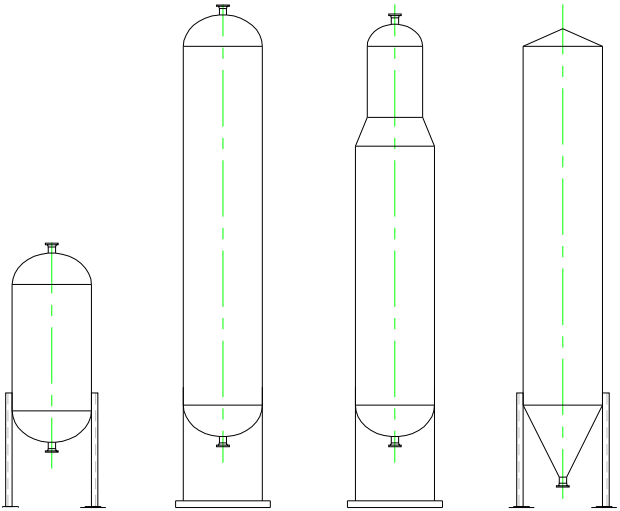

Figure. 3.8: Example of vertical storage with different supports configuration.

Figure 3.9 shows a degasser plant, equipment installed in all industrial power plant in which the production of vapour is

necessary. At the end Figure 3.10 shows and example of typical chemical and pharmaceuticals industrial plant.

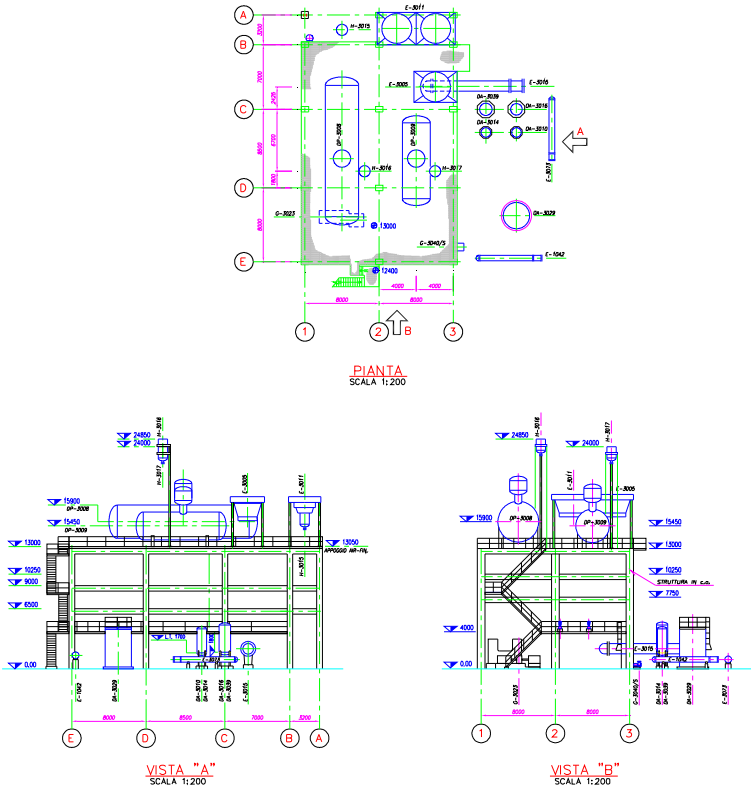

Figure. 3.9: Example of degasser plant.

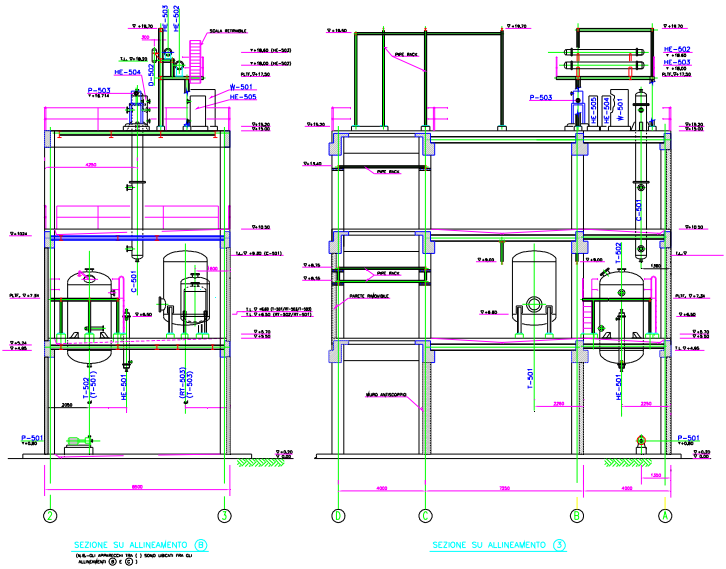

Figure. 3.10: Example of typical chemical and pharmaceuticals industrial plant.

3.2 STRUCTURAL STANDARDIZATION

The above classification of structures located in industrial plants showed the relevance of steel in many applications, especially when pressurised equipments are concerned. Information reported, however, cannot be directly used in the framework of a seismic risk analysis, since critical data cannot be easily found. This is the reason why an effort has been devoted to collect, standardise and report a number of parameters very useful from a seismic perspective.

In particular, steel thickness, properties of materials, connections and masses both at installation and service conditions have been assessed. In the following tables only a reduced number of results can be shown for sake brevity.

HORIZONTAL STEEL TANK								
TANK DIMENSION			MATERIAL: CARBON STEEL PRESSURE MAX 21,8 bar			MATERIAL: STAINLESS STEEL PRESSURE MAX 19,2 bar		
Volume m^3	Diameter m	Height m	Thickness mm	Weight kg	Total Weight kg	Thickness mm	Weight kg	Total Weight kg
1,00	0,8	2,0	5	260	320	4	210	270
2,00	1,0	2,5	5	410	500	4	330	420
3,00	1,2	2,5	5	510	620	4	410	520
4,00	1,2	3,5	5	670	800	5	670	800
5,00	1,3	3,5	6	880	1060	5	730	910
7,50	1,4	4,5	6	1170	1350	6	1170	1350
10,00	1,6	4,5	6	1380	1600	6	1380	1600
15,00	1,8	5,5	6	1850	2130	6	1850	2130
20,00	2,0	6,0	6	2260	2600	7	2640	2980
25,00	2,2	6,0	7	2960	3400	7	2960	3400
30,00	2,4	6,5	7	3500	4030	7	3500	4030
50,00	2,8	8,0	8	5700	6300	8	5700	6300
80,00	3,0	11,0	9	9000	9900	8	8000	8900
100,00	3,2	12,0	10	11200	12300	8	9300	10400

Table 3.1. Summarizing table for horizontal steel tank

ATMOSPHERIC STEEL TANK (FLOATING ROOF)						
TANK DIMENSION			SHELL THICKNESS			
Volume m^3	Diameter m	Height m	Bottom mm	1st Ring mm	Last Ring mm	Total Weight kg
1000	10,97	10,87	7	6	6	44300
2000	14,53	12,19	7	8	6	69600
5000	22,35	12,19	8	11	7	130900
10000	30,48	14,63	8	18	7	244700
25000	45,72	15,24	8	28	8	532100
38000	54,86	15,60	8	34	8	621100
50000	67,06	14,58	8	38	9,5	1049300

Table 3.2. Summarizing table for atmospheric steel tank (Floating roof).

ATMOSPHERIC STEEL TANK (CONIC ROOF)							
TANK DIMENSION			SHELL THICKNESS				
Volume m^3	Diameter m	Height m	Bottom mm	1st Ring mm	Last Ring mm	Roof mm	Total Weight kg
25	2,80	4,00	6	6	5	5	2170
50	3,50	5,50	6	6	5	5	3700
100	4,57	7,31	7	7	5	5	6660
150	4,57	9,14	7	7	5	5	7760
250	6,70	7,31	7	7	5	5	1150
500	7,62	10,97	7	7	5	5	17800
750	10,66	9,14	7	7	5	5	25850
1000	12,19	9,14	7	7	6	5	33100
2000	13,72	14,63	7	8	6	5	52700
5000	24,38	10,97	7	8	7	5	120500
10000	30,48	14,63	7	8	7	5	215000
25000	45,72	15,24	7	8	8	5	483900

Table 3.3. Summarizing table for atmospheric steel tank (Conic roof).

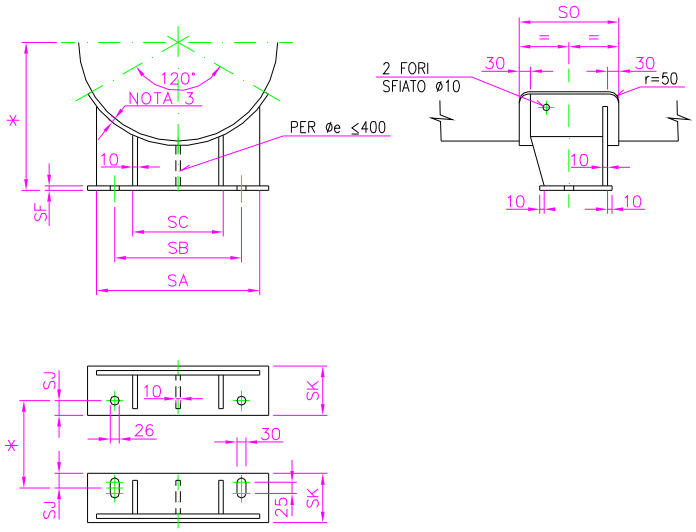

Figure 3.11. Support for horizontal steel tank (Type A).

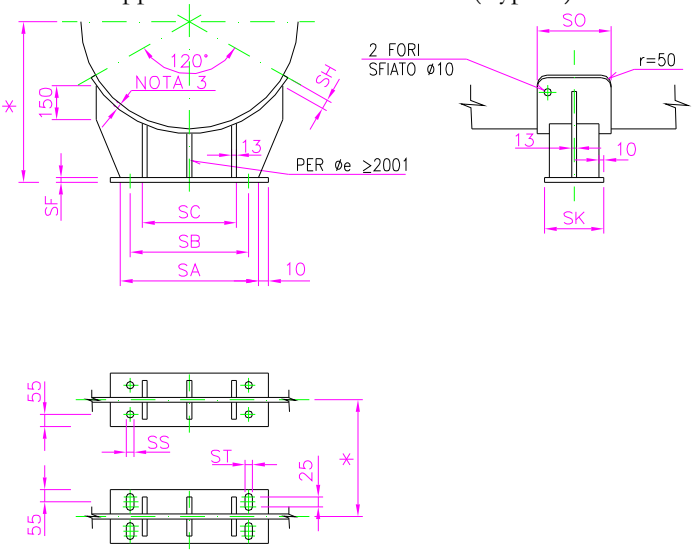

Figure 3.12. Support for horizontal steel tank (Type B).

VERTICAL STEEL TANK

TANK DIMENSION			MATERIAL: CARBON STEEL PRESSURE MAX 21,8 bar			MATERIAL: CARBON STEEL PRESSURE MAX 21,8 bar		
Volume m^3	Diameter m	Height m	Thickness mm	Weight kg	Total Weight kg	Thickness mm	Weight kg	Total Weight kg
1,00	0,90	1,50	5	240	290	4	190	240
2,00	1,10	2,00	5	390	470	4	310	390
3,00	1,20	2,50	6	610	730	4	410	530
4,00	1,30	3,00	6	770	920	5	640	790
5,00	1,40	3,00	6	850	1020	5	700	870
7,50	1,60	3,50	6	1120	1290	5	940	1110
10,00	1,80	3,50	6	1300	1500	5	1100	1300
15,00	2,00	4,50	6	1800	2070	5	1500	1770
20,00	2,20	5,00	7	2560	2950	6	2190	2480
25,00	2,40	5,00	7	2860	3290	6	2450	2880
30,00	2,60	5,50	7	3380	2890	6	2900	3410
50,00	3,00	6,50	8	5240	5770	7	4590	5120
80,00	3,20	9,00	8	7200	7920	7	6300	7000
100,00	3,20	11,50	8	8800	9680	7	7700	8600

Table 3.4. Summarizing table for vertical steel tank.

Diameter	SA	SB	SC	SF	SJ	SK	SO
? 250	180	120	-				
251 ÷ 300	200	140	-	10	50	120	180
301 ÷ 350	250	190	-				
351 ÷ 400	270	210	-				
401 ÷ 450	310	230	130		55	140	210
451 ÷ 500	359	270	170	13			
501 ÷ 550	370	290	190		65	170	250
551 ÷ 600	400	320	220				
601 ÷ 650	470	390	290				
651 ÷ 700	510	430	330				
701 ÷ 750	550	470	370				
751 ÷ 800	570	490	390				
801 ÷ 850	600	520	420	16	80	200	280
851 ÷ 900	640	560	460				
901 ÷ 950	680	600	500				
951 ÷ 1000	710	630	530				
1001 ÷ 1050	750	670	570				

Table 3.5. Summarizing table for support of horizontal steel tank (Figure 3.11).

Diameter	SA	SB	SC	SF	SH	SK	SO	SS	ST
1051 ÷ 1100	590	510	430	16	50	220	320	26	30
1101 ÷ 1150	620	540	460						
1151 ÷ 1200	650	570	490						
1201 ÷ 1300	680	600	520						
1301 ÷ 1400	740	660	580						
1401 ÷ 1500	800	720	640						
1501 ÷ 1600	860	780	700						
1601 ÷ 1700	930	850	740						
1701 ÷ 1800	1000	870	770	19	100	250	380	30	36
1801 ÷ 1900	1060	930	800						
1901 ÷ 2000	1130	1000	870						
2001 ÷ 2100	1200	1070	940						
2101 ÷ 2200	1260	1130	1000						
2201 ÷ 2300	1330	1200	1070						
2301 ÷ 2400	1400	1220	1090						
2401 ÷ 2500	1460	1250	1150						
2501 ÷ 2600	1530	1350	1220						
2601 ÷ 2700	1600	1420	1290						
2701 ÷ 2800	1670	1490	1360						
2801 ÷ 2900	1740	1560	1430						
2901 ÷ 3000	1810	1630	1500						
3001 ÷ 3100	1880	1700	1570						
3101 ÷ 3200	1950	1770	1640						
3201 ÷ 3300	2010	1830	1700						
3301 ÷ 3400	2080	1900	1770						
3401 ÷ 3500	2150	1970	1840						
3501 ÷ 3600	2220	2040	1910						
3601 ÷ 3700	2280	2100	1970						

Table 3.6. Summarizing table for support of horizontal steel tank (Figure 3.12).

CHAPTER 4:

STRUCTURAL DESIGN OF ATMOSPHERIC STORAGE STEEL TANK

4.1 INTRODUCTION

In this section, provisions given in various codes on seismic analysis of tanks are reviewed. As summarized in previous section seismic analysis of liquid storage tanks requires special considerations evaluation of hydrodynamic forces requires suitable modelling and dynamic analysis of tank-liquid system, which is rather complex. The mechanical models used to asses the dynamic behaviour of steel storage tanks, convert the tank-liquid system into an equivalent spring-mass system. Design codes use these mechanical models to evaluate seismic response of tanks. While using such an approach, various other parameters also get associated with the analysis. Some of these parameters are: Pressure distribution on tank wall due to lateral and vertical base excitation, time period of tank in lateral and vertical mode, effect of soil-structure interaction and maximum sloshing wave height. Design Codes have provisions with varying degree of details to suitably evaluate these parameters.

Codes considered are: ACI 350.3 [22], AWWA D-100 [23-24], AWWA D-110 [25-26], API 650[27], Eurocode 8 [28] guidelines. It may be noted that some of these codes deal with only specific types of tanks. Table 4.1 provides details of types of tanks considered in each of these codes. The review will in particular focus on following AWWA D-100, API 650 and Eurocode 8 that are the codes with specific attention on steel tank.

Code	Types of tanks
ACI 350.3	Ground supported circular and rectangular concrete tanks with fixed and flexible base. Pedestal supported elevated tanks.
API 650	Ground supported steel petroleum tanks (Types of base support are not described).
AWWA D-100 & D103	Ground supported steel tanks with fixed and flexible base. Elevated steel tanks with braced frame and pedestal type supporting tower.
AWWA D-110 & D115	Ground supported prestressed concrete tanks with fixed and flexible base.
Eurocode 8	Ground supported circular and rectangular tanks with fixed base. Elevated tanks.

Table 4.1. Types of tanks considered in various codes.

4.2 API 650

The API 650 regulation represents the world reference for storage tank design.

4.2.1 Structural Design

4.2.1.1 Bottom Plate

All bottom plates shall have a minimum nominal thickness of 6 mm exclusive of any corrosion allowance specified by the purchaser for the bottom plates. <unless otherwise agreed the purchaser, all rectangular and sketch plates shall have a minimum nominal width of 1800 mm.

4.2.1.2 Tank Wall

The required shell thickness shall be the greater of the design shell thickness, including any corrosion allowance, or the hydrostatic test shell thickness, but the shell thickness shall not be less than the values shows in table 4.2.

Tank's Diameter [m]	Minimun Thickness [mm]
<15	5
15 ÷ <36	6
36 ÷ 60	8
>60	10

Table 4.2. Minimum thickness of the shell plate according to the API 650

Unless otherwise agreed to by the purchaser, the shell plates shall have a minimum nominal width of 1800 mm. Plates that are to be butt-welded shall be properly squared. The design shell thickness shall be computed on the basis that the tank is filled to a level H with a liquid that has a specific gravity specified by purchaser.

The hydrostatic test shell thickness shall be computed on the basis that the tank is filled to a level H with water. The calculated stress for each shell course shall not be greater than the stress permitted for the particular material used for the course. Not shell course shall be thinner than the course above it.

The tank shell shall be checked for stability against buckling from the design wind velocity, as specified by the purchaser. If required for stability, intermediate girders, increased shell-plate thickness, or both shall be used. If the design wind velocity is not specified, the maximum allowable wind velocity shall be calculated, and the result shall be reported to the purchaser at time of the bid.

The manufacturer shall furnish to the purchaser a drawing that lists the following for each course:

- The required shell thickness for both the design condition (including corrosion allowable) and hydrostatic test condition.
- The nominal thickness used.

- The material specification.
- The Allowable Stress.

The design stress design basis shall be either two-thirds the yield strength or two-fifths the tensile strength, whichever is less. The gross plate thicknesses, including any corrosion allowance, shall be either three-fourths the yield strength or three-sevenths the tensile strength, whichever is less.

4.2.1.2.1 Calculation of Thickness trough 1-Foot Method

The 1-foot method calculates the thicknesses required at design points 0.3 m above the bottom of each shell course. This method shall not be used for tanks larger than 60 m in diameter. The required minimum thickness of shell plates shall to be greater of the values computed by the following formulas:

$$t_d = \frac{4.9D(H-0.3)G}{S_d} + CA\,; \quad t_t = \frac{4.9D(H-0.3)G}{S_t} \qquad (4.1)$$

where:

t_d = design shell thickness, in mm;

t_t = hydrostatic test shell thickness, in mm;

D= nominal tank diameter, in m;

H= design liquid level, in m;

G= design specific gravity of the liquid to be stored, as specified by the purchaser;

CA= corrosion allowable, in mm, as specified by the purchaser;

S_d= allowable stress for design condition, in MPa;

S_t= allowable stress for hydrostatic test condition, in MPa.

4.2.1.2.2 Calculation of Thickness trough Variable-Design-Point

This procedure normally provides a reduction in shell-course thicknesses and total material weight, but more important is its potential to permit construction of larger diameter tanks within the maximum plate thickness limitation.

Design by the variable-design-point method give shell thicknesses at design points that result in calculated stress being relatively close to the actual circumferential shell stresses. This method may only be used when the purchaser has not specified that 1-foot method be used and when the following is true:

$$\frac{L}{H} \leq \frac{1000}{6} \tag{4.2}$$

where:

$L=(500\ D\ t)^{0.5}$, in mm;

D= tank diameter, in m;

t= bottom-course shell thickness, in mm;

H= maximum design liquid level, in m.

The minimum plate thickness for both the design condition and the hydrostatic test condition shall be determined as

outlined. Complete, independent calculations shall be made for all of the courses for the design condition, exclusive of any corrosion allowance, and for the hydrostatic test condition. The required shell thickness for each course shall be the greater of the design shell thickness plus any corrosion allowance or the hydrostatic test shell thickness. When a greater thickness is used for a shell course, the greater thickness may be used for subsequent calculations of the thicknesses of the shell courses above the course that as greater thickness, provided the greater thickness is shown as the required design thickness on the manufacturer's drawing.

To calculate the bottom-course thickness, preliminary values t_{pd} and t_{pt} for the design and the hydrostatic test condition shall first be calculated with the formulas provided in one-foot method.

The bottom-course thicknesses t_{1d} and t_{1t} for the design and the hydrostatic test conditions shall be calculated using the following formulas:

$$t_{1d} = \left(1.06 - \frac{0.463D}{H}\sqrt{\frac{HG}{S_d}}\right)\left(\frac{2.6HDG}{S_d}\right) + CA \qquad (4.3)$$

$$t_{1t} = \left(1.06 - \frac{0.463D}{H}\sqrt{\frac{H}{S_t}}\right)\left(\frac{2.6HD}{S_t}\right) \qquad (4.4)$$

Note: for design conditions t_{1d} need not be greater than t_{pd}; for hydrostatic testing conditions t_{1t} need not be greater than t_{pt}.

To calculate the second-course thicknesses for both the design condition and the hydrostatic test condition, the value of the following ratio shall be calculated for the bottom course:

$$r = \frac{h_1}{\sqrt{rt_1}} \tag{4.5}$$

where:

h_1= height of the bottom shell course, in mm;

r= nominal radius of the tank, in m;

t_1= actual thickness of the bottom shell course, less any thickness added for corrosion allowance, in mm, used to calculate t_2 (design). The total thickness of the bottom shell course shall be used to calculate t_2 (hydrostatic test).

If the value of the ratio (equation 4.5) is less than or equal to 1.375,

$$t_2 = t_1 \tag{4.6}$$

If the value of the ratio (equation 4.5) is greater than or equal to 2.625,

$$t_2 = t_{2a} \tag{4.7}$$

If the value of the ratio (equation 4.5) is greater than 1.375 but less than 2.625,

$$t_2 = t_{2a} + (t_1 - t_{2a})[2.1 - \frac{h_1}{1.25\sqrt{rt_1}}] \quad (4.8)$$

where:

t_2 = minimum design thickness of the second shell course excluding any corrosion allowance, in mm;

t_{2a} = thickness of the second shell course, in mm.

The preceding formula for t_2 is based on the same allowable stress being used for the design of the bottom and second courses. For tanks where the value of the ratio is greater than or equal to 2.625, the allowable stress for the second course may be lower than the allowable stress for the bottom course when the methods preceding methods are used.

To calculate the upper-course thicknesses for both the design condition and the hydrostatic test condition, a preliminary value t_u for the upper-course thickness shall be calculated using the formula 4.1, and then be the distance x of the variable design point from the bottom of the course shall be calculated using the lowest value obtained from the following:

$$x_1 = 0.61\sqrt{rt_1} + 320CH ;$$

$$x_2 = 1000CH ;$$

$$x_3 = 1.22\sqrt{rt_1} \quad (4.9)$$

where:

t_u= thickness of the upper corse at the girth joint, in mm;

$C = [k^{0.5}(K-1)]/(1+k^{1.5})$;

$K = t_L / t_u$;

t_L= thickness of the lower course at the girth joint, in mm;

H = design liquid level, in m.

The minimum thickness t_x for the upper shell courses shall be calculated for both the design condition (t_{dx}) and the hydrostatic test condition (t_{tx}) using the minimum value of x obtained from 4.9:

$$t_{dx} = \frac{2.6D(H-\frac{x}{12})G}{S_d} + CA$$
$$t_{tx} = \frac{2.6D(H-\frac{x}{12})G}{S_t} \qquad (4.10)$$

The steps described shall be repeated using the calculated value of t_x as t_u until there is little difference between the calculated values of t_x in succession (repeating the steps twice is normally sufficient). Repeating the steps provides a more exact location of the design point for the course under consideration and, consequently, a more accurate shell thickness.

4.2.1.2.3 Calculation of Thickness trough Elastic Analysis

For tanks where L/H is greater than 2, the selection of shell thicknesses shall be based on an elastic analysis that shows the calculated circumferential shell stresses to be below the allowable stresses given in table form. The boundary conditions for the analysis shall assume a fully plastic moment caused by yielding of the plate beneath the shell and zero radial growth.

4.2.1.3 Roof

The following definitions apply to roof (Figure 4.1) but shell not be considered as limiting the type of roof permitted:

- A supported cone roof is a roof formed to approximately the surface of a right cone that is supported principally either by after on griders and columns or by rafters on trusses with or without columns.
- A self-supporting cone roof is a roof formed to approximately the surface of a right cone that is supported only at its periphery.
- A self-supporting dome roof is a roof formed to approximately a spherical surface that is supported only at its periphery.
- A self-supporting umbrella roof is modified dome roof formed so that any horizontal section is a

regular polygon with as many sides as there are roof plates that is supported only at its periphery.

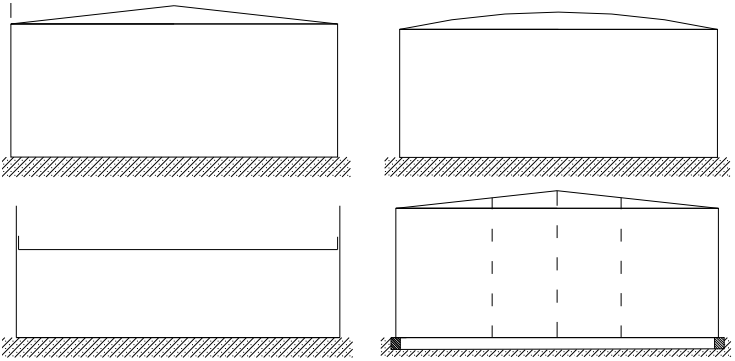

Figure 4.1. Different types of roof.

All roofs and supporting structures shall be designed to support dead load plus a uniform live load of not less than 1.2 kPa of projected area.

Roof plates shall have a minimum nominal thickness of 5 mm. Thicker roof plates may be required for self-supporting roofs. Any required corrosion allowance for the plates of self – supporting roofs shall be added to the calculated thickness unless otherwise specified by the purchaser. Any corrosion allowance for the plates of supported roofs shall be added to the minimum nominal thickness.

Roof plates of supported cone roofs shall not be attached to the supporting members.

All internal and external structural members shall have a minimum nominal thickness of 4.3 mm in any component. The

method of providing a corrosion allowance, if any, for the structural members shall be a matter of agreement between the purchaser and the manufacturer.

For supported cone roofs the slope of the roof shall be 19 mm in 30 mm or greater if specified by the purchaser. If the rafters are set directly on chord girders, producing slightly varing rafter slopes, the slope of the flattest rafter shall conform to the specified or order roof slope.

Roof columns shall be made from structural shapes, or steel pipe may be used subject to the approval of the purchaser. When pipe is used, it must be sealed, or provisions for draining and venting must be made at the purchaser's option.

Self-supporting roofs whose roof plates are stiffened by sections welded to the plates need not conform to the minimum thickness requirements, but the thickness of the roof plates shall not be less than 5 mm when so designed by the manufacturer, subject to the approval of the purchaser.

Self-supporting cone roofs shall conform to the following requirements: $\theta \le 37° ; \theta \ge 9.5°$ (slope 9:12; slope 2:12); minimum thickness = $\frac{D}{4.8 \cdot \sin\theta} \ge 5mm$; maximum thickness = 12.5 mm, exclusive of corrosion allowance.

Where:

θ= angle of the cone elements to the horizontal, in degrees;

D= nominal diameter of tank shell, in m.

The participating area at the roof-to-shell junction shall be equal or exceed the following:

$$\frac{D^2}{0.432\sin\theta} \tag{4.11}$$

Where:

θ= angle of the cone elements to the horizontal, in degrees;

D= nominal diameter of tank shell, in m.

The area calculated from the expression above is based on the nominal material thickness less any corrosion allowance.

Self-supporting dome and umbrella roofs shall conform to the following requirements:

- Minimum radius= 0.8D (unless otherwise specified by the purchaser);
- Maximum radius= 1.2D;
- Minimum thickness= $r_r/2.4$+C.A. $\geq$ 5mm (r_r =roof radium, in m; D =nominal tank diameter, in m)
- Maximum thickness= 1.25 mm, exclusive of corrosion allowance.

The participating area, in mm^2, at the roof-to-shell junction shall be equal or exceed following:

$$\frac{D \cdot r_r}{0.216} \tag{4.12}$$

The area calculated from the expression above is based on the nominal material thickness less any corrosion allowance.

4.2.1.4 Wind Load (Overturnig Stability)

When specified by the purchaser, overturning stability shall be calculated using the following procedure: The wind load or pressure shall be assumed to be 1.4 kPa on vertical plane surfaces, 0.86 kPa on projected areas of cylindrical surfaces, and 0.72 kPa on projected areas of conical and double-curved surfaces. These wind pressure are based on a wind velocity 160 km/h. For structures designed for wind velocities (V) other than 160 km/h, the wind loads specified above shall be adjusted in proportion to the following ratio:

$$\left(\frac{V}{160}\right)^2 \tag{4.13}$$

For unanchored tank, the overturning moment from wind pressure shall not exceed two-thirds of the dead-load resisting moment, excluding any tank contents, and shall calculated as follows:

$$M \leq \frac{2}{3}\left(\frac{WD}{2}\right) \tag{4.14}$$

where:

M = overturning moment from wind pressure, Nm;

W = shell weight available to resist uplift, less any corrosion allowance, plus dead weight supported by the shell minus simultaneous uplift from operating, conditions such as internal pressure on the roof, in N;
D =tank diameter, in m.

4.2.1 Seismic Design

This section provides minimum requirements that may be specified by the purchaser for the design of storage tanks subject to seismic load. These requirements represent accepted practice for application to flat-bottom tanks; however, other procedures and applicable factors or additional requirements may be specified by purchaser or jurisdictional authorities. Any deviation from the requirements of this section must be by agreement between the purchaser and the manufacturer.

The design procedure considers two response modes for the tank and its contents:

- The relatively high-frequency amplified response to lateral round motion of the tank shell and roof, together with the portion of the liquid contents that moves in unison with the shell.
- The relatively low-frequency amplified response of the portion of the liquid contents that moves on the fundamental sloshing mode.

The design requires the determination of the hydrodynamic mass associated with each mode and the lateral force and overturning moment applied to the shell as a result of the response of the masses to lateral ground motion. Provisions are included to assure stability of the tank shell with respect to overturning and to preclude buckling of the tank shell as a result of longitudinal compression.

This section has no provisions for determining the increased hoop tension that would result from earthquake motion. The increased hoop tension, correctly calculated from the lateral force coefficients specified in this section, would not increase the hoop stresses above a generally acceptable stress level that could be used for seismic design of the tank shell.

The overturning moment due to seismic forces applied to the bottom of the shell be determined as follows:

$$M = ZI\left[C_1\left(W_s X_s + W_r H_t + W_1 X_1\right) + C_2 W_2 X_2\right] \qquad (4.15)$$

Where:

M = overturning moment applied to the bottom of the tank shell, in Nm;

Z = seismic zone factor (horizontal seismic acceleration) as determined by the purchaser or the appropriate government authority that has jurisdiction;

I = importance factor;

C_1,C_2 = lateral earthquake force coefficients;

W_s = total weight of the tank, in N;

X_s = height from the bottom of the tank shell to the shell's center of gravity, in m;

W_r = total weight of the tank roof plus a portion of the snow load, if any, specified by the purchaser, in N;

H_t = total height of the tank shell, in m;

W_1 = weight of the effective mass of the tank contents;

X_1 = height from the bottom of the tank shell to the centroid of lateral seismic force applied to W_1 , in m;

W_2 = weight of the effective mass of the tank contents that move in the first sloshing mode, in N;

X_2 = height from the bottom of the tank shell to the centroid of lateral seismic force applied to W_2 , in m.

The effective masses W_1 and W_2 may be determined by multiplying W_T by ratio W_1/W_T and W_2/W_T, respectively, obtained from Figure 4.2 for the ratio D/H.

Where:

W_T = total weight of the tank contents, in N;

D = nominal tank diameter, in m;

H = maximum design liquid level, in m.

The heights from the bottom of the tank shell to the centroids of the lateral seismic forces applied to W_1 and W_2 , X_1 and X_2, may be determined by multiplying H by the ratios X_1/H and X_2/H, respectively, obtained from Figure 4.3 for the ratio D/H.

The lateral force coefficient C_1 shall be less 0.60 unless the product ZIC_1 and the product ZIC_2 are determined.

The lateral force coefficient C_2 shall be determined as a function of the natural period of the first sloshing mode, T, and the soil conditions at the tank. When T is less than or equal to 4.5:

$$C_2 = \frac{0.75S}{T} \tag{4.16}$$

When T is greater than 0.45:

$$C_2 = \frac{3.375S}{T^2} \tag{4.17}$$

where:

S = site coefficient;

T =natural period of the first sloshing mode, in seconds. T may be determined from the following equation:

$$T = 1.81k\left(D^{0.5}\right) \tag{4.18}$$

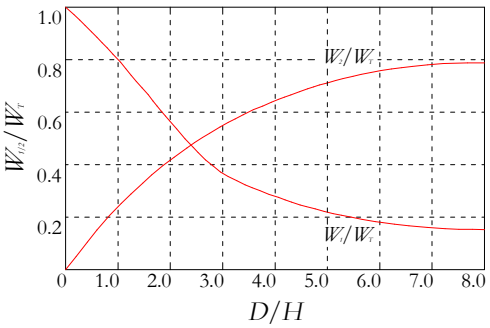

Figure 4.2. Effective masses according to API 650.

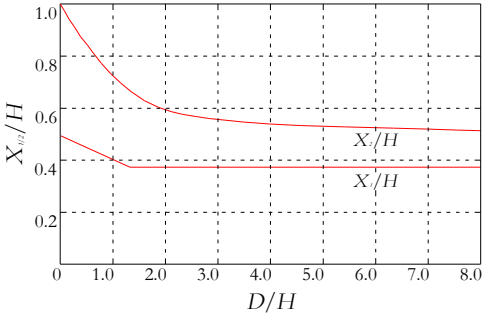

Figure 4.3. Centroids of Seismic Forces according to API 650.

Unanchored Tanks:

For unanchored tanks, the maximum longitudinal compressive force at the bottom of the shell may be determined as follows:

when $\frac{M}{D^2\left(w_t + w_L\right)} \le 0.785$

$$b = w_t + \frac{1.273M}{D^2} \tag{4.19}$$

when $0.785 < \frac{M}{D^2\left(w_t + w_L\right)} \le 1.5$, b may be computed by diagram shows in Figure 4.4.

When $1.5 < \frac{M}{D^2\left(w_t + w_L\right)} \le 1.57$:

$$\frac{b + w_L}{w_t + w_L} = \frac{1.490}{\left[1 - \frac{0.637M}{D^2(w_t + w_L)}\right]^{0.5}} \tag{4.20}$$

where:

w_t =weight of the tank shell and the portion of the fixed roof supported by the shell, in Nm of shell circumference;

w_L =maximum weight of the tank contents that may be used to resist the shell overturning moment, in N/m of shell circumference, $w_L = 98.9 t_b \sqrt{F_{by} HG}$ (t_b =thickness of the bottom plate under the shell, in mm; F_{by} =minimum specified yield strength of the bottom plate under the shell, in MPa; G =design specified gravity of the liquid to be stored, as specified by the purchaser; H =maximum design liquid level, m; D =nominal tank diameter, in m);

b =maximum longitudinal compressive force at the bottom shell, in N/m of shell circumference.

When $M/\left[D^2\left(w_t + w_L\right)\right]$ is greater than 1.57 or when $b/[1000t]$ is greater than F_a, the tank is structurally unstable.

Anchored Tanks:

For anchored tanks, the maximum longitudinal compressive force at the bottom of the shell may be determined as follows:

$$b = w_t + \frac{1.273M}{D^2} \tag{4.21}$$

The maximum longitudinal compressive stress in the shell, $b/1000t$, shall not exceed the maximum allowable stress, F_a, determined by the following formulas for F_a, which take into account the effect of internal pressure due to the liquid contents. When GHD^2/t^2 is greater than or equal to 44:

$$F_a = \frac{83t}{D} \text{ [Mpa]} \tag{4.22}$$

When GHD^2/t^2 is less than 44:

$$F_a = \frac{83y}{2.5D} + 7.5\sqrt{GH} \text{ [Mpa]} \tag{4.23}$$

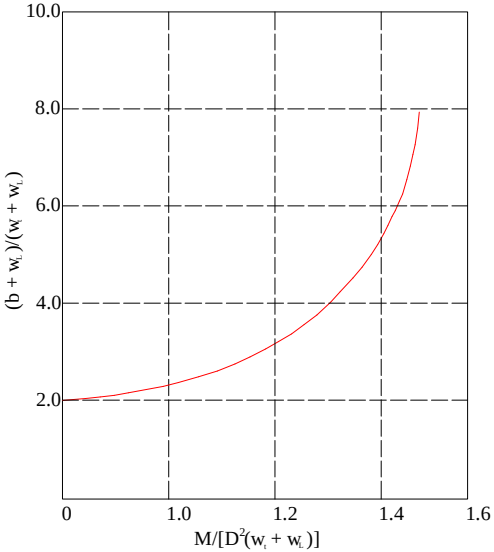

Figure 4.4. Compression Force *b*.

However F_a shall not be greater than F_{by}. If the thickness of the lower shell course calculated to resist the seismic overturning moments is greater than the thickness required for hydrostatic pressure, both excluding any corrosion allowable, then the calculated thickness of each upper shell course for hydrostatic pressure shall be increased in same proportion, unless a special analysis is made to determine the seismic overturning moment and corresponding stresses at the bottom of each upper shell course.

4.3 AWWA D 100-96

American Water Works Association is a code to the design and construction of welded steel tanks for the storage of water, but are also considered standard code for the containment structures for fuel oils. In this section only instructions for the design of atmospheric tanks on the ground are considered, such as neglecting those in elevation and the criteria for design details such as openings in tanks, which go beyond the scope of this thesis. The method adopted is that of allowable stress.

4.3.1 Structural Design

The following loads shall be considered in the design of tank structures and foundations:

- Dead load: dead load shall be the estimated weight of all permanent construction. The unit weights used shall be 7850 kg/m3 for steel and 2310 kg/m3 for concrete.
- Water load: water load shall be the weight of all of the water when the tank is filled to the TCL. The unit weight of water used for water shall be 1000 kg/m3. The weight of water in a wet riser, which is supported directly on foundations, shall not be considered a vertical load on the riser.

- Roof design loads:
    - Design snow load: The allowance for the pressure resulting from the design snow load shall be a minimum of 1205 N/m^2 on the horizontal projection of the tank and external balcony for roof surfaces having a slope of 30° , or less, with the horizontal. For roof surfaces with greater slope, the design snow load allowance may be reduced when the tank is located where the lowest one-day mean low temperature is 5°F (-15°C), or warmer, and local experience indicates that a smaller load may be used.

- The minimum roof design load shall be 720 N/m^2 . The roof plates may deflect between structural supports under design load.
- Wind load:

$$P_w = 1436 \cdot 0.6\left(\frac{v}{45}\right)^2 \ [N/m^2] \qquad (4.24)$$

Where:

P_w = the wind pressure

v = the actual wind velocity; however the value of wind velocity is not be less than 45 m/s;

- Balcony and ladder load: A vertical load (and only one such load in each case) shall be applied as follows: 454 kg to any $0.93m^2$ area on the balcony floor, 454 kg to each platform, 227 kg to any 0.93 m^2 area on the tank roof, and 159 kg on each vertical section of the ladder. All structural parts and connections shall be proportioned properly to withstand such loads. The previously mentioned load need not be combined with the design snow load before referred., but it shall be combined with the dead load. The balcony, platform, and roof plating may deflect between structural supports in order to support the loading.

4.3.1.1 Tank Wall

The shell plates shall always be formed in accordance with the following expression:

$$t = \frac{4.9 h_p D G}{sE} \tag{4.25}$$

where h_p is the height of liquid from top capacity level to the bottom of the shell course being designed, in m; D is the nominal tank diameter, in m; s is the allowable design stress, in N/m^2 and E is the joint efficiency (minus then 1 as described below).

4.3.1.2 Anchorage

The minimum recommended bolt diameter is 31.8 mm for anchor bolts exposed to weather. Smaller anchor bolts may be used, provided consideration is given to possible corrosion. The maximum anchor bolt spacing shall be 10 ft. 0 in. Foundation anchor bolts may be either upset or not upset. They shall be proportioned for the design uplift, using the area at the root of the thread or the not upset bolt diameter, whichever is smaller. The allowable stress is the lesser value of 0.4 times the yield stress or 0.25 times the tensile strength. Foundation anchor bolts may extend to within 3 in. of the bottom of the pier or footing , but not necessarily more than required to develop the anchorage design loads, and shall terminate in a right-angle hook, bend, nut, or washer plate. The anchorage design load

shall be the greater value of the wind uplift force or the lesser of four times the seismic uplift force or the bolt yield capacity. For an unanchored tank, the overturning moment from wind pressure shall not exceed two-thirds of the dead load resisting moment , excluding any tank contents, and shall be calculated as follows:

$$M \le \frac{2}{3}\left(\frac{WD}{2}\right) \tag{4.26}$$

Where M is the overturning moment from wind pressure, W is the shell weight plus roof dead-load reaction on shell available to resist uplift, less any corrosion allowance, minus simultaneous uplift from operating conditions, such as internal pressure on the roof, and D is the nominal tank diameter.

If the overturning moment is greater than two-thirds the resisting forces, then anchors must be used.

In this case the design tension load per anchor shall be calculated as follows:

$$P_B = 4\left(\frac{M}{Nd}\right) - \frac{W}{N} \tag{4.27}$$

Where P_B is design tension load per anchor; d is diameter of anchor circle; N is number of anchors; M and W are defined as previously specified.

Corrosion Allowance

Careful considerations shall be given by the purchaser to the proper allowance for corrosion. This allowance will depend on the corrosive nature of the stored water, the proximity of the tank to salt water or other causes of atmospheric corrosion, ad the care with which the paint or other protection will be maintained. If corrosion allowance is desired, the purchaser shall specify the allowance for parts that will be in contact with water. The corrosion allowance specified by the purchaser is to be added to the required thickness determined by design, and to the minimum thicknesses specified by rules, unless otherwise specified by the purchaser. The corrosion allowance for beams and channels need only be added to the webs and not to the flanges. Corrosion allowance on structural sections shall be clearly specified per surface or total per web.

Minimum Thickness

The minimum thickness for any part of the structure shall be 4.76 mm for parts not in contact with water, except that the minimum thickness of roof plates for ground-supported tanks with cone roofs may be 4.55 mm. The minimum thickness for parts other than cylindrical shell plates that will be in contact with water when the tank is full shall be 6.35 mm except that double butt-welded knuckles in ground-supported tanks less than 14.6 m in height and not greater than 15.2 m in diameter may be 4.76 mm. The minimum thickness for tubular columns

and tubular struts shall be 6.35 mm. The controlling thickness of rolled shapes for the purposes of the foregoing stipulations shall be taken as the mean thickness of the flanges , regardless of web thickness. Bars used for wind bracing shall have a minimum diameter of 19 mm. Other shapes, if used, shall have a total net area at least equal to 19 mm round bar. Cylindrical shell plates in contact with water shall have minimum thickness that changes with the diameter and takes value in the range from 4.75 mm (for tanks with nominal diameter lesser than 6.1m) to 9.52 mm (for tanks with nominal diameter greater than 61m).

4.3.1.3 Welding

Welded structural joints shall be proportioned so that the stresses on a section through the throat of the weld, exclusive of weld reinforcement, do not exceed the appropriate percentage of the allowable tensile working stress of the structural material joined. This percentage is calculated taking into account welding' s working conditions.

4.3.1.4 Foundation

Flat-bottom tanks shall be supported on a ringwall, footing, concrete slab, or structurally compacted granular berm, with or without concrete or steel retainer rings, as specified by the purchaser. The tank that require anchor bolts shall be supported on a ringwall or a concrete slab.

Foundations for flat-bottom tanks shall be one of the following types:

- Tanks supported on a ringwall footing.
- Tanks supported on a concrete slab.
- Tanks within ringwalls: tanks may be placed on a sand cushion within a concrete ringwall. The cushion base shall consist of a minimum of 152 mm cushion of clean sand or fine crushed stone saturated with a heavy-base petroleum oil unless preclude by environmental requirements as discussed above.
- Tanks supported on granular berms.
- Tanks supported on granular berms with steel retainer rings.

The tops of concrete foundations shall be a minimum of 152 mm above the finished grade, unless specified otherwise by the purchaser. The foundation shall be graded to slope uniformly upward to the center of the tank. A slope of 25 mm vertical to 3.00 m horizontal is suggested as a minimum. The minimum depth of foundation shall be 300 mm. If a pile-supported foundation is required, the purchaser shall by specified the pile type and depth existing grade to be used for bidding and design capacities for live and dead loads, combined with wind or seismic loads, or both.

4.3.1.4 Seismic Design

The seismic design of ground-supported tanks recognizes the reduction in seismic load due to the sloshing of the contained liquid. Anchored tanks could be susceptible to tearing of the shell if anchorage is not properly designed. Care must be taken to ensure that anchor bolt attachments are stronger than the anchor bolt. Experience shows that properly designed anchored tanks retain greater reserve strength to seismic overload than unanchored tanks. Anchorage shall be designed such that anchor bolts yield before the shell attachment fails.

Seismic resistance of unanchored tank is related to the height to diameter ratio of the structure. The Figure 4.5 shows the relative seismic resistance of typical unanchored tanks. For tanks having a combination of dimensions and horizontal accelerations falling below the given tank diameter limit line shown in Figure 4.5, seismic analysis of the shell and bottom may be omitted unless vertical acceleration is specified. Vertical acceleration causes an increase in the apparent density of the water stored in the tank, thus increasing tensile hoop stress.

The effective mass procedure considers two response modes of the tank and its contents:

- The high-frequency amplified response to lateral ground motion of the tank shell and roof together with a portion of the liquid contents that moves in unison with the shell, and

The low-frequency amplified response of a portion of the liquid contents in the fundamental sloshing mode.

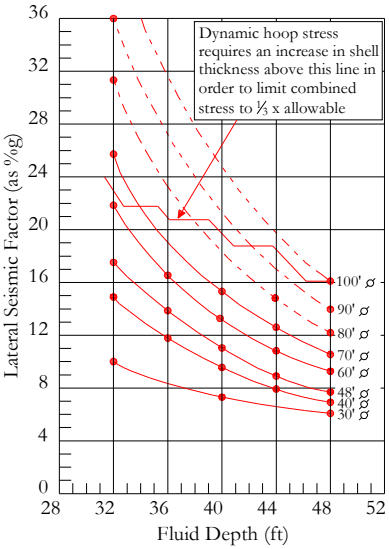

Figure 4.5. Relative seismic resistance of typical unanchored flat-bottom tanks.

The design requires the determination of the hydrodynamic mass associated with each mode and the lateral force and overturning moment applied to the shell resulting from the response of the mass to lateral ground motion.

The base shear and overturning moment due to seismic forces applied to the bottom of the shell shall be determined in accordance with the following formulas.

Base Shear

$$V = \frac{18ZI}{R_w}\left[0.14\left(W_s + W_r + W_f + W_1\right) + SC_1W_2\right] \quad (4.28)$$

where:

V = lateral base shear;

Z = seismic zone coefficient;

I = use factor;

R_w = force reduction coefficient;

W_s = total weight of tank shell and significant appurtenances;

W_r = the total weight of tank roof plus permanent loads;

W_f = total weight of bottom;

W_1 = the total weight of effective mass of tank contents that moves in unison with the tank shell;

S = the site amplification factor;

W_2 = the weight of effective mass of the first mode sloshing contents of the tank;

C_1 is determined as follows:

For the condition where $T_w < 4.5$:

$$C_1 = \frac{1}{6T_w} \quad (4.29)$$

For the condition where $T_w \geq 4.5$:

$$C_1 = \frac{0.85}{T_w^2} \tag{4.30}$$

In the equations 4.29 and 4.30 T_w represent the first mode sloshing wave, in seconds, which is determined by equation 4.31.

$$T_w = K_p D^{1/2} \tag{4.31}$$

The coefficient K_p presents in the equation 4.31 shall be determined using the Figure 4.6.

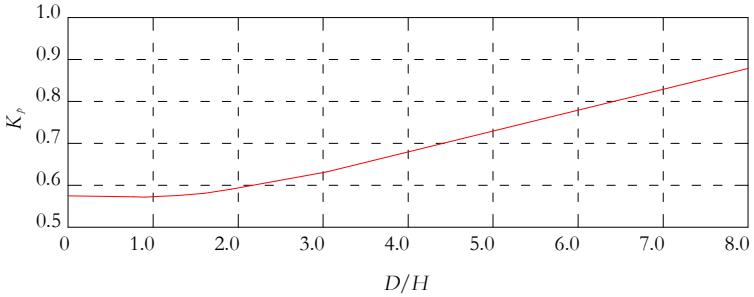

Figure 4.6. Curve for obtaining factor K_p.

Overturning Moment:

$$M = \frac{18ZI}{R_w}\left[0.14\left(W_s X_s + W_r H_t + W_1 X_1\right) + SC_1 W_2 X_2\right] \tag{4.32}$$

where:

M = overturning moment applied to the bottom of the tank shell;

X_s = height from the bottom of the tank shell to center of gravity of the shell;

H_t = total height of the tank shell;

X_1 = height from the bottom of the tank shell to the centroid of lateral seismic force applied to W_1;

X_2 = height from the bottom of the tank shell to the centroid of lateral seismic force applied to W_2;

The weight of the effective mass of the tank contents, which moves in unison with the tank shell W_1, and the weight of the effective mass of the first mode sloshing contents W_2 may be determined by multiplying W_T by the ratio W_1/W_T and W_2/W_T, respectively, obtained from Figure 4.7 for the ratio D/H.

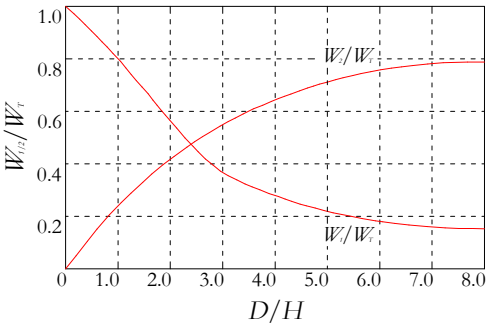

Figure 4.7. Effective masses according to AWWA D100-96.

The heights X_1 and X_2 from the bottom of the tank shell to the centroids of the lateral seismic forces applied to W_1 and

W_2 may be determined by multiplying H by ratio D/H and D/H, respectively obtained by Figure 4.8.

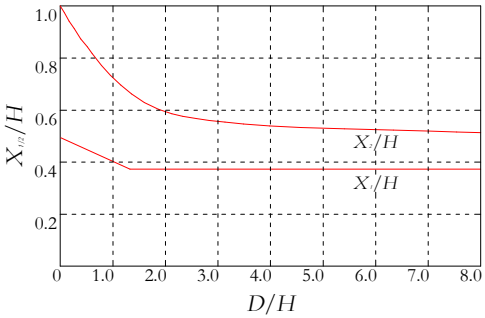

Figure 4.8. Centroids of Seismic Forces.

Where response spectra are used, the accelerations of two masses shall replace the seismic coefficient as follows:

$$\frac{A_i}{R_F} \text{ replaces } 0.14\frac{18ZI}{R_w} \tag{4.33}$$

$$\frac{A_c}{R_F} \text{ replaces } \frac{18ZIC_1S}{R_w} \tag{4.34}$$

where:

A_i = spectral acceleration of impulsive mass;

A_c = spectral acceleration of convective mass;

R_F = reduction factor;

A 2-percent damped curve is recommended for determining acceleration of a structure and a 0.5-percent damped curve is

recommended for determining acceleration of the sloshing liquid. Scaling down a site-specific response spectra is appropriate for ductile modes of failure such as hoop tension, and nonductilite buckling such as the elephant foot buckle at the base of ground-supported tanks. Buckling loads that may result in total collapse of the structure shall not be scaled down. Scaling down will depend on the return period of the earthquake used to generate the response spectra. A reduction factor R_F of 2.5 shall be used for ground motion with mean recurrence interval of 10000 years. Where information is not available to determine a recurrence level accurately, the maximum credible ground motion based on seismology, geology, and seismic and geologic history of the site may be used to determine a site-specific response spectra. For lower-recurrence spectra, the spectra may be scaled down.

Resistance to the overturning moment at the bottom of the shell may be provided by the weight of the tank shell, weight of roof reaction on shell W_{rs}, and by the weight of a portion of the tank contents adjacent to the shell for unanchored tanks or by anchorage of the tank shell. For unanchored tanks, the portion of the contents that may be used to resist overturning is dependent on the width of the bottom annulus. The annulus may be a separate ring or an extension of the bottom plate if the required thickness does not exceed the bottom thickness.

The weight of annulus that lifts off the foundation shall be determined by formula:

$$w_L = 98.9 t_b \sqrt{\sigma_y HG} \ \ [\mathrm{N/m}] \tag{4.35}$$

where:

w_L = maximum weight of tank contents that may be used to resist the shell overturning moment;

t_b = thickness of the bottom annulus;

σ_y = minimum specified yield strength of bottom annuls;

H = maximum depth of water;

D = tank diameter;

G = specific gravity of liquid;

The maximum longitudinal shell compression stress at the bottom of the shell when there is no uplift shall be determined by formula:

$$\sigma_c = \left(w_t + \frac{1{,}273M}{D^2} \right) \frac{1}{1000 t_s} \ \ [\mathrm{Mpa}] \tag{4.36}$$

where:

σ_c = maximum longitudinal stress compression stress;

t_s = thickness of the bottom shell course;

w_t = weight of the tank shell and portion of the roof reacting on the shell, determined as $w_t = W_S / \pi D + w_{rs}$;

where w_{rs} is the roof load acting on the shell.

The maximum longitudinal shell compression stress at the bottom of the shell when there is uplift shall be determined by the formula:

$$\sigma_c = \left(\frac{w_t + w_L}{0.607\text{-}0.18667\left[\frac{M}{D^2 \left(w_t + w_L \right)} \right]^{2.3}} \right) \frac{1}{1000 t_s} \qquad (4.37)$$

The uplift condition is expressed by the equation 4.38:

$$\frac{M}{D^2 (w_t + w_L)} \leq 0.785 \qquad (4.38)$$

The allowable shell compression stress is:

$$\sigma_e = 1.333 \left(\sigma_a + \frac{\Delta C_c E t}{2} \right) [\text{Mpa}] \qquad (4.39)$$

ΔC_c is showed in Figure 4.9.

Hydrodynamic seismic hoop tensile stresses shall be determined by the following formulas:
When vertical acceleration is not specified

$$\sigma_s = \frac{N_i + N_c}{1000 t} \ [\text{Mpa}] \qquad (4.40)$$

where for $D/H > 1.33$

$$N_i = 21.4\left(\frac{ZI}{R_w}\right)GHD\left[\frac{Y}{H} - 0.5\left(\frac{Y}{H}\right)^2\right]\tanh\left(0.866\frac{D}{H}\right) \qquad (4.41)$$

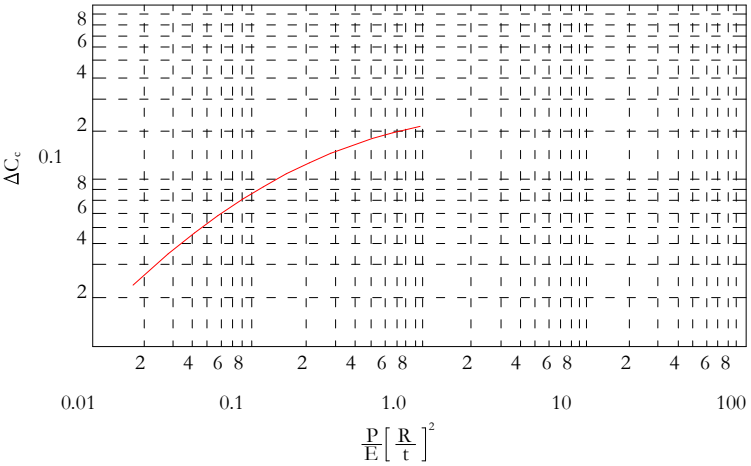

Figura 4.9. Increase in axial-compressive buckling-stress coefficient of cylinders due to internal pressure.

Hydrodynamic seismic hoop tensile stresses shall be determined by the following formulas:

When vertical acceleration is not specified

$$\sigma_s = \frac{N_i + N_c}{1000t} \text{ [Mpa]} \qquad (4.42)$$

where for $D/H > 1.33$

$$N_i = 21.4\left(\frac{ZI}{R_w}\right)GHD\left[\frac{Y}{H} - 0.5\left(\frac{Y}{H}\right)^2\right]\tanh\left(0.866\frac{D}{H}\right) \qquad (4.43)$$

for $D/H > 1.33$ and $Y < 0.75D$

$$N_i = 13.6\left(\frac{ZI}{R_w}\right)GD^2\left[\frac{Y}{0.75D} - 0.5\left(\frac{Y}{0.75D}\right)^2\right] \tag{4.44}$$

for $D/H < 1.33$ and $Y > 0.75D$

$$N_i = 6.6\left(\frac{ZI}{R_w}\right)GD^2 \text{ [kN]} \tag{4.45}$$

for all proportions of D/H

$$N_c = 33.1\left(\frac{ZI}{R_w}\right)C_1SGD^2\left[\frac{\cosh\left[\frac{3.68(H-Y)}{D}\right]}{\cosh\left[\frac{3.68H}{D}\right]}\right] \tag{4.46}$$

When vertical acceleration is not specified

$$\sigma_s = \frac{\sqrt{N_i^2 + N_c^2 + (N_h a_v)^2}}{1000t} \text{ [Mpa]} \tag{4.47}$$

In previous equations have:

σ_s = hydrodynamic hop stress;

N_i = impulsive hoop force;

N_c = convective hoop force;

N_h = hydrostatic force;

a_v = vertical acceleration;

t = thickness of the shell ring under consideration;

Y = distance from fluid surface;

The sloshing wave height may be calculated by the following formula:

$$d = 7.53D\left[\frac{ZIC_1S}{R_w}\right] \tag{4.48}$$

4.4 EUROCODE

The Eurocode 3 [29-30] at 4.2 deals with the design of atmospheric steel tanks while the seismic design is postponed in the Part 4 of Eurocodice 8 [28].

4.4.1 Structural Design

4.4.1.1 Bottom Plate

The thickness of the bottom plate depends on the type of welded connection and the material used in the construction as shown in Table 4.3.

Material	Lap welded	Butt welded
Ferrous Steel	6 mm	5 mm
Stainless Steel	5 mm	3 mm

Table 4.3. Minimum thickness of the bottom plate according to the Eurocodes

For tanks with a diameter greater than 12.5 m the bottom plates must have a minimum thickness of 6 mm or one third the thickness of the shell which are welded to which we must add 3 mm.

The exposed width of the bottom plate (distance of the rim of the bottom plate from the inside edge of the mantle) must be at least 500 mm or

$$w_a = 240 e_a / H^{0.5} \text{ [mm]} \tag{4.49}$$

where:

w_a = exposed width of the bottom plate;

e_a = thickness of first shell course;

H = design liquid level;

The thickness of the outer edge of the base plate must not be lower greatest among 50 mm and 10 times the thickness shell.

4.4.1.2 Tank Wall

The mantle must verify different ultimate limit states: balance and global stability; collapse; cyclical buckling; instability of shell; effort.

Damage limitation states for which the structure must be checked are: deformations, displacements or vibrations that may adversely affect the use of the property or likely to cause

damage to non-structural elements. The threshold values that trigger these limitation states should be decided case-by-case.

In the analysis of shell must take account of any openings in the shell, in particular the latter can be neglected in the review to the instability if

$$\left(\frac{r^0}{\sqrt{Rt}}\right) \leq 0.6\,;\; r^0 = (a+b)/4 \tag{4.50}$$

The anchorages must be designed taking into account the wind load for a two-dimensional system and must be attached to the shell and not the bottom plate. They must allow the thermal and hydrostatic pressure deformation of the shell.

For design of shell at any level must be satisfied the following expression for internal pressure:

$$\left[\gamma_F \rho g H^* + p_d\right](r/t) \leq f_{yd} \tag{4.51}$$

where:

$\rho =$ design specific gravity of the liquid to be stored, as specified by the purchaser;

$g =$ gravity acceleration;

$H^* =$ the height from the bottom of the mantle level considered;

$p_d =$ design value of pressure above the liquid;

The fixed roof tanks must be properly stiffened to the top of the shell structure. The tanks opened in the top must have a primary stiffening ring at the level of finish coat. The section of this ring must have an elastic modulus of cross section minimum:

$$W_{el} = \frac{r^2 H_0}{4300000} \tag{4.52}$$

where:

$H_0 =$ tank height;

$r =$ tank radius;

If the tank is off 30 m value of r is limited to 30. Other stiffened rings may be necessary to prevent the local shell instability. The height from the top of the roof of this ring is:

$$H_E = \sum h \left(\frac{t_{\min}}{t} \right)^{2.5} \tag{4.53}$$

where:

$h =$ is the height of each level;

$t =$ thickness of considered level;

$t_{\min} =$ thickness of top level;

The height above which the shell with thickness $t_{\min}$ is stable is:

$$H_P = 0.46\left(\frac{E}{p_d}\right)\left(\frac{t_{\min}}{r}\right)^{2.5} rK \tag{4.54}$$

If $H_E \le H_P$ stiffened rings are unnecessary otherwise H_E should be divided into stiffened rings to prevent local shell instability. If the secondary ring is not on a level of a minimum thickness mantle is a need for a change:

4.4.1.3 Anchorage

Anchorages are required for tanks with a fixed roof if one of the following conditions occurs. The next conditions indicates a possible uplifting of the base plate of the tank from its foundation:

- Uplift of a vacuum tank for the internal pressure being countered by the weight of the structure and permanent no-structural element;
- Uplift of a tank for the internal pressure combined with wind load countered by the weight of the structure and permanent no-structural element and weight of the contents always present in the tank;
- Uplift of a vacuum tank for the wind countered by the weight of the structure and permanent no-structural element. In this case, the uplifting forces can be calculated by reference to the theory of the

beam with a rigid section of the shell. Local uplifting is accept under these assumptions.

- Uplift of a tank for leakage of contents countered by the weight of the structure and permanent no-structural element.

The anchorages are to be connected primarily to cloak and not only to the base plate. Attacks have a minimum section 500 mm^2 to ensure greater resistance than the screws. The anchorages must not preload start.

4.4.1.4 Roof

The roofs must be designed to support the ultimate limit states, in particular: instability; resistance connections; failure for internal pressure. The roof can be conical or dome can be self-supported or supported by columns.

The support structure may not have the specific connections with the roof. The roof self-supported can design using the theories of great displacements. Connections with the shell must be designed to support the weight of their own, such as overloads the snow and the internal pressure (negative). Damage limitation states for the roofs are the same as for the shell. The welded roofs without stiffened welded must check that:

$$\left(P_{0d}R_1\right)/2t \le jf_{yd} \text{ for spherical roof} \qquad (4.55)$$

$$\left(P_{0d}R_r\right)/t \le jf_{yd} \text{ for conical roof} \tag{4.56}$$

where:

$t =$ is the roof thickness;

$j =$ is the connection efficiency (1 butt welded, 0.5 lap welded);

$P_{0d} =$ radial component of load;

$R_r =$ roof radius;

For verification of stability the following equation shall be used:

$$P_{id} \le 0.05\left[1.21E\left(t/R_r\right)^2\right] \tag{4.57}$$

where:

$P_{id} =$ radial component of design roof load;

Roof plate should not have a thickness less than 3 mm in stainless steel, or 5 mm for traditional steel. For spherical roof design values for the axial force and moment due to action of permanent loads and overload accidental is calculated with following equation:

$$N_d = 0.375\left(r/h\right)P_d \tag{4.58}$$

$$M_d = \left[\left(1-\left(x/r^3\right)-0.366\left(y/h\right)\right)\right]P_d\left(r/\left(1-\varepsilon\right)\right) \tag{4.59}$$

$P_d = \left(\pi r^2 / n\right) p_{R,d}$ $P_{rd} \geq 1.2$ kN/m^2 (maximum component of vertical design load on the roof included the weight of its support structure)

$$\varepsilon = N_d \left(0.6r\right)^2 \Big/ \left(\pi^2 E I_y\right) \tag{4.60}$$

r, h, x, y as in Figure 4.10.

b_k, h_k, A_0, A_u as in Figure 4.11.

n number of beam in the floor.

I_y inertia moment of the beam structure.

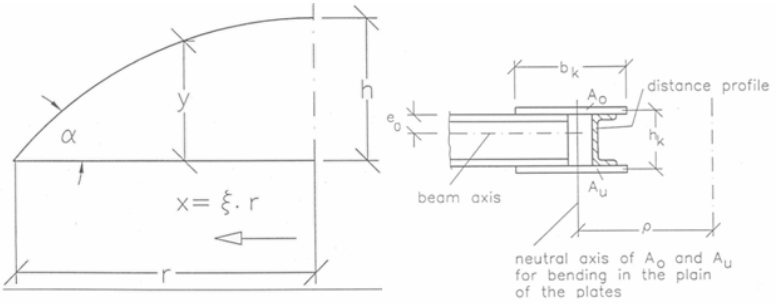

Figure 4.10 e 4.11. Types of roof.

4.4.2 Seismic Design

The model to be used for the determination of the seismic effects shall reproduce properly the stiffness, the strength, the damping, the mass and the geometrical properties of the containment structure, and shall account for the hydrodynamic response of the contained liquid and, where necessary, for the

effects of interaction with the foundation soil. Tanks shall be generally analyzed considering elastic behavior, unless proper justification is given for the use of nonlinear analysis in particular cases. The non linear phenomena admitted in the seismic design situation for which the ultimate limit state is verified shall be restricted so as to not affect the global dynamic response of the tank to any significant extent. Possible interaction between different tanks due to connecting piping shall be considered whenever appropriate.

Damage limitation state shall be ensured that under the seismic actions to the "full integrity" limit state and to the "minimum operating level" limit state:

Full integrity:

The tank system maintains its tightness against leakage of the contents. Adequate freeboard shall be provided, in order to prevent damage to the roof due to the pressures of the sloshing liquid or if the tank has no rigid roof, to prevent the liquid from spilling over;

The hydraulic systems which are part of, or are connected to the tank, are capable of accommodating stress and distortions due to relative displacements between tanks or between tanks and soil, without their functions being impaired;

Minimum operating level:

Local buckling, if it occurs, does not trigger collapse and is reversible; for instance, local buckling of struts due to stress concentration is acceptable.

Ultimate limit stress shall be ensured that under the seismic design situation:

The overall stability of the tank refers to rigid body behavior and may be impaired by sliding or overturning;

Inelastic behavior is restricted within limited portions of the tank, and the ultimate deformations of the materials are not exceeded;

The nature and the extent of buckling phenomena in the shell are adequately controlled;

The hydrodynamic systems which are part of, or connected to the tank are designed so as to prevent loss of the tank content following failure of any of its components.

A rational method based on the solution of the hydrodynamic equations with the appropriate boundary conditions shall be used for the evaluation of the response of the tank system. In particular, the analysis shall properly account for the following, where relevant.

The convective and impulsive components of the motion of the liquid;

The deformation of the tank shell due to hydrodynamic pressures and the interaction effects with the impulsive component;

The deformability of the foundation soil and ensuring modification of the response.

For the purpose of evaluating the dynamic response under seismic actions, the liquid may be generally assumed as incompressible.

Determination of the maximum hydrodynamic pressures induced by horizontal and vertical excitation requires in principle use of nonlinear dynamic analysis. Simplified methods allowing for a direct application of the response spectrum analysis may be used, provided that suitable conservative rules for the combination of the peak modal contributions are adopted.

4.4.2.1 Rigid Tanks

The complete solution of the Laplace equation for the motion of the fluid contained in a rigid cylinder can be expressed as the sum of two separate contributions, called rigid impulsive, and convective, respectively. The rigid impulsive component of the solution satisfies exactly the boundary conditions at the wall and at the bottom of the tank (compatibility between the velocity of the fluid and of the tank), but gives (incorrectly, due to the presence of the waves) zero pressure at the free surface of the fluid. A second term must therefore be added, which does not alter those boundary conditions that are already satisfied, and reestablished the correct equilibrium condition at the top.

Use is made of a cylindrical coordinate system (Figure 4.12): *r, z, θ,* with origin at the centre of the tank bottom, and the z

axis vertical. The height and radius of the tank are denoted by *H* and *R*, respectively, ρ is the mass density of the liquid, and $\xi = r/R$, $\zeta = z/H$, are the nondimensional coordinates.

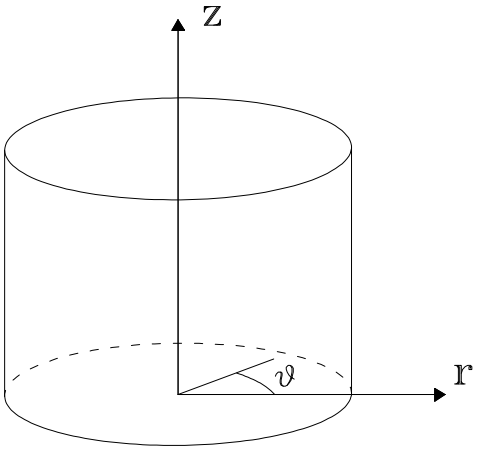

Figure 4.12 Cylindrical coordinate system.

4.4.2.1.1 Impulsive-Rigid pressure

The spatial-temporal variation of this component is given by the expression:

$$p_i(\xi,\varsigma,\vartheta,t) = C_i(\xi,\varsigma)\rho H \cos\vartheta A_g(t) \tag{4.61}$$

where:

$$C_i(\xi,\varsigma) = \sum_{n=0}^{\infty} \frac{(-1)^n}{I_1(\nu_n/\gamma)\nu_n^2} \cos(\nu_n\varsigma) I_1\left(\frac{\nu_n}{\gamma}\xi\right) \tag{4.62}$$

in which:

$$\nu_n = \frac{2n+1}{2}\pi \tag{4.63}$$

$$\gamma = \frac{H}{R} \tag{4.64}$$

and I_1 e I_1' denote the modified Bessell function of order 1 and its derivate.

The time-dependence of the pressure p_i in equation 4.61 is given by the function $A_g(t)$, which represents the free-field motion of the round (the peak value of $A_g(t)$ is denoted by a_g). The distribution along the height of p_i in equation 4.61 is given by the function C_i and is represented in Figure 4.13 for $\xi = 1$ (i.e. at the wall of the tank) and $\cos\theta = 1$ (i.e. on the plane which contains the motion), normalized to $\rho R a_g$ and for three values of $\gamma = H/R$.

Impulsive Base Shear:

By making use of equation 4.61 and performing the appropriate integrals one gets:

$$Q_i = m_i A_g(t) \tag{4.65}$$

Where m_i indicates the mass of the contained fluid which moves together with the tank walls, is called impulsive mass, and has the following expression:

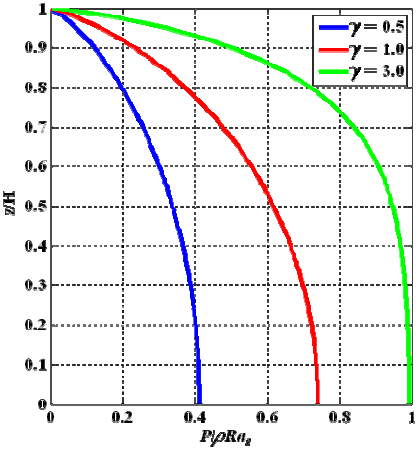

Figure 4.13 Variation along the height of the impulsive pressure for three values of $\gamma = H/R$.

$$m_i = m2\gamma\sum_{n=0}^{\infty}\frac{I_1(\nu_n/\gamma)}{\nu_n^3 I_1'(\nu_n/\gamma)} \tag{4.66}$$

With $m = \rho\pi R^2$ total contained mass of the fluid.

Impulsive Base Moment:

$$M_i = m_i h_i' A_g(t) \tag{4.67}$$

The Figure 4.14 shows the variability of m_i and h_i' as a function of m_i.

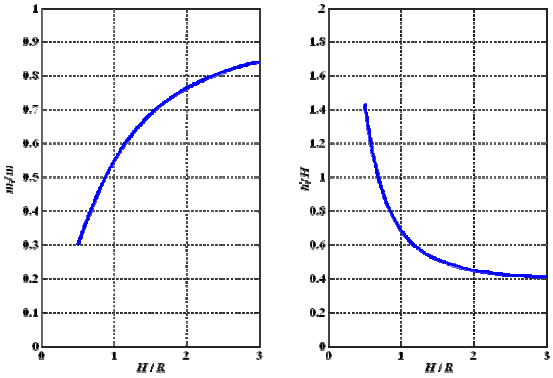

Figure 4.14 Ratios m_i/m and h'/H as functions of the slenderness of the tank.

4.4.2.1.2 Convective pressure

The spatial-temporal variation of this component is given by the following expression:

$$p_c(\xi,\varsigma,\theta,t) = \rho\sum_{n=1}^{\infty}\psi_n \cosh(\lambda_n\gamma\varsigma)... \\ ...J_1(\lambda_n\xi)\cos\theta A_n(t) \tag{4.68}$$

with:

$$\psi_n = \frac{2R}{(\lambda_n^2-1)J_1(\lambda_n)\cosh(\lambda_n\gamma)} \tag{4.69}$$

$$\lambda_1 = 1.8112 \quad \lambda_2 = 5.3314 \quad \lambda_3 = 8.5363$$

J_1 = Bessel function of the first order;

$A_n(t)$ = response acceleration of a single degree of freedom oscillator having a frequency ω_{cn}:

$$\omega_{cn}^2 = g\frac{\lambda_n}{R}\tanh(\lambda_n\gamma) \tag{4.70}$$

and a damping factor value appropriate for fluid.

The equation 4.68 shows that the total pressure is the combination of an infinite number of modal terms, each one corresponding to a wave form of the oscillating liquid. Only the first oscillating, or sloshing, mode and frequency, needs in most cases to be considered for design purposes. The vertical distribution of the sloshing pressures for first two modes are shown in Figure 4.15.

One can observe from Figure 4.15 that in a squat tanks the sloshing pressures maintain relatively high values down to the bottom, while in slender tanks the sloshing effect is superficial. For the same value of response acceleration, the contribution of the second mode is seen to be negligible.

Pressure Resultants:

The base shear is given by:

$$Q_c(t) = \sum_{n=1}^{\infty} m_{cn} A_n(t) \tag{4.71}$$

with the nth modal convective mass:

$$m_{cn} = m\frac{2\tanh\left(\lambda_n\gamma\right)}{\gamma\lambda_n\left(\lambda_n^2-1\right)} \tag{4.72}$$

From equation 4.71 one can note that the total shear force is given by the instantaneous sum of the forces contributed by the (infinite) oscillators having masses m_{cn}, attached to the rigid tank by means of springs having stiffnesses: $k_{cn} = \omega_{cn}^2 m_{cn}$. The tank is subjected to the ground acceleration $A_g(t)$ and the masses respond with acceleration $A_n(t)$.

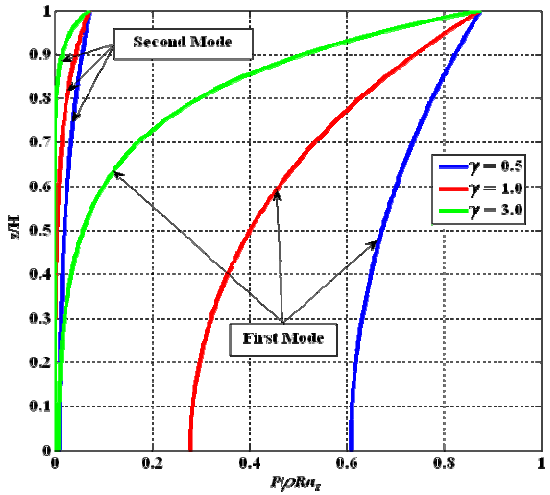

Figure 4.15 Variation along the height of the first two sloshing modes pressure for three values of $\gamma = H/R$.

The total moment can be expressed as:

$$M_c(t) = \sum_{n=1}^{\infty} \left(m_{cn} A_n(t) \right) h_{cn} \tag{4.73}$$

where h_{cn} is the level where the equivalent oscillator has to be applied in order to give the correct value of M_{cn}.

$$h_{cn} = H \left(1 + \frac{2 - \cosh(\lambda_n \gamma)}{\lambda_n \gamma \sinh(\lambda_n \gamma)} \right) \tag{4.74}$$

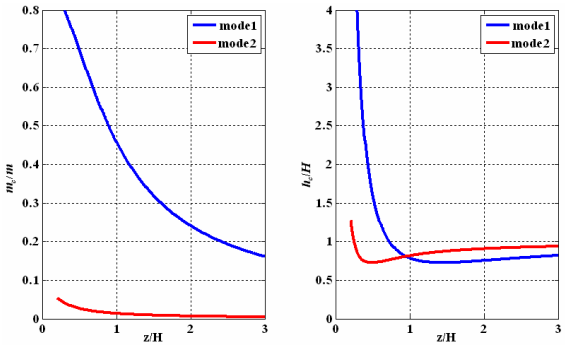

Figure 4.16 First two sloshing modal masses and corresponding heights h_{c1} and h_{c2} as functions of the slenderness of the tank.

The values of m_{c1} and m_{c2}, and the corresponding values of h_{c1} and h_{c2} are shown in Figure 4.16, as a function of γ. The predominant contribution to the sloshing wave height is

provided by the first mode, and the expression of the peak at the edge is:

$$d_{\max} = 0.84RS_e\left(T_{c1}\right) \tag{4.75}$$

4.4.2.1.3 Combination of impulsive and convective pressures

The time-history of the total pressure is the sum of the two time-histories, the impulsive one being driven by $A_g(t)$, the convective one by $A_{c1}(t)$ (neglecting higher order components). If, as it is customary in design practice, a response spectrum approach is preferred, the problem of suitably combining the two maxima arises. Given the generally wide separation between the central frequencies of the ground motion and the sloshing frequency, the "square root of the sum of squares" rule may become unconservative, so that the alternative, upper bound, rule of adding the absolute values of the two maxima is recommended for general use. For steel tanks, the inertia forces acting on the shell due to its own mass are small in comparison with the hydrodynamic forces, and can normally be neglected.

4.4.2.2 Flexible-Impulsive pressure

When the tank cannot be considered as rigid (this is almost always the case for steel tanks) the complete solution of the

Laplace equation is ordinarily sought in the form of the sum of three contributions, referred to as: "rigid impulsive", "sloshing" and "flexible".

The third contribution is new with respect to the case of the rigid tanks: it satisfies the condition that the radial velocity of the fluid along the wall equals the deformation velocity of the tank wall, plus the conditions of zero vertical velocity at the tank bottom and zero pressure at the free surface of the fluid.

Since the deformation of the wall is also due to the sloshing pressures, the sloshing and the flexible components of the solution are theoretically coupled, a fact which makes the determination of the solution quite involved. Fortunately, the dynamic coupling is very weak, due to the separation which exists between the frequencies of the two motions, and this allows to determine the third component independently of the others with almost complete accuracy. The rigid impulsive and the sloshing components examined in previous sections remain therefore unaffected.

No closed-form expression is possible for the flexible component, since the pressure distribution depends on the modes of vibration of the tank-fluid system, and hence on the geometric and stiffness properties of the tank. These modes cannot be obtained directly from usual eigenvalue algorithms, since the participating mass of the fluid is not known a priori and also because only the modes of the type:

$f(\varsigma,\theta)=f(\theta)\cos\theta$ are of interest (and these modes may be laborious to find among all other modes of a tank). Assuming the modes as known the flexible pressure distribution has the following form: :

$$p_f(\varsigma,\theta,t)=\rho H\psi\sum_{n=0}^{\infty}d_n\cos(\nu_n\varsigma)\cos\theta A_f(t) \qquad (4.76)$$

with:

$$\psi=\frac{\int_0^1 f(\varsigma)\left[\frac{\rho_s s}{\rho H}+\sum_{n=0}^{\infty}b_n'\cos(\nu_n\varsigma)\right]d\varsigma}{\int_0^1 f(\varsigma)\left[\frac{\rho_s s}{\rho H}f(\varsigma)+\sum_{n=0}^{\infty}d_n\cos(\nu_n\varsigma)\right]d\varsigma} \qquad (4.77)$$

$$b_n'=2\frac{(-1)^n I_1(\nu_n/\gamma)}{\nu_n^2 I_1'(\nu_n/\gamma)} \qquad (4.78)$$

$$d_n=2\frac{\int_0^1 f(\varsigma)\cos(\nu_n\varsigma)d\varsigma I_1(\nu_n/\gamma)}{\nu_n I_1'(\nu_n/\gamma)} \qquad (4.79)$$

ρ_s is the mass density of the shell, s is its thickness and p_f in equation 4.76 provides the predominant contribution to the total pressure, due to the fact that, while the rigid impulsive term varies with the ground acceleration $A_g(t)$, the flexible term varies with the response acceleration which, given the

usual range of periods of the tank-fluid systems, is considerably amplified with respect to $A_g(t)$.

Pressure resultants:

Starting from equation 4.76, the resultant base shear and total moment at the base can be evaluated, arriving at expressions in the form:

Base Shear

$$Q_f(t) = m_f A_f(t) \quad (1st \bmod e\ only) \tag{4.80}$$

with:

$$m_f = m\psi\gamma\sum_{n=0}^{\infty}\frac{(-1)^n}{\nu_n}d_n \tag{4.81}$$

Base Shear

$$M_f(t) = m_f A_f(t) h_f \tag{4.82}$$

with:

$$h_f = H\frac{\left[\gamma\sum_{n=0}^{\infty}d_n\frac{(-1)^n\nu_n - 2}{\nu_n^2} + \frac{d_n I_1'(\nu_n/\gamma)}{\nu_n}\right]}{\gamma\sum_{n=0}^{\infty}d_n'\frac{(-1)^n}{\nu_n}} \tag{4.83}$$

4.5 COMPARISON BETWEEN DIFFERENT INTERNATIONAL CODES

In this section, as summary of previous section, a comparison between different international codes on dynamic analysis of liquid storage tank is presented. The comparison will in particular focus on following aspects:

i) Mechanical model and its parameters

ii) Hydrodynamic pressure due to lateral and vertical excitation

iii) Time period of tank in lateral and vertical mode

iv) Effect of soil flexibility

4.5.1 Mechanical models

As explained earlier, the mechanical model adopted by international codes for dynamic analysis of steel storage tank is a spring-lumped mass system, which considerably simplifies the evaluation of hydrodynamic forces (Figure 4.17).

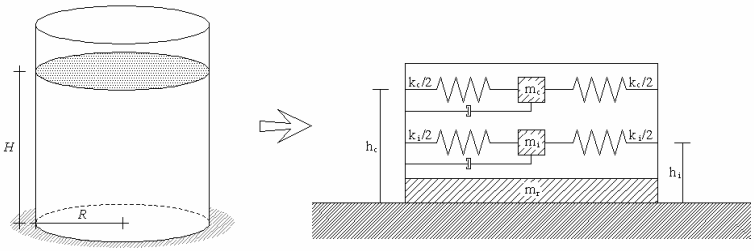

Figure 4.17. One-dimensional dynamic model of tank .

Various quantities associated with a mechanical model are: impulsive mass (M_i), convective mass (M_c), height of impulsive mass (h_i), height of convective mass (h_c) and convective mode time period (Tc).

Various codes use one or the other mechanical models described in previous section. AWWA D-100, and API 650 use mechanical model of Housner [31] with modifications of Wozniak and Mitchell [32]. AWWA D- 100 and API 650 deal with circular steel tanks, which are flexible tanks. However, since there is no appreciable difference in the parameters of mechanical models of rigid and flexible tank models, these codes evaluate parameters of impulsive and convective modes from rigid tank models. Eurocode 8 mentions mechanical model of Veletsos and Yang [33] as an acceptable procedure for rigid circular tanks. For flexible circular tanks, models of Veletsos [34] and Haroun and Housner [35] are described along with the procedure of Malhotra et. al. [36]. For rigid rectangular tanks it suggests model of Housner [31]. An important point while using a mechanical model pertains to combination rule used for adding the impulsive and convective forces. Except Eurocode 8, all the codes suggest SRSS (square root of sum of square) rule to combine impulsive and convective forces. Eurocode 8 suggests use of absolute summation rule. For evaluating the impulsive force, mass of tank wall and roof is also considered along with impulsive fluid mass. Eurocode 8 suggest a reduction factor to suitably reduce the mass of tank

wall. Such a reduction factor was suggested by Veletsos [34] to compensate the conservativeness in the evaluation of impulsive force.

4.5.2 Time period of impulsive mode

Impulsive mode refers to lateral mode of tank-liquid system. Lateral seismic force on tank depends on the impulsive mode time period. Time period of tank-fluid system depends on the flexibility of support also. Table 4.4 gives details of the expressions used in various codes to evaluate the impulsive mode time period.

Type of tank	Code	Expression	Note
Circular tanks with fixed base	AWWA D-100 and D-103		Expression is not required in the analysis.
	API 650		Expression is not required in the analysis.
	Eurocode 8	$T_i = \frac{2R}{C_i}\sqrt{\frac{\rho R}{Et}}$	C_i is a function of h\R given by exprion.
Circular tanks with flexible base	AWWA D-100 and D-103		Expression is not required in the analysis.
	API 650		No expression are given
	Eurocode 8		

Table 4.4. Expressions for impulsive time period given in various codes.

For fixed base circular tanks, Eurocode 8 has followed the expression given by Sakai et. al. [37]. Eurocode 8 also gives the expression suggested by Malhotra for evaluation of impulsive

mode time period. AWWA D-100 and API 650 prescribe a constant value of design spectral acceleration and hence impulsive time period is not needed in these codes.

For circular tanks resting on flexible base, the expressions for impulsive time period is not gives by codes; only ACI 350.3 and AWWA 350.2 gives this expression.

4.5.3 Hydrodinamic pressure distribution due to lateral excitation

Stresses in the tank wall depend on distribution of hydrodynamic pressure along the wall height. Housner [31] had derived the expressions for distribution of hydrodynamic pressure on a rigid tank wall due to lateral base excitation. Impulsive as well as convective components of hydrodynamic pressure were considered. Veletsos [34] has also obtained the distribution of hydrodynamic pressure on rigid as well as flexible wall. It may be mentioned that flexibility of tank wall does not influence the convective hydrostatic pressure. However, it does affects the impulsive hydrodynamic pressure distribution, particularly for the slender tanks. Evaluation of impulsive pressure distribution in flexible tanks is quite involved and can be done only through iterative procedures [34]. All the codes use pressure distribution of rigid tanks. AWWA D-100 and D-103 provide expressions of Housner [31] to obtain distribution of impulsive and convective

hydrodynamic pressure. Eurocode 8 use approach of Veletsos [34] to get hydrodynamic pressure distribution in circular tanks.

4.5.4 Response to vertical base excitation

Under the influence of vertical excitation, liquid exerts axisymmetric hydrodynamic pressure on tank wall. Knowledge of this pressure is essential in properly assessing the safety and strength of tank wall against buckling. In all the codes effect of vertical acceleration is considered. Response to vertical excitation is mainly governed by the time period of fundamental breathing mode or axisymmetric mode of vibration of tank-liquid system. Expression for exact time period of axisymmetric mode of a circular tank is quite involved. However, considering certain approximations like, mass of tank wall is quite small as compared to fluid mass, some simple closed form expressions have been given by Veletsos [34] and Haroun and Tayel [38]. Other than API 650, all codes do have provisions to consider tank response under vertical excitation. These expressions refer to circular tanks only. Eurocode 8 has used expression from Haroun and Tayel [38].

4.5.5 Sloshing wave height

The sloshing component of liquid mass undergoes vertical displacement and it is necessary to provide suitable free board to prevent spilling of liquid. All the codes, except API 650, give

explicit expressions to evaluate maximum sloshing wave height. These expressions are given in Table 4.5.

Code	Expression of Sloshing wave
API 650	Non Mentioned
AWWA D-100 and D-103	$0.84 A_1 R$
Eurocode 8	$0.84 A_1 R$

Table 4.5. Expressions of sloshing wave given in various codes.

CHAPTER 5:

DYNAMIC RESPONSE AND MODELLING

5.1 INTRODUCTION

Liquid storage tanks are important components of lifeline and industrial facilities. They are critical elements in municipal water supply and fire fighting systems, and in many industrial facilities for storage of water, oil, chemicals and liquefied natural gas. Behaviour of large tanks during seismic events has implications far beyond the mere economic value of the tanks and their contents. If, for instance, a water tank collapses, as occurred during the 1933 Long Beach and the 1971 San Fernando earth-quakes, loss of public water supply can have serious consequences. Similarly, failure of tanks storing combustible materials, as occurred during the 1964 Niigata, Japan and the 1964 Alaska earthquakes, can lead to extensive uncontrolled fires. Many researchers have investigated the dynamic behaviour of liquid storage tanks both theoretically and experimentally. Investigations have been conducted to seek possible improvements in the design of such tanks to resist earthquakes.

5.2 DYNAMIC BHEAVIOUR OF STORAGE TANK: HYSTORICAL BACKGROUND

First developments of the seismic response of liquid storage tanks considered the tank to be rigid, and focused attention on the dynamic response of the contained liquid , such as the work performed by Jacobsen [39], Graham and Rodriguez [40], and Housner [41]. Housner proposed a simplified model for seismic analysis of anchored tanks with rigid walls [31]. According to this model, a tank with a free liquid surface subjected to horizontal ground acceleration is characterised by a given fraction of the liquid that is forced to participate in this motion as rigid mass; on the other hand the motion of the tank walls excites the liquid into oscillations which result in a dynamic force on the tank. This force is assumed to be the same of a lumped mass, known as a convective mass, that can vibrate horizontally restrained by a spring.

Later, the 1964 Alaska earthquake caused large scale damages to tanks of modern design [43] and profoundly influenced research into vibrational characteristics of flexible tanks. Different solution techniques and simplified models were employed to obtain the seismic response of flexible anchored liquid storage tanks.

A different approach to the analysis of flexible containers was developed by Veletsos [44]. He presented a simple procedure for evaluating hydrodynamic forces induced in

flexible liquid-filled tanks. The tank was assumed to be have as a single degree of freedom system, to vibrate in a prescribed mode and to remain circular during vibrations. Hydrodynamic pressure distribution, base shears and overturning moments corresponding to several assumed modes of vibration w ere presented. Later, Veletsos and Yang [33-45] estimated maximum base overturning moment induced by a horizontal earthquake motion by modifying Housner's model to consider the first cantilever mode of the tank. They presented simplified formulas to obtain the fundamental natural frequencies of liquid-filled shells by the Rayleigh-Ritz energy method.

Rosenblueth and Newmark [46] modified later the relationships suggested by Housner to estimate the convective and rigid masses and gave updated formulations for the evaluation of the seismic design forces of liquid storage tanks.

In 1980 and 81, Haroun and Housner [47] used a boundary integral theory to drive the fluid added mass matrix, rather than using the displacement based fluid finite elements. The former approach substantially reduced the number of unknowns in the problem. They conducted a comprehensive study [35-48-49-50-51-52] which led to the development of a reliable method for analysing the dynamic behaviour of deformable cylindrical tanks. A mechanical model [35], which takes into account the deformability of the tank wall, was derived and parameters of the model were displayed in charts to facilitate the computational work.

In Haron's model [50] a part of the liquid moves independently with respect to the tank shell, again convective motion, while another part of the liquid oscillates at unison with the tank. If the flexibility of the tank wall is considered, a part of this mass moves independently (impulsive mass) while the remaining accelerates back and forth with the tank (rigid mass). Figure 5.1 shows the idealised structural model of liquid storage tank. The contained continuous liquid mass is lumped as convective, impulsive and rigid masses are referred as m_c, m_i and m_r, respectively. The convective and impulsive masses are connected to the tank wall by different equivalent springs having stiffness k_c and k_i, respectively. In addition, each spring can be associated to an equivalent damping ratio ξ_c and ξ_i. Damping for impulsive mode of vibration can be assumed about 2% of critical for steel tanks, while the damping for convective mode can be assumed as 0,5% of critical. Under such assumptions, this model for anchored storage tank has been extended to analyse unanchored base-isolated liquid storage tanks [38].

Effective masses are given in Equations (5.1-5.4) as a fraction of the total mass m (Equation 5.5). Coefficients Y_c, Y_i, and Y_r depend upon the filling ratio S=H/R, where H is the liquid height and R is the tank radius, as clearly shown in Figure 5.1.

$$m_c = mY_c \tag{5.1}$$

$$m_i = mY_i \tag{5.2}$$

$$m_r = mY_r \tag{5.3}$$

$$m_{tot} = m_c + m_i + m_r \tag{5.4}$$

$$m = \pi R^2 H \rho_w \tag{5.5}$$

Similarly, natural frequencies of convective mass, ω_c and impulsive mass, ω_i (Equations 5.6-5.7) can be retrieved from [53]:

$$\omega_c = \sqrt{1.84\left(\frac{g}{R}\right)\tan\left(1.84\frac{H}{R}\right)} \tag{5.6}$$

$$\omega_c = \frac{P}{H}\sqrt{\frac{E}{\rho_s}} \tag{5.7}$$

where E and ρs are the modulus of elasticity and density of tank wall respectively; g is the acceleration due to gravity; and P is a dimensionless parameter depending on the ratio H/R as well.

In the same period, the evolution of digital computers and associated numerical techniques allowing the use of FEM models to estimation of dynamic behaviour of steel tank. The first example of FEM analysis was conducted by Edwards [54]. He employed the finite element method and a refined shell

theory to predict seismic stresses and displacements in a vertical cylindrical tank having a height to diameter ratio smaller than one.

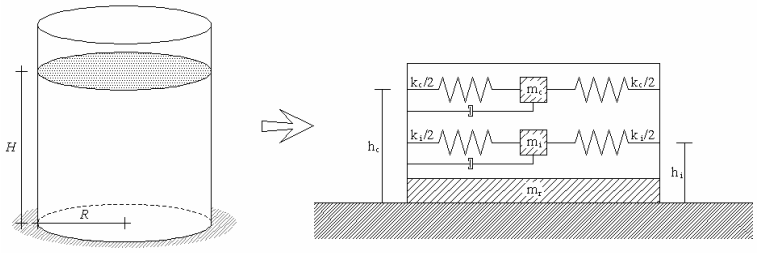

Figure 5.1. One-dimensional dynamic model of tank as in [53].

The finite element method combined with the boundary element method was used by several investigators, such as Grilli [55], Huang [56] and Kondo [57], to investigate the problem. Hwang [58-59] employed the boundary element method to determine the hydrodynamic pressures associated with small amplitude excitations and negligible surface wave effects in the liquid domain. He obtained frequency-dependent terms related with the natural modes of vibration of the elastic tank and incorporated them into a finite element formulation of an elastic tank in frequency domain.

In order to simplify the problem, former investigations ignored some nonlinear factors that may affect the response of anchored liquid storage tanks. Several researchers tried to refine the analysis by including the effects of these factors in the analysis. Sakai and Isoe [60-61] investigated the nonlinearity due

to partial sliding of the anchored tank base plate on its foundation. Huang [62] performed geometrically nonlinear analysis of tanks to investigate the large deflection effect.

Uras et al [63] studied the influence of geometrical imperfections on the dynamic stability of liquid-filled shells under horizontal ground excitations. He introduced a general imperfection pattern in the circumferential direction to analyze the geometrical stiffness term. Imperfection effects on buckling of liquid-filled shells were also discussed in [64-65-66].

5.3 ANALITICAL APPROACH

The response of vertical liquid storage tanks to earthquakes is characterised by four pressure components:

- Fluid pressure p_1 due to the ground acceleration (considering the tank wall as being rigid), named impulsive pressure;
- Fluid pressure p_2 due to sloshing (liquid surface displacement) only, named convective pressure;
- Fluid pressure p_3 caused by the wall deformation relative to the base circle due to the deformability of the tank wall;
- Fluid pressure p_v due to the vertical motion of the tank.

Since the fluid motion due to the ground acceleration (pressure p_1) and the wall deformation (pressure p_3) produces a

distribution of the displacement of the fluid surface, a coupling exists between the pressure components p_1, p_3 and the pressure p_2 due to sloshing.

Since numerical methods are able to solve complicated fluid-structure interaction problems, recently the finite element method for the tank shell and the boundary element method for the liquid were applied to treat a fully coupled system solid/tank/liquid, see e.g. Lay [67] or the work by Bo and Tag [68] which investigates specifically the influence of a base isolation on the sloshing behaviour. The pressure wave equation can be solved by means of a series expansion for various sets of boundary conditions. Although the leading form of the differential equations exist (see e.g. Flugge' s exact equations in [69]), a closed form analytical solution for the wall deformation is not available, mainly because of the fact that in practice the tank wall thickness varies over the tank's height. Therefore, various types of the relative wall deformation shape are assumed. This assumption is based on practical observations and numerical studies [70]. Tall tanks with the ratio ($H/R>1$) (R radius of the tank, H height of the tank) often show a more or less linear variation of the deformation over the tank' s height. Broad tanks with ratio ($H/R<1$) often show a typical concave or convex wall deformation shape which can be approximated by sin- or (1-cos)-type functions, respectively.

Assuming the model shows in Figure 5.2, with z being the coordinate in the axial direction of the tank, we finally assume the radial displacement of the tank wall relative to the base circle as $w(t)\psi(z)\cos\varphi$. The function $w(t)$ represents a time history, which is the same for all points along one generator. $\psi(z)$ represents the type of the deformation. The function $\cos\varphi$ shows that circular tanks for which a horizontal base excitation activates basic radial modes (wave number 1) only [70]. Modes with higher wave numbers would not contribute to over-all resultant forces or moments.

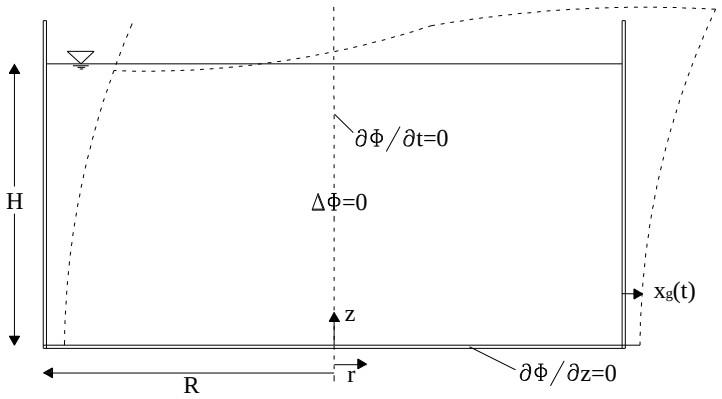

Figura 5.2 Conditions for potential of velocity.

5.3.1 Hydrodynamic pressure

The liquid pressure distribution in a deformable tank (radius R, height H) which is horizontally exited (base acceleration $\ddot{x}_g$)

is described assuming an ideal fluid (incompressible, non-rotational) as described by:

$$\Delta\phi = \frac{\partial^2\phi}{\partial r^2} + \frac{1}{r}\frac{\partial\phi}{\partial r} + \frac{1}{r^2}\frac{\partial^2\phi}{\partial\varphi^2} + \frac{\partial^2\phi}{\partial z^2} = 0 \tag{5.8}$$

where ϕ is the velocity potential; the velocity v being-grad ϕ, i.e.:

$$v^T = \left(-\frac{\partial\phi}{\partial r}, -\frac{1}{r}\frac{\partial\phi}{\partial\varphi}, -\frac{\partial\phi}{\partial z}\right) \tag{5.9}$$

The linearized Bernoulli equation for pressure is:

$$p = \rho\frac{\partial\phi}{\partial t} \tag{5.10}$$

where ρ is the mass density of the liquid.

In the following considerations only the first mode of the Fourier expansion of ϕ and p with respect to the circumference coordinate φ,

$$\phi = P(r, z; t)\cos\varphi \tag{5.11}$$

is studied, since only this component leads to a resultant eternal force moment. The following boundary value problem must be considered:

$$r = 0: \qquad \frac{\partial P}{\partial t} = 0; \tag{5.12}$$

as the pressure distribution is antisymmetric,

$$r = R: \qquad -\frac{\partial P}{\partial t} = \ddot{x}_g(t) + v_r(z,t); \tag{5.13}$$

As the fluid velocity must coincide with the wall velocity, which is the sum of the ground velocity $\dot{x}_g$ and the velocity $v_r(z,t)$ relative to the ground,

$$z = 0: \qquad \frac{\partial P}{\partial z} = 0; \tag{5.14}$$

as the fluid velocity component in z-direction is 0 at z=0,

$$z = H: \qquad \frac{\partial^2 P}{\partial t^2} + g\frac{\partial P}{\partial z} = 0; \tag{5.15}$$

as the sloshing of the liquid leads, up to linearized terms, to the condition $p(H,r,t) = d(H,r,t)\rho g$, where d is the displacement of the liquid surface $(-\partial\phi/\partial z = d)$.

The function P is now split into three parts,

$$P = P_1 + P_2 + P_3 \tag{5.16}$$

- P_1 potential due to the ground acceleration $\dot{x}_g$ only (impulsive solution),
- P_2 potential due to the sloshing only (convective solution),
- P_3 potential due to the relative wall velocity $v_r(z,t)$.

The set of boundary conditions for P_1, P_2, P_3 are listed below:

$$\begin{aligned} P_1:\ r=0 \Rightarrow \frac{\partial P_1}{\partial t}=0;\quad r=R \Rightarrow\ -\frac{\partial P_1}{\partial r}=\ddot{x}_g(t);\\ z=0 \Rightarrow \frac{\partial P_1}{\partial z}=0;\quad z=H \Rightarrow\ -\frac{\partial P_1}{\partial t}=0; \end{aligned} \tag{5.17}$$

$$\begin{aligned} P_2:\ r=0 \Rightarrow \frac{\partial P_2}{\partial t}=0;\quad r=R \Rightarrow\ -\frac{\partial P_2}{\partial r}=0;\\ z=0 \Rightarrow \frac{\partial P_2}{\partial z}=0;\quad z=H \Rightarrow \frac{\partial^2 P_2}{\partial t^2}+g\frac{\partial P_2}{\partial z}= \\ =-g\left(\frac{\partial P_1}{\partial z}+\frac{\partial P_3}{\partial z}\right); \end{aligned} \tag{5.18}$$

$$\begin{aligned} P_3:\ r=0 \Rightarrow \frac{\partial P_3}{\partial t}=0;\quad r=R \Rightarrow\ -\frac{\partial P_3}{\partial r}=v_r(z,t);\\ z=0 \Rightarrow \frac{\partial P_3}{\partial z}=0;\quad z=H \Rightarrow\ \frac{\partial P_3}{\partial t}=0; \end{aligned} \tag{5.19}$$

Due to the linearity of the problem the sum $\left(P_1+P_2+P_3\right)\cos\varphi$ describes the original problem as defined by equations 5.8-5.15. The solution of problem (equation 5.17), for $\varphi=0$ as:

$$p_{1,0}=\rho\frac{\partial P_1}{\partial t}=-\ddot{x}_g\left(t\right)\rho H\ldots$$
$$\ldots\sum_{i=1}^{\infty}8\frac{\left(-1\right)^{i+1}}{\left[\left(2i-1\right)\pi\right]^2}\times\ldots \tag{5.20}$$
$$\ldots\frac{I_1\left[\left(2i-1\right)\frac{\pi}{2}\frac{z}{H}\right]}{I_1^{'}\left[\left(2i-1\right)\frac{\pi}{2}\frac{r}{H}\right]}\cos\left[\left(2i-1\right)\frac{\pi}{2}\frac{z}{H}\right]$$

where $I_1\left(y\right)$ is the Bessel modified function of first kind of order 1 with the argument y and $I_1^{'}\left(y\right)$ is its derivate.

The solution of problem 5.19 can also be derived analytically for given relative wall velocity $v_r\left(z,t\right)=\dot{w}\left(t\right)\psi\left(z\right)$ for $\varphi=0$ as:

$$p_{3,0} = \rho \frac{\partial P_3}{\partial t} = -\ddot{w}(t)\,\rho H \sum_{i=1}^{\infty} 4 \frac{\beta_i}{(2i-1)\pi} \times \ldots\ldots \\ \ldots\ldots \frac{I_1\left[(2i-1)\frac{\pi}{2}\frac{z}{H}\right]}{I_1'\left[(2i-1)\frac{\pi}{2}\frac{r}{H}\right]} \cos\left[(2i-1)\frac{\pi}{2}\frac{z}{H}\right] \tag{5.21}$$

$$\beta_i = \frac{1}{H}\int_0^H \psi(z)\cos\left[(2i-1)\frac{\pi}{2}\frac{z}{H}\right]dz = \ldots\ldots \\ \ldots\ldots \int_0^1 \psi(\xi)\cos\left[(2i-1)\frac{\pi}{2}\xi\right]dz \tag{5.22}$$

For the solution of the problem (equation 5.18) more discussion are required. Firstly, it can be immediately seen from equation 5.20 and 5.21 that $\left(\partial^2 P_1/\partial t^2\right)$ and $\left(\partial^2 P_3/\partial t^2\right)$ are zero at $z = H$, and therefore, these terms do not appear in the boundary condition for P_2 at $z = H$. Secondary, as is well known in the literature [71], a homogeneous solution to problem 5.18 is:

$$P_{2,i} = C_i J_i\left(\lambda_i \frac{r}{R}\right)\cosh\left(\lambda_i \frac{z}{R}\right) f_i(t); \\ P_2 = \sum_{i=1}^{\infty} P_{2,i} \tag{5.23}$$

where $J_1(y)$ is the Bessel function of the first kind of order 1 with the argument y, $J_1'(y)$ is its derivate, C_i's are constants, and $f_i(t)$'s represents some time dependent functions, λ_i are the zeros of $J_1'(y)$. Considering the boundary condition at $z = H$ which leads to:

$$\begin{aligned}
&\sum_{i=1}^{\infty} C_i J_i\left(\lambda_i \frac{r}{R}\right)\left[\ddot{f}_i(t)\cosh\left(\frac{\lambda_i H}{R}\right)+\ldots\right.\\
&\left.\ldots+g\frac{\lambda_i}{R}\sinh\left(\frac{\lambda_i H}{R}\right) f_i(t)\right]=\\
&=-g\sum_{i=1}^{\infty}\left[\frac{4}{(2i-1)\pi}\dot{x}_g+2\beta_i(-1)^{i-1}\dot{w}\right]\ldots\\
&\ldots\times\frac{I_1\left[(2i-1)\frac{\pi}{2}\frac{r}{R}\right]}{I_1\left[(2i-1)\frac{\pi}{2}\frac{R}{H}\right]}
\end{aligned} \tag{5.24}$$

If should be noted that the second term within the brackets on the r.h.s., i.e. the one with $\dot{w}$ which represents the coupling with the wall deformation, is omitted in Yang's derivation [72]. In the case of free vibrations the circular frequencies $\omega_i f_i(t) = \exp(i\omega_i t)$, where calculated as

$$\omega_i^2 = \frac{\lambda_i g}{R}\tanh\left(\frac{\lambda_i H}{R}\right) \tag{5.25}$$

with ω_i's being the sloshing frequencies. Since $J_1\left(\lambda_i\left(r/R\right)\right)$ is an eigenfunction corresponding to the eigenvalue λ_i, orthogonality condition holds

$$\int_0^1 J_1\left(\lambda_i r'\right) J_1\left(\lambda_n r'\right) r' dr' = \frac{\lambda_n^2 - 1}{2\lambda_n^2} J_1^2\left(\lambda_n\right)\delta_{i,n}$$
$$r' = \frac{r}{R} \tag{5.26}$$

where $\delta_{i,n}$, is the Kronecker delta symbol. The dependence on r in equation 5.24 disappears by multiplying both sides of equation 5.24 with $J_1\left(\lambda_n\left(r/R\right)\right)\left(r/R\right)$ and integrating over $0 \le \left(r/R\right) \le 1$. Now the following relation for the product $C_n f_n\left(t\right)$ can be derived:

$$
\begin{aligned}
&C_n\left[\ddot{f}_n(t)\cosh\left(\frac{\lambda_n H}{R}\right)+\ldots\right.\\
&\left.\ldots g\frac{\lambda_n}{R}\sinh\left(\frac{\lambda_n H}{R}\right)f_n(t)\right]=\\
&=-4g\frac{H}{R}\frac{\lambda_n^2}{J_1(\lambda_n)(\lambda_n-1)}\ldots\\
&\ldots\sum_{i=1}^{\infty}\left[\dot{x}_g+(-1)^{i-1}(2i-1)\frac{\pi}{2}\beta_i\dot{w}\right]\ldots\\
&\ldots\times\frac{1}{(\lambda_n H/R)^2+\left[(2i-1)\frac{\pi}{2}\right]^2}
\end{aligned}
\tag{5.27}
$$

Using the identity,

$$
\sum_{i=1}^{\infty}\frac{2}{x^2+\left[(2i-1)\frac{\pi}{2}\right]^2}=\frac{1}{x}\tanh x \tag{5.28}
$$

and equation 5.25 the following differential equation for $C_n f_n(t)=\tilde{f}_n(t)$ can be derived:

$$\ddot{\tilde{f}}_n + \omega_n^2 \tilde{f}_n = -2g \frac{\lambda_n}{J_1(\lambda_n)\left(\lambda_n^2 - 1\right)} \times \ldots$$

$$\ldots \left[\frac{\sinh\left(\lambda_n \frac{H}{R}\right)}{\cosh^2\left(\lambda_n \frac{H}{R}\right)} \dot{x}_g + 2\frac{H}{R} \frac{\lambda_n}{\cosh\left(\lambda_n H/R\right)} \ldots \right. \tag{5.29}$$

$$\left. \ldots \times \sum_{i=1}^{\infty} \frac{(-1)^{i+1}(2i-1)\frac{\pi}{2}\beta_i}{\left(\lambda_n \frac{H}{R}\right)^2 + \left[(2i-1)\frac{\pi}{2}\right]^2} \dot{w} \right]$$

with

$$\kappa_n = 2 \frac{\lambda_n \frac{H}{R}}{\tanh\left(\lambda_n \frac{H}{R}\right)} \ldots$$

$$\ldots \sum_{i=1}^{\infty} \frac{(-1)^{i+1}(2i-1)\frac{\pi}{2}\beta_i}{\left(\lambda_n \frac{H}{R}\right)^2 + \left[(2i-1)\frac{\pi}{2}\right]^2} \tag{5.30}$$

This leads to:

$$\ddot{\tilde{f}}_n + \omega_n^2 \tilde{f}_n = -2g \frac{\lambda_n}{J_1(\lambda_n)\left(\lambda_n^2 - 1\right)} \cdots$$
$$\cdots \frac{\sinh\left(\lambda_n \frac{H}{R}\right)}{\cosh^2\left(\lambda_n \frac{H}{R}\right)} \left(\dot{x}_g + \kappa_n \dot{w}\right) \tag{5.31}$$

The coefficient κ_n is evaluated numerically for the integer variable n and different types of wall deformation shapes $\psi(\xi)$:

$$T1: \qquad \psi(\xi) = \sin\frac{\pi}{2}\xi$$

$$T2: \qquad \psi(\xi) = \xi$$

$$T3: \qquad \psi(\xi) = 1 - \cos\frac{\pi}{2}\xi$$

$$T4: \qquad \psi(\xi) = 1$$

The solution of equation 5.31 can be found by following Duhamel's principle, taking $\tilde{f}_n(0) = \dot{\tilde{f}}(0) = 0$, as

$$\tilde{f}_n(t) = -2g \frac{\lambda_n}{J_1(\lambda_n)(\lambda_n^2 - 1)} \frac{\sinh\left(\lambda_n \frac{H}{R}\right)}{\cosh^2\left(\lambda_n \frac{H}{R}\right)} \times \frac{1}{\omega_n} \int_0^t \sin(\omega_n(t-\tau)) \left[\dot{x}_g(\tau) + \kappa_n \dot{w}(\tau)\right] d\tau \tag{5.32}$$

Using equation 5.25 this leads to:

$$\tilde{f}_n(t) = -2R \frac{\omega_n}{J_1(\lambda_n)(\lambda_n^2 - 1)} \frac{1}{\cosh(\lambda_n H/R)} \ldots \ldots \int_0^t \sin(\omega_n(t-\tau)) \left[\dot{x}_g(\tau) + \kappa_n \dot{w}(\tau)\right] d\tau \tag{5.33}$$

In this relation the time history $\dot{x}_g$ is given, namely the round velocity excitation by the earthquake. However, $\dot{w}(t)$ is not known in advance. The time derivate of the integral on the right hand side equation 5.33 can be obtained after integration by parts with $\dot{x}_g(0) = \dot{w}(0) = 0$ as:

$$\frac{d}{dt}\int_0^t \sin\left(\omega_n(t-\tau)\right)\left[\dot{x}_g(\tau)+\kappa_n\dot{w}(\tau)\right]d\tau = \omega_n\int_0^t \cos\left(\omega_n(t-\tau)\right)\left[\dot{x}_g(\tau)+\kappa_n\dot{w}(\tau)\right]d\tau = \int_0^t \sin\left(\omega_n(t-\tau)\right)\left[\ddot{x}_g(\tau)+\kappa_n\ddot{w}(\tau)\right]d\tau \tag{5.34}$$

Using the equations 5.10, 5.23 and 5.34 the pressure distribution due to sloshing can now be found for $\varphi = 0$ as:

$$p_{2,0} = \rho\frac{\partial P_2}{\partial t} = -2\rho R... \\ ...\sum_{n=1}^{\infty}\frac{\omega_n}{\left(\lambda_n^2-1\right)}\frac{J_1\left(\lambda_n\frac{r}{R}\right)}{J_1\left(\lambda_n\right)}\frac{\cosh\left(\lambda_n\frac{z}{R}\right)}{\cosh\left(\lambda_n\frac{H}{R}\right)}... \\ ...\int_0^t \sin\left(\omega_n(t-\tau)\right)\left[\ddot{x}_g(\tau)+\kappa_n\ddot{w}(\tau)\right]d\tau \tag{5.35}$$

It is important to note that the hydrodynamic pressure due to sloshing now reflects the influence of the wall displacement by the term $\kappa_n\ddot{w}(\tau) = 0$ in addition to $\ddot{x}_g$. The sloshing pressure reported in the literature contains only the $\ddot{x}_g$ term. This additional term represents the substantial new condition to the research in the field of earthquake loaded liquid storage tanks, and the question, whether or not it can be disregarded, or

under which conditions it might become essential, is to be answered.

For the sake of brevity a parameter b_i is introduced as

$$b_i = \frac{1}{(2i-1)\frac{\pi}{2}\frac{R}{H}} \frac{I_1\left[(2i-1)\frac{\pi}{2}\frac{R}{H}\right]}{I_1'\left[(2i-1)\frac{\pi}{2}\frac{R}{H}\right]} \tag{5.36}$$

The parameter b_i can easily be estimated using asymptotic expansions. For small arguments of the Bessel function we obtain $b_i \approx 1$ and for large arguments

$$b_i \approx \frac{1}{(2i-1)\frac{\pi}{2}\frac{R}{H} - 1} \tag{5.37}$$

Finally, using equations 5.20, 5.21, 5.22 and 5.35 the pressure on the tank wall at $\varphi = 0$ can be calculated as:

$$
\begin{aligned}
&p_0(z;t) = \left[p_{1,0} + p_{2,0} + p_{3,0}\right]_{r=R} = \\
&-2\rho R\left\{\ddot{x}_g(t)\sum_{i=1}^{\infty}\frac{2(-1)^{i+1}}{(2i-1)\pi}b_i \ldots\right. \\
&\ldots\cos\left[(2i-1)\frac{\pi}{2}\frac{z}{H}\right] + \ddot{w}(t)\ldots \\
&\ldots\sum_{i=1}^{\infty}\beta_i b_i \cos\left[(2i-1)\frac{\pi}{2}\frac{z}{H}\right] + \ldots \\
&\ldots\sum_{i=1}^{\infty}\frac{\omega_i}{\lambda_i^2 - 1}\frac{\cosh\left(\lambda_i\frac{z}{R}\right)}{\cosh\left(\lambda_i\frac{H}{R}\right)}\ldots \\
&\left.\int_0^t \sin\omega_i(t-\tau)\left[\ddot{x}_g(\tau) + \kappa_i\ddot{w}(\tau)\right]d\tau\right\}
\end{aligned}
\tag{5.38}
$$

5.4 MODEL IN THE ANALYSES

The simplified model uses in the analyses analysed in chapter 6 is showed in the Figure 5.1. According to this model, a tank with a free liquid surface subjected to horizontal ground acceleration is characterised by a given fraction of the liquid that is forced to participate in this motion as rigid mass; on the other hand the motion of the tank walls excites the liquid into oscillations which result in a dynamic force on the tank. This force is assumed to be the same of a lumped mass, known as a convective mass, that can vibrate horizontally restrained by a

spring. Another part of the liquid oscillates at unison with the tank. If the flexibility of the tank wall is considered (as in the analyses of chapter 6), a part of this mass moves independently (impulsive mass) while the remaining accelerates back and forth with the tank (rigid mass). Figure 5.1 shows the idealised structural model of liquid storage tank. The contained continuous liquid mass is lumped as convective, impulsive and rigid masses are referred as m_c, m_i and m_r, respectively. The convective and impulsive masses are connected to the tank wall by different equivalent springs having stiffness k_c and k_i, respectively. In addition, each spring can be associated to an equivalent damping ratio ξ_c and ξ_i. Damping for impulsive mode of vibration can be assumed about 2% of critical for steel tanks, while the damping for convective mode can be assumed as 0,5% of critical. However, liquid damping effects are herein neglected without any loss of generality and relevance of results. Under such assumptions, this model for anchored storage tank has been extended to analyse unanchored base-isolated liquid storage tank [53].

Effective masses are given in Equations (5.45-5.49) as a fraction of the total mass m (Equation 5.49). Coefficients Y_c, Y_i, and Y_r depend upon the filling ratio S=H/R, where H is the liquid height and R is the tank radius, as clearly shown in Figure 1.

$$m_c = mY_c \tag{5.45}$$

$$m_i = mY_i \tag{5.46}$$

$$m_r = mY_r \tag{5.47}$$

$$m_{tot} = m_c + m_i + m_r \tag{5.48}$$

$$m = \pi R^2 H \rho_w \tag{5.49}$$

Similarly, natural frequencies of convective mass, ω_c and impulsive mass, ω_i (Equations 5.50-5.51) can be retrieved from [53]:

$$\omega_c = \sqrt{1.84\left(\frac{g}{R}\right)\tanh\left(1.84\frac{H}{R}\right)} \tag{5.50}$$

$$\omega_i = \frac{P}{H}\sqrt{\frac{E}{\rho_s}} \tag{5.51}$$

where E and ρ_s are the modulus of elasticity and density of tank wall respectively; g is the acceleration due to gravity; and P is a dimensionless parameter depending on the ratio H/R as well.

5.4.1 Unanchored Storage Tank

Motion of unanchored tanks can be affected by large-displacement phenomena: during the ground motion the tank can slide with respect to the foundation and the base plate may uplift due to overturning moment.

The sliding depends on the base shear: once it reaches the limit value corresponding to the frictional resistance (Equation 5.52), relative motion between the tank and the foundation starts. Sliding reduces the maximum acceleration suffered by the tank; this reduction is dependent upon to the frictional factor (μ), but relatively small values of the latter may produce large relative displacements.

Different models can be used in a sliding system to describe the frictional force. In fact, the latter can be generally modelled according two different models: conventional model and hysteretic [73]. The conventional model is discontinuous and a number of stick-slide conditions leads to solve different equations and to repeated check at every stage; on the other hand the hysteretic model is continuous and the required continuity is automatically maintained by the hysteretic displacement components. In the analyses showed in the chapter 6 the conventional model is used for the frictional force, but this assumption actually does not represent a limitation of the approach.

In detail, the friction force is evaluated by considering the equilibrium of the base: the system remains in the non-sliding

phase if the frictional force in time t is lower than the limit frictional force expressed by Equation 5.52; where g represent the gravitational acceleration.

$$F_{\lim} = m\mu g \tag{5.52}$$

Therefore the motion can be subdivided in non-sliding and sliding phases. Whenever the tank does not slide, the dynamic equilibrium of forces in Equation 5.53 applies in the case of one horizontal component, while Equation (5.54) fits the case of both horizontal components acting together.

$$F_x = -\left(m_c \ddot{x}_c + m_i \ddot{x}_i + m_{tot} \ddot{x}_b + m_{tot} \ddot{u}_{gx}\right) \tag{5.53}$$

$$\begin{cases} F_x = -\left(m_c \ddot{x}_c + m_i \ddot{x}_i + m_{tot} \ddot{x}_b + m_{tot} \ddot{u}_{gx}\right) \\ F_y = -\left(m_c \ddot{y}_c + m_i \ddot{y}_i + m_{tot} \ddot{y}_b + m_{tot} \ddot{u}_{gy}\right) \end{cases} \tag{5.54}$$

In addition, another large-displacement mechanism can be addressed according to field observations of the seismic response of unanchored liquid storage tanks; it is represented by the partial uplift of the base plate [74]. This phenomenon reduces the hydrodynamic forces in the tank, but increases significantly the axial compressive stress in the tank wall. In fact, base uplifting in tanks supported directly on flexible soil foundations does not lead to a significant increase in the axial compressive stress in the tank wall, but may lead to large foundation penetrations and several cycles of large plastic

rotations at the plate boundary [75-76]. Flexibly supported unanchored tanks are therefore less prone to elephant-foot buckling damage, but more prone to uneven settlement of the foundation and fatigue rupture at the plate-shell connection. A particularly interesting aspect is represented by the force-displacement relationship for the plate boundary. The definition of this relationship is complicated by the nonlinearities arising from: 1) the continuous variation of the contact area of the interface between the base plate and the foundation; 2) the plastic yielding of the base plate; and 3) the effect of the membrane forces induced by the large deflections of the plate.

In the following, partially uplift of the base plate is not considered in compliance with the primary objective of the paper. However, the numerical procedure that has been implemented to solve the equation of motion can be easily enhanced to take account of the phenomenon.

5.4.2 Equation of motion

The equations of motion for the unanchored tank under a two-dimensional input ground motion, for non-sliding and sliding phase, can be expressed in the following matrix format as in Equation 5.55.

$$[M]\{\ddot{z}\}+[B]\{\dot{z}\}+[K]\{z\}+\{F\}=-[M][r]\{\ddot{u}_g\} \qquad (5.55)$$

In the case of non-sliding phase (rest) of the system the equations of the motion are reported in Equation 5.56.

$$\begin{cases} m_c\ddot{x}_c + b_c\dot{x}_c + k_c x_c = -m_c\ddot{u}_{gx} \\ m_i\ddot{x}_i + b_i\dot{x}_i + k_i x_i = -m_i\ddot{u}_{gx} \\ m_c\ddot{y}_c + b_c\dot{y}_c + k_c y_c = -m_c\ddot{u}_{gy} \\ m_i\ddot{y}_i + b_i\dot{y}_i + k_i y_i = -m_i\ddot{u}_{gy} \end{cases} \quad (5.56)$$

Where x_c and y_c are the components of displacements of convective masses relative to the base; x_i and y_i are the components of displacements of impulsive masses relative to the base; x_b and y_b are the component of displacement of the base relative to the ground; $\ddot{u}_{gx}$ and $\ddot{u}_{gy}$ are the two horizontal components of ground acceleration.

In this case m_c and m_i represent two simple oscillators and there is not coupling between two directions of motion and the dimension of matrices is four, as reported in Equation 5.57 and 5.58.

$$[M] = \begin{bmatrix} m_c & 0 & 0 & 0 \\ 0 & m_i & 0 & 0 \\ 0 & 0 & m_c & 0 \\ 0 & 0 & 0 & m_i \end{bmatrix}; [B] = \begin{bmatrix} b_c & 0 & 0 & 0 \\ 0 & b_i & 0 & 0 \\ 0 & 0 & b_c & 0 \\ 0 & 0 & 0 & b_i \end{bmatrix};$$

$$[K]=\begin{bmatrix} k_c & 0 & 0 & 0 \\ 0 & k_i & 0 & 0 \\ 0 & 0 & k_c & 0 \\ 0 & 0 & 0 & k_i \end{bmatrix} \tag{5.57}$$

$$\{z\}=\begin{Bmatrix} x_c \\ x_i \\ y_c \\ y_i \end{Bmatrix}; \quad \{F\}=\begin{Bmatrix} 0 \\ 0 \\ 0 \\ 0 \end{Bmatrix}; \quad [r]=\begin{bmatrix} 1 & 0 \\ 1 & 0 \\ 0 & 1 \\ 0 & 1 \end{bmatrix}; \quad \{\ddot{u}\}=\begin{Bmatrix} \ddot{u}_{gx} \\ \ddot{u}_{gy} \end{Bmatrix} \tag{5.58}$$

If the system slides the motion depends on the dynamic equilibrium for convective and impulsive masses and for the system as a whole according to Equation 5.59; the matrices are given in Equation 5.60 and 5.61.

$$\begin{cases} m_c\ddot{x}_c + m_c\ddot{x}_b + b_c\dot{x}_c + k_c x_c = -m_c\ddot{u}_{gx} \\ m_i\ddot{x}_i + m_i\ddot{x}_b + b_i\dot{x}_i + k_i x_i = -m_i\ddot{u}_{gx} \\ m_c\ddot{x}_c + m_i\ddot{x}_i + m_{tot}\ddot{x}_b - m_{tot}\mu g\cos(\alpha) = -m_{tot}\ddot{u}_{gx} \\ m_c\ddot{y}_c + m_c\ddot{y}_b + b_c\dot{y}_c + k_c y_c = -m_c\ddot{u}_{gy} \\ m_i\ddot{y}_i + m_i\ddot{y}_b + b_i\dot{y}_i + k_i y_i = -m_i\ddot{u}_{gy} \\ m_c\ddot{y}_c + m_i\ddot{y}_i + m_{tot}\ddot{y}_b - m_{tot}\mu g\sin(\alpha) = -m_{tot}\ddot{u}_{gy} \end{cases}$$

(5.59)

The Equation (5.60) shows that convective and impulsive masses are no more two simple oscillators, but there is an inertial coupling. As shows in Equation (5.62) the sliding motion leads both to an inertial coupling and the coupling between two directions of motion.

$$[M]=\begin{bmatrix} m_c & 0 & m_c & 0 & 0 & 0 \\ 0 & m_i & m_i & 0 & 0 & 0 \\ m_c & m_i & m_{tot} & 0 & 0 & 0 \\ 0 & 0 & 0 & m_c & 0 & m_c \\ 0 & 0 & 0 & 0 & m_i & m_i \\ 0 & 0 & 0 & m_c & m_i & m_{tot} \end{bmatrix} \tag{5.60}$$

$$\{z\}=\begin{Bmatrix} x_c \\ x_i \\ x_b \\ y_c \\ y_i \\ y_b \end{Bmatrix}; \quad [B]=diag[b_c,b_i,0,b_c,b_i,0] \quad [K]=diag[k_c,k_i,0,k_c,k_i,0] \quad \{\ddot{u}\}=\begin{Bmatrix} \ddot{u}_{gx} \\ \ddot{u}_{gy} \end{Bmatrix} \quad [r]=\begin{bmatrix} 0 & 0 & 1 & 0 & 0 & 0 \\ 0 & 0 & 0 & 0 & 0 & 1 \end{bmatrix}^T \tag{5.61}$$

$$\{F\} = -m_{tot}\mu g \begin{Bmatrix} 0 \\ 0 \\ \cos(\alpha) \\ 0 \\ 0 \\ \sin(\alpha) \end{Bmatrix} \tag{5.62}$$

CHAPTER 6:

SEISMIC DEMAND AND FRAGILITY FOAM

6.1 INTRODUCTION

The numerical study presented herein aims at showing the capability of simplified model, shows in the previous section, to solve the dynamic problem for storage steel tank. In this framework the influence of various parameters of model on the seismic demand assessment can be estimated. In particular the results of incremental dynamic analysis with two horizontal ground acceleration components are discussed. In the second time the output of incremental Dynamic Analyses is used to a fragility analysis for steel storage tank. The last step of analysis consist in a FEM analysis of steel storage tank. The results of FEM analyses are compared with those obtained according to simplified design procedures.

6.2 ANALYSES WITH SIMPLIFIED MODELS

6.2.1 INCREMENTAL DYNAMIC ANALYSES

Incremental Dynamic Analysis (IDA) is adopted to analyse the seismic response of tanks under seismic loads [77] and characterise the related structural demand.

IDA requires to analyze a model under a suite of ground motion records, all scaled to several levels of intensity. The output is represented by some curves of response that relate the selected Demand Measure (DM) to the ground motion intensity, generally given by a scalar intensity measure (IM). In the following, IDA analyses taking into account generalised, two-dimensional ground motion records are presented.

Figure 1 reports the main phases of the procedure. It is worth noting that the seismic demand at a selected ground motion intensity level is obtained scaling the Peak Ground Acceleration (PGA) of the real record. The scaling factor χ varies to let PGA range between 0,05 g and 2,00 g. In order to assess the influence on seismic demand of geometrical and functional parameters, different volume capacities were considered (5000 m^3 and 30000 m^3). Furthermore, three different filling conditions were analysed (25%-50%-80%), and anchored and unanchored configuration of the tanks

were used. In the last case of unanchored tanks, a set of friction coefficients, μ, were used.

The solution of the equations presented in the previous sections was achieved by a MatLab computer code using the Wilson theta method [78].

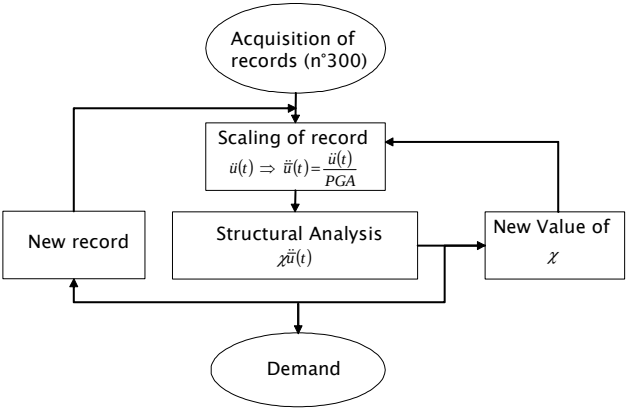

Figure 6.1. Flow chart of incremental dynamic analysis.

6.2.1.1 Matlab code

The solution of dynamics equations presented in the previous sections was achieved by a MatLab computer code. The flow chart of the procedure able to perform the time history analysis for storage tanks is shown in Figure 6.2. Firstly the check of the base velocity at time *t* has to be performed: whenever it is zero, the full knowledge of the phase of motion requires an additional check of the value of the base shear. If the base shear at time *t* is lower than the limit frictional value, the motion is rest (no-sliding) type in

$[t,t+\Delta t[$; otherwise the system, in the same time interval, slides.

If the system does not slide the check of the value of the base shear at $t+\Delta t$ is also needed. Whenever it is lower than F_{lim} the integration of the equation of dynamic equilibrium for the next Δt is possible; otherwise the computation of the time t^*, intermediate between t and $t+\Delta t$ and corresponding to base shear that reaches the limit value is needed. In other words, between t and t^* the tank does not slide while between t^* and $t+\Delta t$ slides. In order to compute the intermediate time t^* a linear variation of base shear is assumed in the time interval $[t,t+\Delta t[$.

If at time t the velocity is not equal to zero the system is in sliding phase and another check at $t+\Delta t$ is necessary; when the velocity has changed its signum between t and $t+\Delta t$ the computation of t^* corresponding to the point zero velocity is performed. Otherwise the integration of the equation of dynamic equilibrium for the next Δt can take place. The time t^* is calculated again via a linear variation of velocity. Between t and t^* the system slides but the type of motion between t^* and $t+\Delta t$ depends on the base shear at t^*: if it is lower than the limit then the system is in no-sliding (rest) between t^* and $t+\Delta t$ otherwise it is sliding. The number of equations and the number of unknowns depends on the type of motion at time t (sliding or rest).

The Figure 6.3 and 6.4 shows an example of graphic interface of implemented procedure.

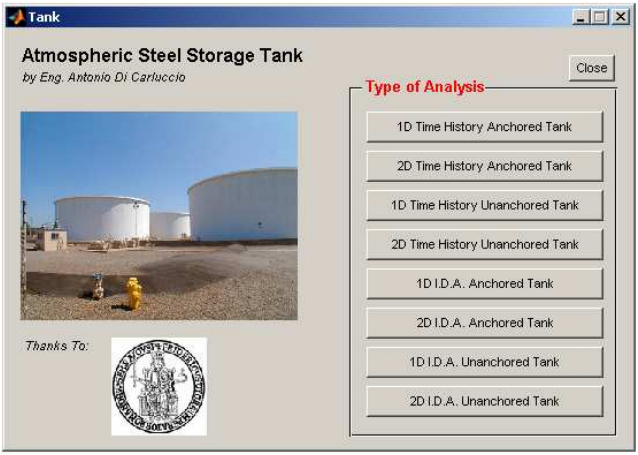

Figure 6.3. Manager window of procedure.

The Figure 6.3 shows the manager windows of procedure; is possible in this window chose the type of analysis. In the procedure, in fact, 8 types of analyses are implemented:

- 1D Time History Anchored Tank
- 2D Time History Anchored Tank
- 1D Time History Unanchored Tank
- 2D Time History Unanchored Tank
- 1D I.D.A. for Anchored Tank
- 2D I.D.A. for Anchored Tank
- 1D I.D.A. for Unanchored Tank
- 2D I.D.A. for Unanchored Tank

The Figure 6.4 shows, as example, the interface of procedure for 2D time history analyses for anchored storage tank. It's possible insert geometric and mechanical parameters for tank and for liquid; it's also possible chooses in a database of 300 earthquakes European records the record for the time history analysis and know its characteristics in terms of PGA and duration (Figure 6.5). In this window is also possible view the output of analyses.

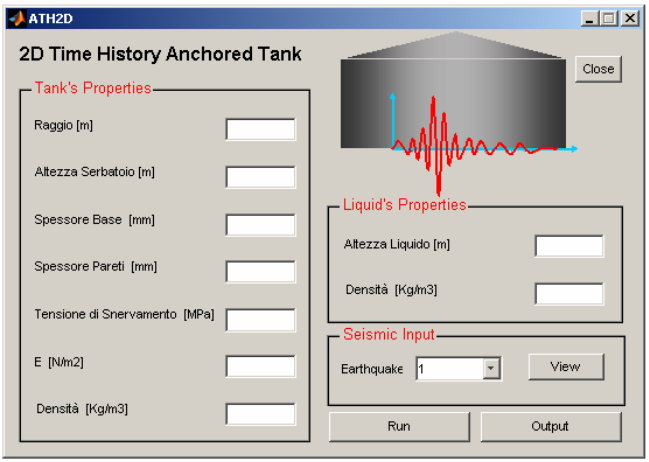

Figure 6.4. Example of graphic interface of MatLab implemented procedure.

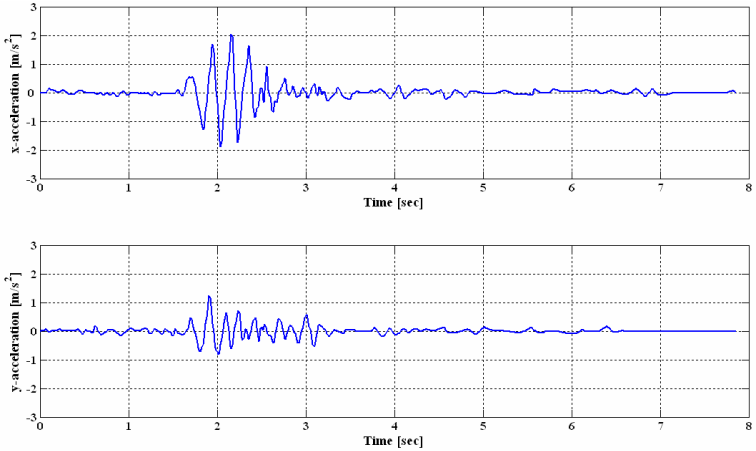

Figure 6.5. Example of graphic visualization of the horizontal components of record used for analysis.

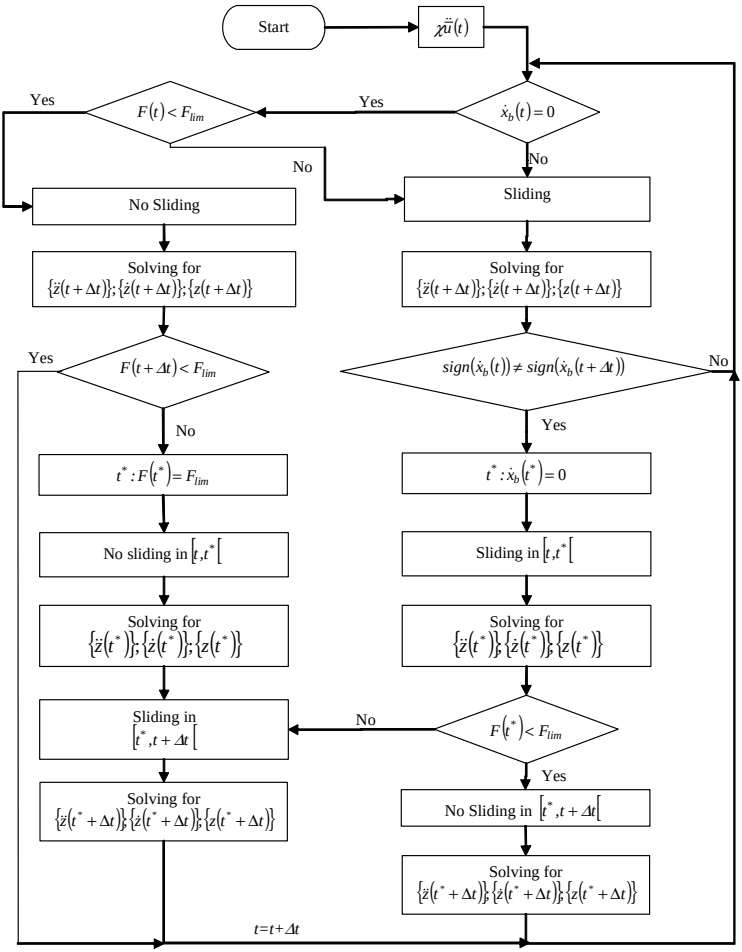

Figure 6.2. Algorithm flow chart.

6.2.2 RESULT AND DISCUSSION

The parameters of the investigated tanks are described in Table 6.1; t_b is the base plate thickness and t_s is the shell thickness; H is the height of liquid in the tank, ϱ_s and ϱ_l are the specific weights of steel and liquid respectively and E is the modulus of elasticity of the tank structure. In the parametric analysis μ (friction factor) varies from 0.1 to 0.7 (with step of 0.1).

Volume [m^3]	R [m]	h (tank) [m]	Filling [%]	H liquid [m]	ρ_s [kgm^{-3}]	ρ_l [kgm^{-3}]	E [GPa]	tb [m]	ts [m]
5000	12.25	10.80	25%	2.700	7850	1000	210	0.008	0.007
			50%	5.400	7850	1000	210	0.008	0.007
			80%	8.640	7850	1000	210	0.008	0.007
30000	22.75	18.50	25%	4.625	7850	1000	210	0.008	0.007
			50%	9.250	7850	1000	210	0.008	0.007
			80%	14.800	7850	1000	210	0.008	0.007

Table 6.1. Tank parameters.

For the analysis presented in the thesis a suitable set of 300 ground motion records are used. Selected earthquake ground motions records are all stiff soil records to avoid specific problems related to site effects.

Appendix A reports some data concerning the selected ground motion records used in the analysis needed to reproduce the analysis. All the accelerograms herein employed come from the European Strong Motion Database (http://www.isesd.cv.ic.ac.uk/) and can be easily retrieved from there.

Figure 6.6 shows an example of the demand curve in term of axial compressive stress [MPa] obtained from the bi-directional model. Curves include media and 1β bounds (β is the standard deviation of the logarithms of the demand).

Figures 6.7 and 6.8 shows as surface the seismic demand in term of axial compressive stress for all configurations. Figures shows the influence on seismic demand of boundary conditions and filling one. It appears that when filling increases seismic demand increases and the same happens when friction factor increases.

The base-displacement demand curve depending on the g.m. PGA for the set of ground motions is shown in Figure 6.9; again the median and ±1 β curves are given.

This curve represent, point to point, the median of probability distribution of the parameter which is investigated. In the case of the rigid displacement the probability distribution is conditioned not only to g.m. PGA but also to sliding motion, because not all records with an assigned value of g.m. PGA cause the sliding motion.

Figure 6.10 and 6.11 summarises the probability of sliding motion at the different $PGA_{g.m.}$ levels depending on the filling level and the friction factor μ. As could be expected, for a given value of filling level and μ, the higher is $PGA_{g.m.}$ the higher is the probability of sliding motion. At same level of $PGA_{g.m.}$ the probability of sliding motion increases as the

filling level increases, while it decreases as the friction factor grows.

Figure 6.12 and 6.13 shows the influence of filling level on the compressive stress demand, for anchored and unanchored tank respectively

Figure 6.14 and 6.15 shows the influence of filling level and friction factor on the rigid displacement respectively. For the same value of friction factor the rigid displacement increases when filling level increases. The variability of filling level have influence both on the mean value and on standard deviation. The variability of friction factor, as shows in Figure 6.15, has the same influence; in fact for the same value of filing level the rigid displacement increases when friction factor decreases.

Figures 6.16 and figure 6.17 shows the influence of filling level on the probability of failure 30000 m^3. It is worth noting that the probability of failure for EFB is strictly related to the filling level and it increases when the felling level increase. In figure 6.18 it's showed the of friction factor on probability of failure EFB. The figure shows the effect of base restraint of the tank. In fact, it shows the different between fragility curve for different values of friction factor. Plots also point out the positive effect of sliding on the probability of failure for EFB failure mode. The effect of sliding is similar to the effect of seismic base isolator; it

reduce the acceleration on liquid mass and so reduce the overturning moment and compressive stress in the wall tank.

In Figure 6.19 are plotted the numerical probability of failure previous calculated (F_{calc}) and observational fragility (F_{obs}) and the relative ratio of EFB respect to the observational fragility are also showed . The specific failure mode here analysed is more effective at high PGA whereas at low PGA.

Figure 6.20 and 6.21 report some numerical results able to demonstrate the effects of contemporary presence of the two horizontal components; thus a comparison between uni-directional and bi-directional results in terms of base-displacement can be done. These two analyses are not equivalent; in fact, the maximum base displacement in X direction for the one-dimensional analysis is 0.0692m while when the second component is taken into consideration the displacement goes to 0.1584m. The same effect can be recognised in terms of displacements along Y direction, that are characterised by a maximum equal to 0.0379m when one-dimensional analysis is performed and equal to 0.1162m when the two components are introduced. In the Figure 6.22, as example, the trajectory of tank is plotted. It represents the displacement of tank's geometric barycentre for the 000187-Iran earthquake.

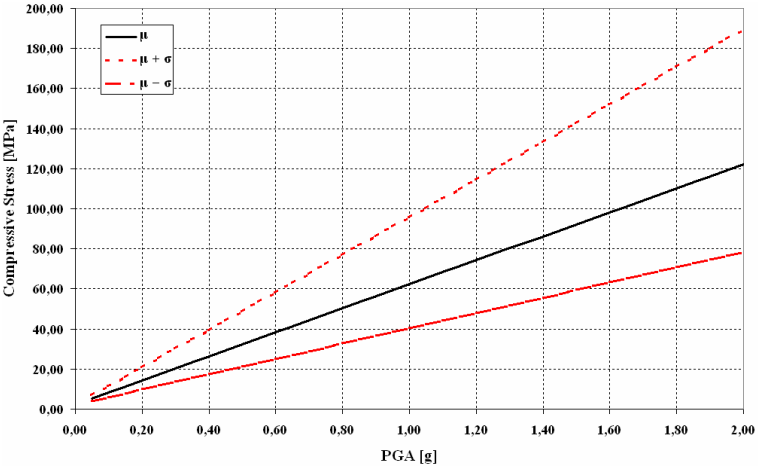

Figure 6.6. IDA curve for the compressive axial stress for the anchored storage tank with V= 30000 m^3 and filling level equal to 50%.

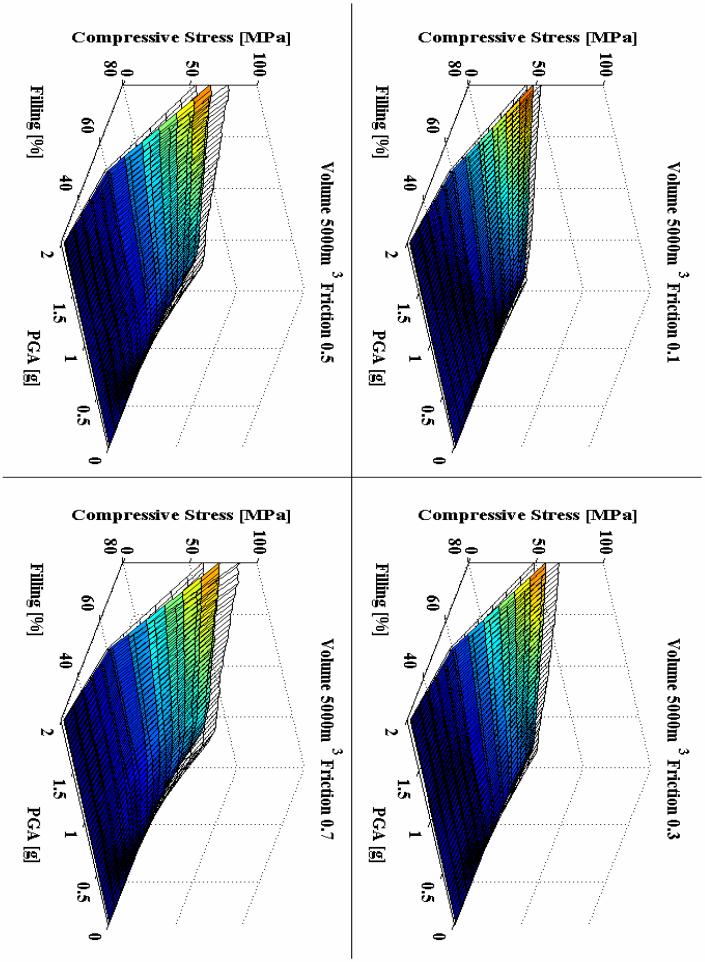

Figure 6.7. Seismic demand results analyses for the unanchored storage tank with V= 5000 m³.

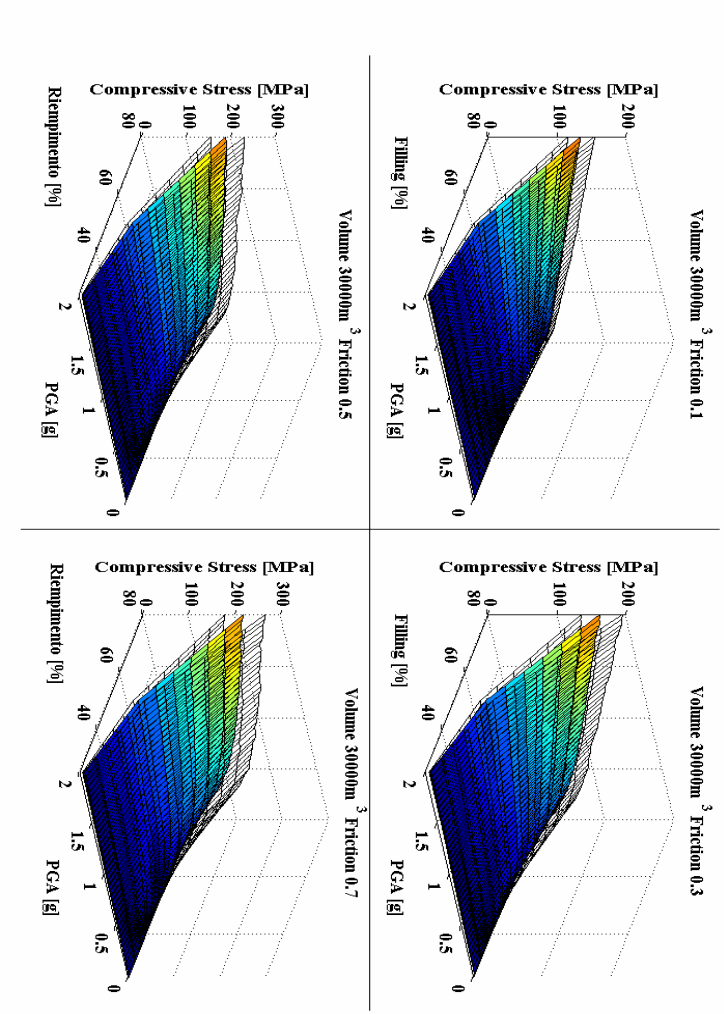

Figure 6.8. Seismic demand results analyses for the unanchored storage tank with V= 30000 m^3.

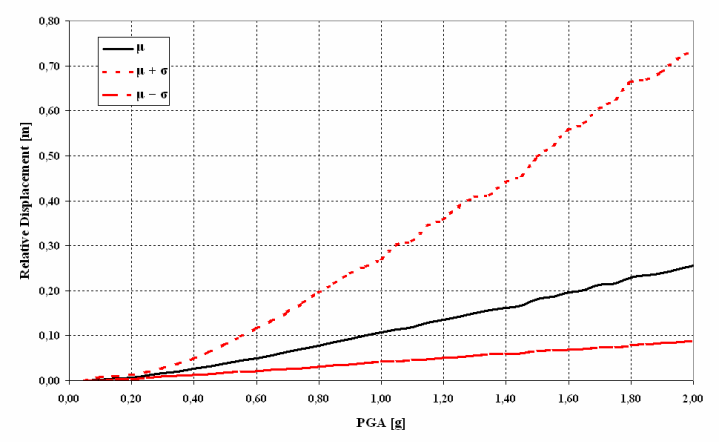

Figure 6.9. IDA for the sliding-induced displacement for the bi-directional analysis for the unanchored storage tank with V= 5000 m³, filling level equal to 80% and friction factor equal to 0.3.

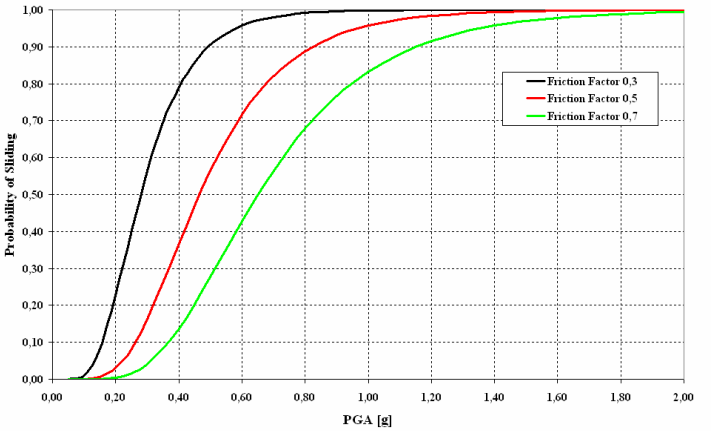

Figure 6.10. Probability of sliding for unanchored storage tank with V= 30000 m³, filling level equal to 50%, and friction factor equal to 0.7, 0.5 and 0.3.

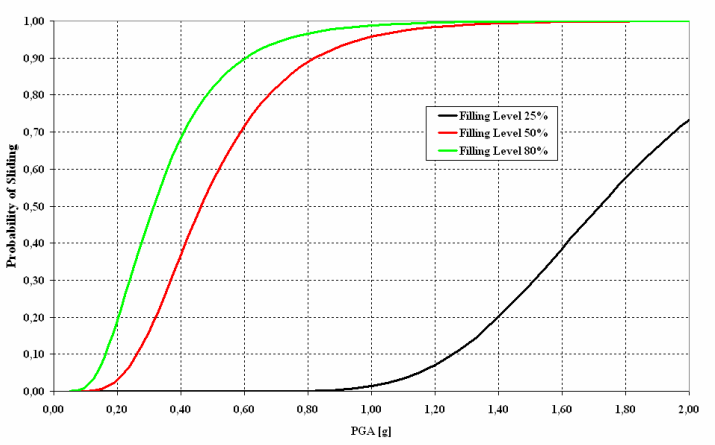

Figure 6.11. Probability of sliding for unanchored storage tank with V= 30000 m³, friction factor equal to 0.5 and filling level equal to 25%, 50% and 80%.

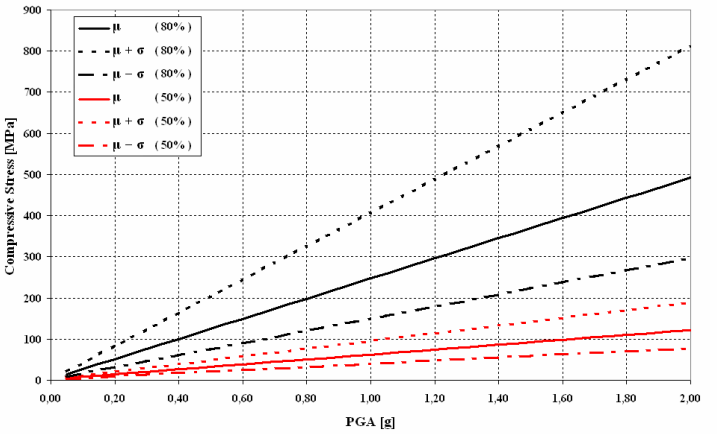

Figure 6.12. IDA curve for the compressive axial stress for the anchored storage tank with V= 30000 m³ and filling level equal to 80% and 50%.

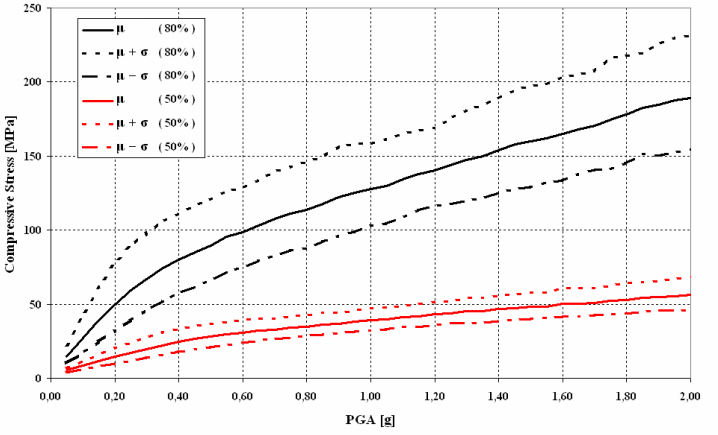

Figure 6.13. IDA curve for the compressive axial stress for the unanchored storage tank with V= 5000 m³, filling level equal to 80% and 50% and friction factor equal to 0.5.

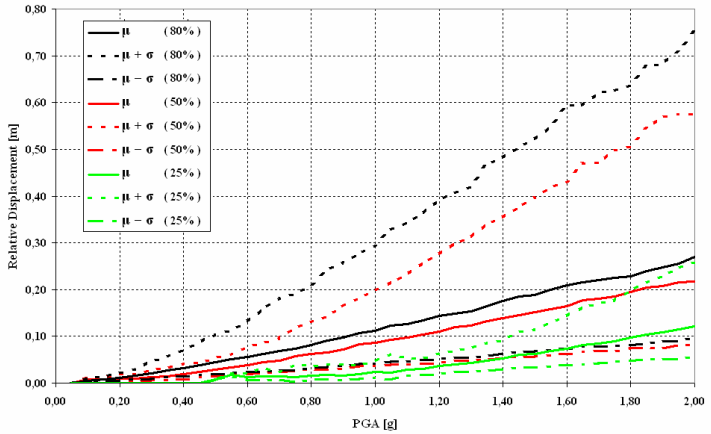

Figure 6.14. IDA for the sliding-induced displacement for the bi-directional analysis for the unanchored storage tank with V= 30000 m³, filling level equal to 80%, 50% and 25% and friction factor equal to 0.3.

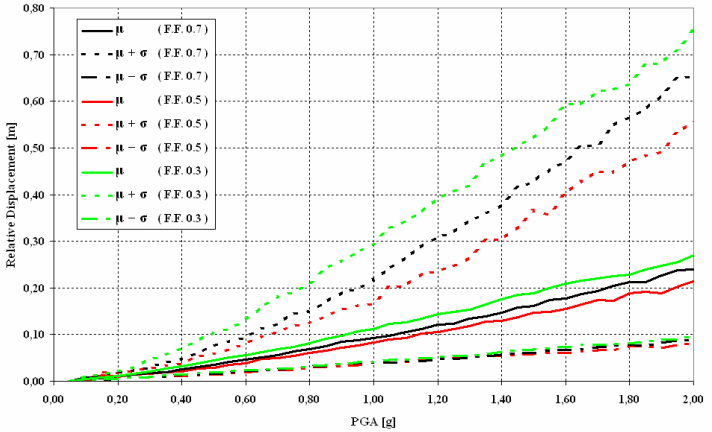

Figure 6.15. IDA for the sliding-induced displacement for the bi-directional analysis for the unanchored storage tank with V= 30000 m^3, filling level equal to 80%, and friction factor equal to 0.7, 0.5 and 0.3.

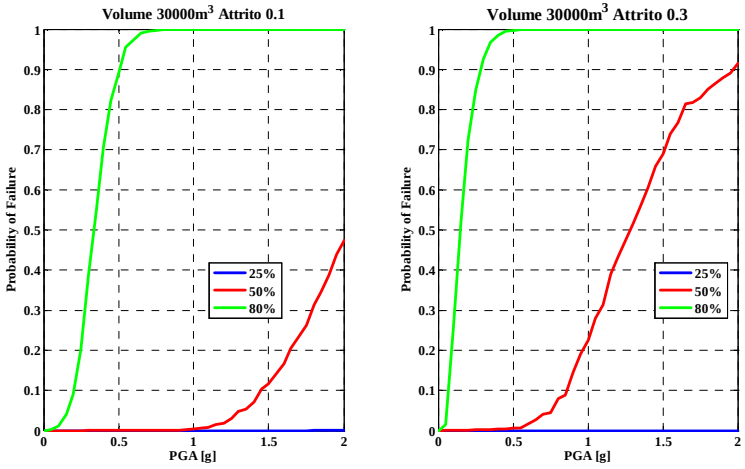

Figure 6.16. Probability of failure for EFB failure mode for tank with 30000 m^3 .

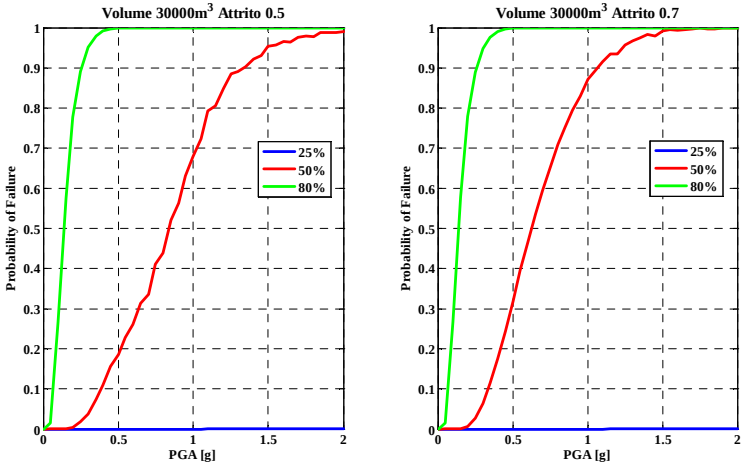

Figure 6.17. Probability of failure for EFB failure mode for tank with 30000 m^3 .

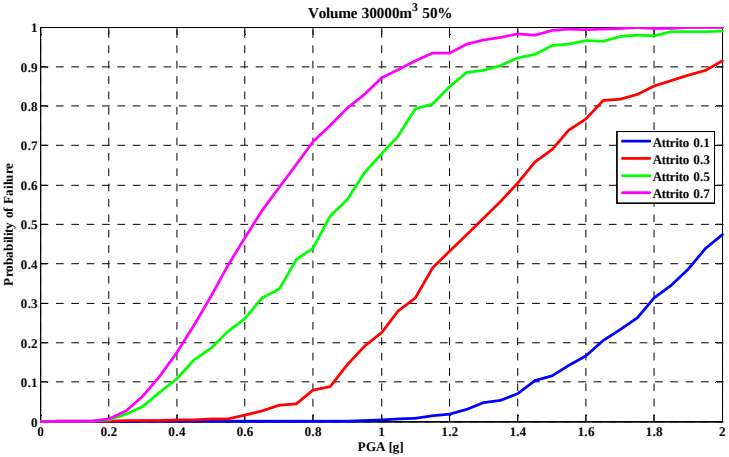

Figure 6.18. Probability of failure for EFB failure mode for tank with 30000 m^3 , filling 50% and different value of friction factor.

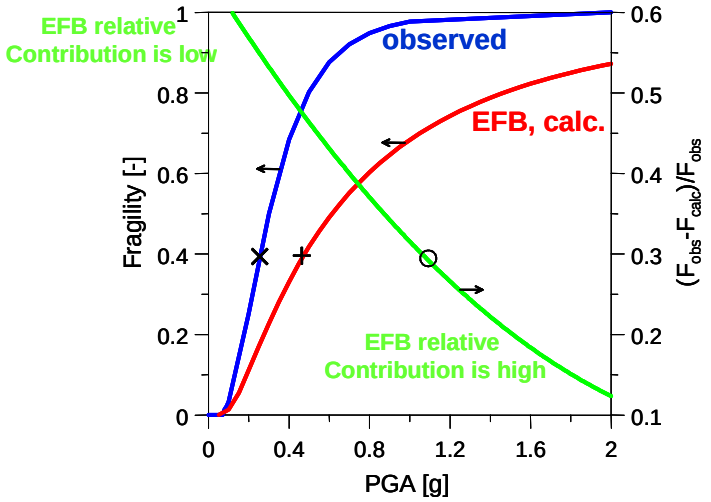

Figure 6.19. probability of failure in terms of calculated (F_{calc}, +) and observational (F_{obs}, x) fragility and relative contribution of EFB over the total fragility (o) with respect to PGA.

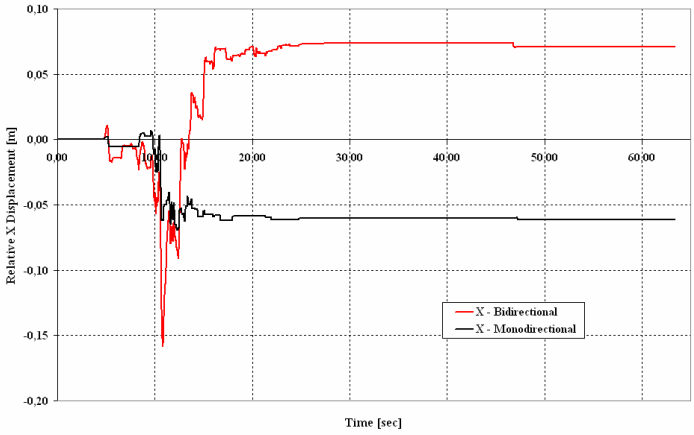

Figure 6.20. Comparison of uni-directional and bi-directional analyses, along x axis, for the 000187 earthquake.

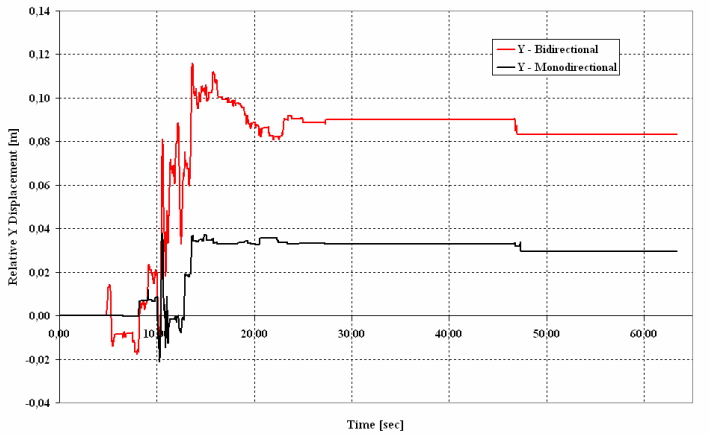

Figure 6.21. Comparison of uni-directional and bi-directional analyses, along x axis, for the 000187 earthquake.

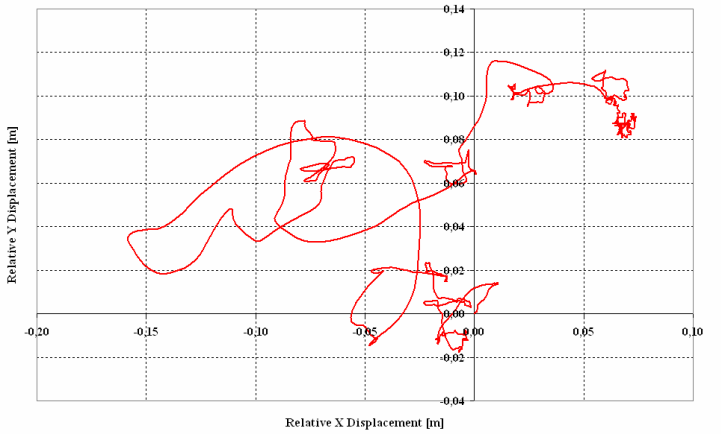

Figure 6.22. Trajectory of Tank for the 000187 earthquake.

6.3 FEM ANALYIS AND VALIDATION OF SIMPLIFIED MODELS

6.2.1 INCREMENTAL DYNAMIC ANALYSES

In the present section, three different geometric configurations have been considered, depending on the filling level γ. Tanks have however similar volume capacity, about 5000 m^3. Geometrical properties of the different models analyzed are summarized in the Table 6.2; the mechanical parameters used are the following:

$$E = 2.1E+11\ N/m^2\ ,\ \rho_s = 7850\ kg/m^3\ ,$$
$$\rho_l = 1000\ kg/m^3\ ,\ \nu = 0.3$$

	Radius R [m]	Height Tank [m]	Height Liquid H [m]	Filling Level	Thickness [m]	Volume [m^3]
Model A	14.50	8.50	7.50	0.5	0.008	4951.39
Model B	11.60	12.60	11.60	1.0	0.008	4901.21
Model C	8.00	25.00	24.00	3.0	0.008	4823.04

Table 6.2: Steel tanks relevant data.

For each configuration a time history analysis with LsDyna's finite element program and a calculation with the simplified procedures reported in section 3 have been carried out. As the lumped mass is concerned, a trial evaluation of the response neglecting damping has been performed. The record used for time history analysis is showed in Figure 6.23.

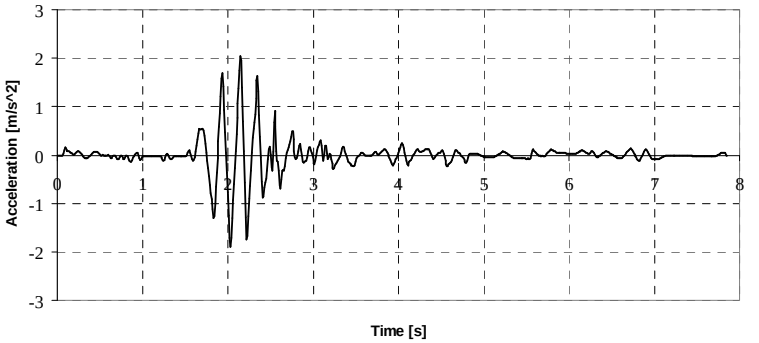

Figure. 6.23: Earthquake code 173; station code 132; European Strong-Motion Data used for analysis.

The finite element analyses (Figure 6.24) presented have been performed with Ls-Dyna code using a Lagrangian approach. The Finite Element program used in the analysis is Ls-Dyna [79, 80]. Ls-Dyna uses an explicit Lagrangian numerical method to solve nonlinear, three dimensional, dynamic, large displacement problems. Implicit, arbitrary Lagrangian-Eulerian, Smoothed Particle Hydrodynamics (also known as SPH) are also available. The most advantageous feature of Ls-Dyna consists of its advanced contact algorithms. For the modeling of tank wall three and four joints shell elements has been used; the liquid has been modelled with solid elements. Details on the analysed models are shown in Figure 6.24 and Table 6.3.

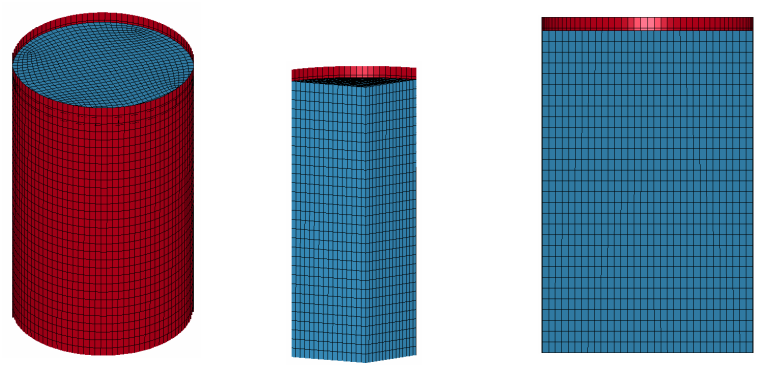

Figure. 6.24: LsDyna Finite Element models.

The material models used are MAT_1 for the steel and MAT_9 for the liquid. The MAT_1 in LsDyna is an isotropic elastic material and is available for beam, shell, and solid elements. In this elastic material the code compute the co-rotational rate of deviatoric Cauchy stress tensor and pressure as follows:

$$S_{ij}^{\nabla^{n+\frac{1}{2}}} = 2G\dot{\varepsilon}_{ij}^{'\,n+\frac{1}{2}} \quad p^{n+1} = -K\ln V^{n+1} \tag{6.1}$$

Where G and K are the elastic shear modulus and bulk modulus and V is the relative volume, i.e., the ratio of the current volume to the initial volume. The MAT_9 is the NULL material. This material takes account of the equation of state without computing deviatoric stress and also this material has no shear stiffness. It has no yield strength and behaves in fluid-like manner. For the analyses presented the

equation of state associated with MAT_9 the Grunesein's equation of state (EOS_4). The Gruneisen's equation of state with cubic shock velocity-particle velocity defines pressure for compressed material:

$$p = \frac{\rho_0 C^2 \mu \left[1 + \left(1 - \frac{\gamma_0}{2} \right) \mu - \frac{a}{2} \mu^2 \right]}{\left[1 - (S_1 - 1)\mu - S_2 \frac{\mu^2}{\mu + 1} - S_3 \frac{\mu^3}{(\mu + 1)^2} \right]} + \ldots \quad (6.2)$$
$$\ldots (\gamma_0 + \alpha\mu) E$$

Where E is the internal energy for initial volume, C is the intercept of the u_s-u_p curve, S_1, S_2 and S_3 are the coefficients of the slope of the u_s-u_p curve, γ_0 is the Gruneisen gamma, and a is the first order volume correction to γ_0. The compression is defined in terms of the relative volume, V, as $\mu = 1/V - 1$. For the atmospheric liquid all parameters of EOS_4 must be equal to zero except the sound velocity C. As contact type a Contact Node to Surface is used. For the three analyses a dynamic relaxation of 2 seconds has been considered, as clearly shown in the time histories reported in Figures 6.25-6.26-6.27.

	Shell elements	Solid elements	Solution time (sec.)
Model A	18447	13500	7402
Model B	26880	21000	13957
Model C	35900	29280	18422

Table. 6.3: Description of LsDyna Finite Element models.

The latter reports for each configuration the comparison between the base shear evaluated according to EC8 simplified procedure discussed in previous section, the lumped mass dynamic model and the full stress LsDyna FEM analysis. In Figures 6.28-6.29-6.30 FEM results are given in terms of liquid displacements along the earthquake direction. In particular, the surfaces characterised by the same displacement are shown. It is thus possible to observe the differences in terms of volume activated by the base motion depending on the aspect ratio of the tank. As base shear is concerned, direct evaluation of the peak base shear according to EC8 seems to be in good agreement with time histories results and FEM analyses in particular. It is also clearly shown that despite the large scatter in terms of computational effort, lumped mass models, that in any case reflects the absence of damping, and LsDyna FEM results are not so different in terms of seismic demand evaluation.

Figures 6.31 and 6.32 shows the displacement along earthquake direction of the joints on the vertical gravity line and the vertical displacement of freeboard surface of liquid.

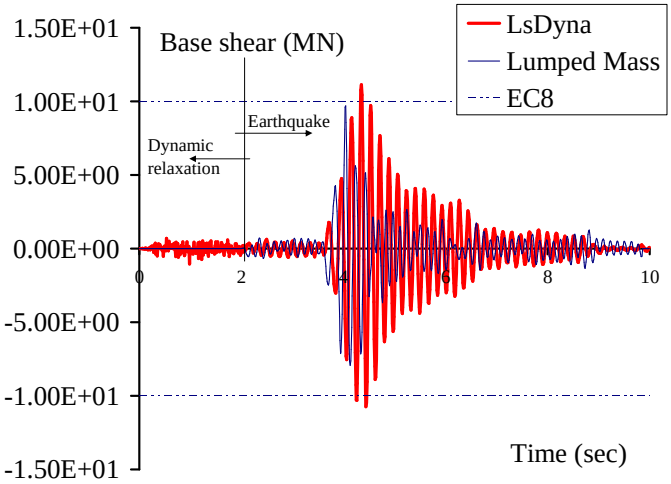

Figure. 6.25: Comparison of results for model A.

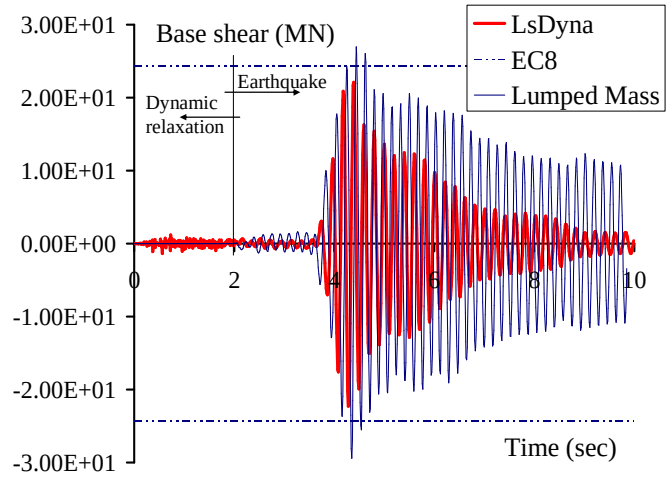

Figure. 6.26: Comparison of results for model B.

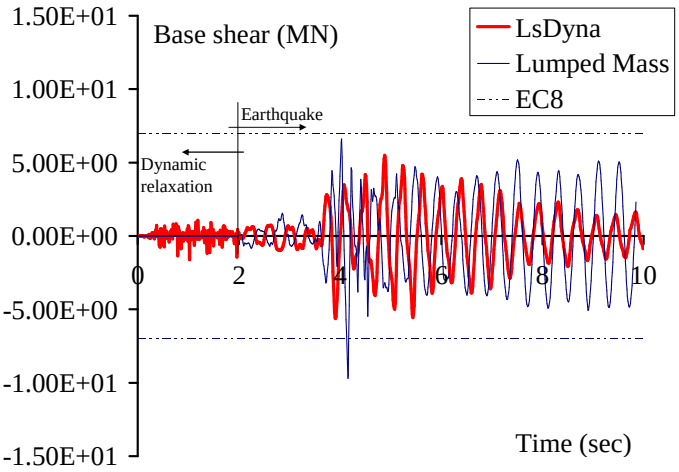

Figure. 6.27: Comparison of results for model C.

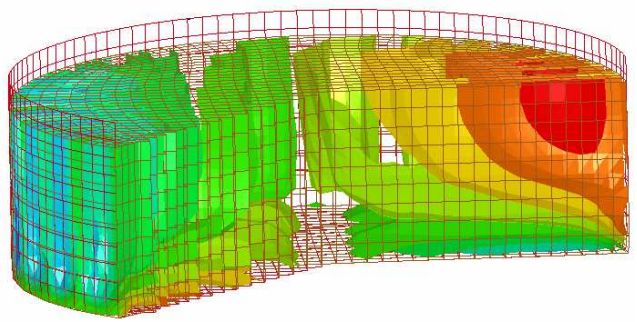

Figure. 6.28: Iso-surface of x-displacement for model A.

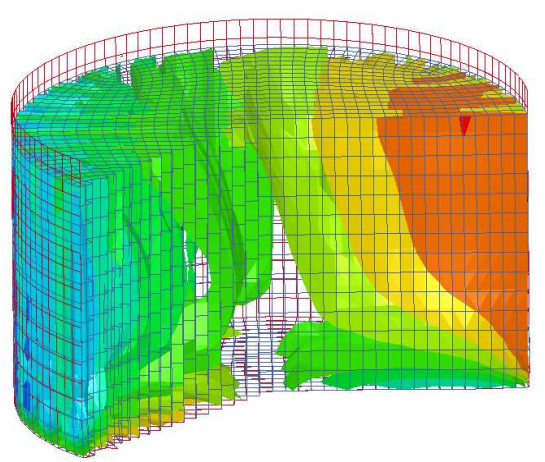

Figure. 6.29: Iso-surface of x-displacement for model B.

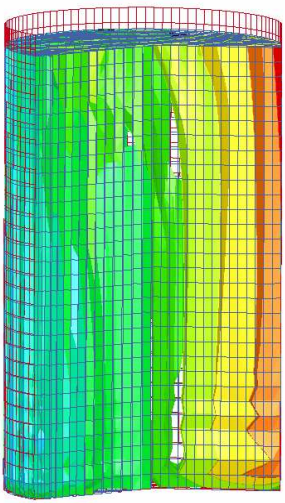

Figure. 6.30: Iso-surface of x-displacement for model C.

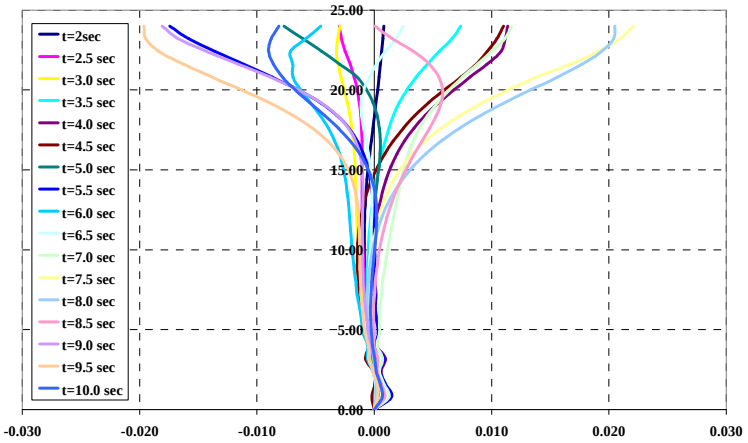

Figure. 6.31: Displacement of joints on vertical gravity line along earthquake direction for Model C.

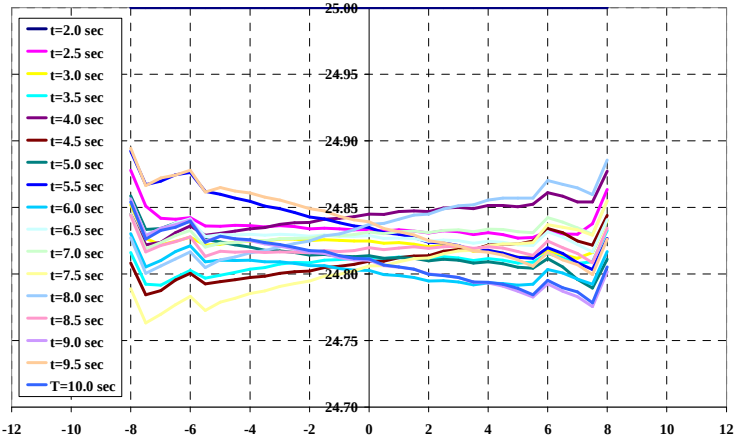

Figure. 6.32: Vertical displacement of freeboard surface for Model C.

CHAPTER 7:

CONCLUSIONS

The work done during the doctorate activity is inserted within a research activity very broad and interdisciplinary which seeks to quantify the industrial risk. Among possible external events attention has been paid to the seismic event.

The main objective is the definition of a clear classification of industrial constructions from the structural engineering perspective. The study represents a useful support for QRA analysts in seismic areas, because it ensures a simulated design of constructions and processes even when data are not available. Standardisation of details, supports, anchorages and structural solutions, has been reached and a number of design tables has been issued covering critical equipments.

Among the various structural equipment presents in a industrial plant has decided to focus attention on the atmospheric storage steel tanks. This choice was determined by different factors. First of all, they are components that are intrinsic hazard due to the fact that very often contain hazardous materials. Moreover, a large database of post earthquake damage exists and finally are present in many

industrial plants. For this reasons a seismic fragility analysis of this structure has been made. The seismic response of anchored and unanchored atmospheric steel tanks for oil storage is investigated in terms of limit states relevant for industrial risk analysis (Elephant Foot Buckling and base-sliding). Algorithms to integrate equations of motions have been formulated for both one-directional. The model does not include the base uplifting, which may affect compressive stress demand, but it is ready to. The model has been employed to produce incremental dynamic analysis demand curves as for building-like structures. Comparison of the two models has also been carried out, results show that the unidirectional results may be un-conservative, at least in terms of base-displacement demand for sliding tanks.

IDA curves can also be similarly developed for bidirectional ground motion, for example using as ground motion intensity measure the geometric mean of the PGA in the two directions, and therefore the model showed in previous section was used effectively for the computation of numerical seismic fragility curves.

Advanced FEM analysis have been carried out and a comparison between simplified procedures proposed by Eurocode 8 and used to develop seismic fragility of tanks has been discussed. A satisfactory capacity of simplified models to fit the overall response of tanks has been shown. This circumstance is by far more relevant, since

computational efforts for full stress analyses are huge compared to those required by simplified methods. Another interesting aspect is related to the capacity of simplified procedures suggested by Eurocode to give good estimates of the peak base shear. Further investigations are needed to confirm such results and collect a significant number of case studies.

REFERENCES

[1] Salzano, E., Di Carluccio, A., Agreda, A.G., Fabbrocino, G., Manfredi, G., The Interaction of Earthquakes with Process Equipment in the Framework of Risk Assessment, 41st Annual Loss Prevention Symposium, Houston (TX), 2007.

[2] Salzano, E., Di Carluccio, A., Agreda, A.G., Fabbrocino, G., Risk Assessment and Early Warning Systems for Industrial Facilities in Seismic Zones, 12th International Symposium Loss Prevention and Safety Promotion in the Process Industries., 2007.

[3] Council Directive 96/82/EC of 9 December 1996 on the control of major-accident hazards involving dangerous substances, Official Journal of the European Communities, L 10/13, Brussels, 1997.

[4] F.P. Lees, Loss Prevention in the Process Industries, second ed., Butterworth-Heinemann, Oxford, 1996.

[5] Generic Letter 88-20, Supplement No. 4, Individual Plant Examination of External Events (IPEEE) for Severe Accident Vulnerabilities - 10 CFR 50.54(f), U.S. Nuclear Regulatory Commission, April 1991.

[6] NUREG-1407, Procedural and Submittal Guidance for Individual Plant Examination of External Events (IPEEE) for Severe Accident Vulnerabilities, U.S. Nuclear Regulatory Commission, June 1991.

[7] NUREG/CR-5042, Evaluation of External Hazard to Nuclear Power Plants in the United States, U.S. Nuclear Regulatory Commission, December 1987.

[8] NUREG/CR-5042 Supplement 2, Evaluation of External Hazard to Nuclear Power Plants in the United States - Other External Events, U.S. Nuclear Regulatory Commission, February 1989.

[9] NUREG/CR-2300, PRA Procedure Guide: A Guide to the Performance of Probabilistic Risk Assessments for Nuclear Power Plants, U.S. Nuclear Regulatory Commission, 1983.

[10] NUREG/CR-4839, Methods for External Event Screening Quantification: Risk Methods Integration and Evaluation Program (RMIEP), U.S. Nuclear Regulatory Commission, July 1992.

[11] NUREG/CR-6033, NRC Seismic Margin Methodology: Update and Supplementary Guidance, U.S. Nuclear Regulatory Commission, 1992.

[12] Campbell, K.W., Strong ground motion attenuation relationships; a ten-year perspective, Earthquake Spectra 1, pp. 759-804, 1985.

[13] Joyner, W.B., Boore, D.M., Measurement, characterization, and prediction of strong ground motion, Proc. Of Earthquake Engineering & Soil Dynamics II, GT Div/ASCE, Park City, Utah, June 27-30, pp.43-102, 1988.

[14] Di Carluccio, A., Iervolino, I., Manfredi, G., Fabbrocino, G., Salzano, E., Quantitative probabilistic seismic risk analysis of storage facilities, in: Proc. CISAP-2, Chem. Eng. Trans. 9, 215, 2006.

[15] Guidelines For Seismic Evaluation and Design of Petrochemical Facilities, Task committee on seismic evaluation and design of petrochemical facilities, The American Society of Civil Engineers Petrochemical Energy Committee.

[16] NUREG-75/087, Standard Review Plan for the Review of Safety Analysis for Nuclear Power Plants, U.S. Nuclear Regulatory Commission, July 1975.

[17] Vesely, W.E., Goldberg, FR, Roberts, N.H., Haasl, D.F., Fault Tree Handbook, 1981.

[18] Perry, R.H., and Green, D., Perry's chemical engineering handbook. 6th ed. New York: McGraw-Hill. (ISBN 0-07-049479-7), 1984.

[19] Martin, R.J., Ali Reza, A., Anderson, L.W., What is an explosion? A case history of an investigation for the insurance, Journal of Loss Prevention in the Process Industries, 13, pp. 491-497, 2000.

[20] CCPS, Center for Chemical Process Safery of the American Institute of Chemical Engineers, Guidelines for chemical process quantitative risk analysis, Center for Chemical Process Safety of the American Institute of Chemical Engineers, New York, 1989.

[21] CCPS, Center for Chemical Process Safety of the American Institute of Chemical Engineers, Guidelines for evaluating the characteristics of VCEs, Flash Fires and BLEWs, Center for Chemical Process Safety of the American Institute of Chemical Engineers, New York, 1994.

[22] ACI 350.3, Seismic design of liquid containing concrete structures", An American Concrete Institute Standard, 2001.

[23] AWWA D-100, Welded steel tanks for water storage", American Water Works Association, Colorado, 1996.

[24] AWWA D-103, Factory-coated bolted steel tanks for water storage, American Water Works Association, Colorado, 1997.

[25] AWWA D-110, Wire- and strand-wound circular, prestressed concrete water tanks, American Water Works Association, Colorado, 1995.

[26] AWWA D-115, Circular prestressed concrete water tanks with circumferential tendons, American Water Works Association, Colorado, 1995.

[27] API 650, Welded storage tanks for oil storage, American Petroleum Institute Standard, Washington D. C., 1998.

[28] Eurocode 8, Design provisions for earthquake resistance of structures, Part 1-General rules and Part 4–Silos, tanks and pipelines, European committee for Standardization, Brussels, 1998.

[29] Eurocode 3, Design of Steel Structures, Part 4-2, European committee for Standardization, Brussels, 1998.

[30] Eurocode 3, Design of Steel Structures, Part 1-6: General Rules: Supplementary Rules for the Strength and Stability of Shell Structures, European committee for Standardization, Brussels, 1998.

[31] Housner,G.W., Dynamic analysis of fluids in containers subjected to acceleration, Nuclear Reactors and Earthquakes, Report No. TID 7024, U.S. Atomic energy Commission, Washington D.C,1963.

[32] Wozniak, R.S., Mitchell, W.W., Basis of seismic design provisions for welded steel oil storage tanks, American Petroleum Institute 43rd midyear meeting, session on Advances in Storage Tank Design, Toronto, Canada, 1978.

[33] Veletsos, A.S., Young, Earthquake response of liquid storage tanks, Proc. of 2nd Engg. Mechanics specialty conf. ASCE Raleigh, 1-24, 1977.

[34] Veletsos, A.S., Seismic response and design of liquid storage tanks, Guidelines for Seismic design of oil & gas pipelines system, ASCE, NY, 255-370, 1984.

[35] Haroun, M.A., Housner, G.W., Seismic design of liquid storage tanks, Journal of Technical Councils of ASCE, Vol. 107, No. TC1, 191-207, 1981.

[36] Malhotra, P.K., Wenk, T., Wieland, M., Simple procedure for seismic analysis of liquid storage tanks, Structural Engineering, IABSE, Vol. 10, No.3, 197-201, 2000.

[37] Sakai, F., Ogawa, H., Isoe, A., Horizontal, vertical and rocking fluid elastic response and design of cylindrical liquid storage tanks, Proc. of 8th World conference on Earthquake Engineering, San Francisco, Calif. Vol. V, 263-270, 1984.

[38] Haroun, M.A., Tayel, M.A., Axisymmetrical vibrations of tanks-Numerical, Journal of Engineering Mechanics, ASCE, Vol. 111, No. 3, 329-345, 1985.

[39] Jacobsen, L.S., Impulsive Hydrodynamics of Fluid Inside a Cylindrical Tank and of a Fluid Surrounding a Cylindrical Pier, Bulletin of the Seismological Society of America, Vol. 39, pp. 189-204, 1949.

[40] Graham, E.W., Rodriguez, A.M., The Characteristics of Fuel Motion Which Affect Airplane Dynamics, Journal of Applied Mechanics, Vol. 19, No. 3, pp. 381-388,1952.

[41] Housner, G., Dynamic Pressure on Accelerated Fluid Containers, Bulletin of the Seismological Society of America, Vol. 47, pp. 15-35, 1957.

[42] Housner, G.W., Dynamic behaviour of water tanks, Bulletin of Seismological Society of America, (53), 381-387, 1963.

[43] Hanson, R.D., Behaviour of Liquid Storage Tanks, Report, National Academy of Sciences, Washington D.C., pp. 331-339, 1973.

[44] Veletsos, A.S., Seismic Effects in Flexible Liquid Storage Tanks, Proceedings of the 5h World Conference on Earthquake Engineering, Rome, Italy, Vol. l, pp. 630-639, 1974.

[45] Veletsos, A.S., Yang, J.Y., Dynamics of Fixed Base Liquid Storage Tanks, Proceedings of U.S.-Japan Seminar on Earthquake Engineering Research with Emphasis on Lifeline Systems, Japan Society for Promotion of Earthquake Engineering, Tokyo, Japan, pp. 317-341, November 1976.

[46] Rosenblueth, E. & Newmark, N.M., Fundamentals of Earthquake Engineering, Prentice-Hall: NJ, 1971.

[47] Haroun, M.A., Dynamic Analyses of Liquid Storage Tanks, Earthquake Engineering Research Laboratory, Report No. EERL 80-4, California Institute of Technology, February 1980.

[48] Haroun, M.A., Stress Analysis of Rectangular Walls Under Seismically Induced Hydrodynamic Loads, Bulletin of the Seismological Society of America, Vol. 74, N o. 3, pp. 1031-1041, June 1984.

[49] Haroun, M.A., Warren, W.L., TANK-A Computer Program for Seismic Analysis of Tanks, Proceedings of the Third Conference on Computing in Civil Engineering, ASCE, California, pp. 665-674, April 1984.

[50] Haroun, M. A., Vibration Studies and Tests of Liquid Storage Tanks, Journal of Earthquake Engineering and Structural Dynamics, Vol. 11, pp. 179-206, 1983.

[51] Haroun, M.A., Housner, G.W., Complications in Free Vibration Analysis of Tanks, Journal of Engineering Mechanics, ASCE, Vo1.108, pp. 801-818, 1982.

[52] Haroun, M.A., Housner, G.W., Dynamic Characteristics of Liquid Storage Tanks, Journal of Engineering mechanics, ASCE, Vo1.108, pp. 783-800, 1982.

[53] Shrimali, M.K., R.S. Jangid, Seismic response of liquid storage tanks isolated by sliding bearings, Engineering Structures, 24, 909-921, 2002.

[54] Edwards, N.W., A Procedure for Dynamic Analysis of Thin Walled Cylindrical Liquid Storage Tanks subjected to Lateral Ground Motions, Ph.D. Thesis, University of Michigan, Ann Arbor, 1969.

[55] Grilli, S.T., Skourup, J., Svendsen, L.A.., The Modelling of Highly Nonlinear Water-Waces-A Step Toward a Numerical Wave Tank, Proceedings of the 10th International Conference on Boundary Element Methods, Southampton, England, pp. 549-5GG, 1988.

[56] Huang, Y.Y., Wang, S.K., Cheng, W.M., Fluid-Structure Coupling Boundary Element Method for Analyzing Free-Vibration of Axisymmetric Thick-Walled Tanks, Proceedings of the 10th International Conference on Boundary Element Methods, Southampton, England, pp. 521-534, 1988.

[57] Kondo, H., Yamamoto, S., Sasaki, Y., Fluid-Structure Interaction Analysis Program for Axisymmetric Structures, JSME International Journal, Series III-Vibration Control Engineering for Industry, Vo1.33, No.3, pp. 315-322, September 1990.

[58] Hwang, LT., Ting, K., Boundary Element Method for Fluid-Structure Interaction Problems in Liquid Storage

Tanks, Journal of Pressure Vessels Technology, Vol. III, No.4, pp. 435-440, November 1989.

[59] Hwang, LT., Ting, K., Dynamic Analysis of Liquid Storage Tanks Including Hydrodynamic Interaction Boundary Element Method, Proceedings of the 9th International Conference on Structural Mechanics in Reactor Technology (SMIRT-9), Lausanne, Switzerland, pp. 429-434, August 1987.

[60] Sakai, F., Isoe, A., Partial Sliding During Earthquakes in an Anchor-Strapped Cylindrical Tank, Proceedings of the Pressure Vessels and Piping Conference, Flow-Structure Vibration and Sloshing, ASME, PVP, Vol.191, Tennessee, pp. 69-74, June 1990.

[61] Sakai, F., Isoe, A., Influence of Partial Sliding of Bottom Plate in an Anchored Cylindrical Tank During Earthquakes, Gakkai Rombun Hokokushu, No.410, pt. l-12, pp. 385-393, October 1989.

[62] Huang, C.Y., Ansourian, P., Non linear Analysis of Tanks, Research Report No. R535, University of Sydney, School of Civil and Mechanical Engineering, November 1968.

[63] Uras, R., Liu, W., Chen, Y., Study of the Influence of Imperfections on the Dynamic Stability of Tanks, Proceedings of the Pressure Vessels and Piping Conference, Flow-Structure Vibration and Sloshing, ASME, PVP, Vol. 191, Tennessee, pp. 47-54, June 1990.

[64] Aita, S., Combescure, A., Gibert, R.J., Imperfections on Thin Axisymmetric Shells-Fluid Structure Interaction Aspects, Proceedings of the 9th International Conference on Structural Mechanics in Reactor Technology (SMIRT-9), Lausanne, Switzerland, August 1987.

[65] Clarke, M.J., Rotter, J.M., Technique for the Measurement of Imperfections in Prototype Silos and Tanks, Research Report, University of Sydney, School of Civil and Mechanical Engineering, No. RSGS, March 1988.

[66] Tani, S., Hori, N., Yamaguchi, K., Nonlinear Dynamic Analysis of Cylindrical Tanks with Imperfect Circular Section Containing Liquid, Proceedings of the 8th World Conference on Earthquake Engineering, Vol. 5, California, pp. 247-254, July 1984.

[67] Lay, KS., Seismic coplued modelling of axisymmetric tanks containing liquid, ASCE J Engng Mech; 119:1747-1761, 1993.

[68] Bo, L., Tang, J-X., Vibration studies of base-isolated liquid storage tanks, Computer and Structures; 52:1051-1059, 1994.

[69] Gupta, RK., Free vibrations of partially filled cylindrical tanks. Engng Struct; 17:221-230, 1995.

[70] Fischer, FD., Rammerstorfer, RG., Scharf K., Earthquake resistant design of anchored and unanchored liquid storage tanks under three-dimensional earthquake excitation, In: Schueller GI, editor. Structural dynamics-recent advances, Berlin: Springer, pp. 317-371, 1991.

[71] Tokuda, N., Sakurai, T., Teraoku, T., Sloshing analysis method using existing FEM structural analysis code, ASME J Pres Ves Techn; 117:268-272, 1995.

[72] Yang, JY., Dynamic behaviour of fluid-tank systems, PhD Thesis, Rice University, Houston, USA, 1976.

[73] Costantinou, M.C., Mokha, A.S., Reinhorn A.M., Teflon bearing in base isolation II: modelling, Journal of Structural Engineering, ASCE, 116(2):455-74, 1990.

[74] Malhotra, P.K., Veletsos, A.S., Seismic response of unanchored and partially anchored liquid- storage tanks,

Report TR-105809, Eletric Power Research Institute, Paolo Alto, 1995.

[75] Malhotra, P.K., Base uplifting analysis of flexibly supported liquid-storage tanks, Journal of Earthquake Engineering and Strustural Dynamics, 24(12), 1591-1607, 1995.

[76] Malhotra, P.K., Seismic response of soil-supported unanchored liquid-storage tanks, Journal of Earthquake Engineering, ASCE, New York, 123(4), 440–450, 1997.

[77] Vamvatsikos, D., Cornell, C. A., Incremental Dynamic Analysis, Earthquake Engineering and Structural Dynamics; 31(3):491-514, 2002.

[78] Chopra, A.K., Dynamics of Structures, "Theory and applications to earthquake engineering", Prentice Hall.

[79] Hallquist, J.O., LS-DYNA Theoretical Manual, Livermore Software Technology Corporation, 1998.

[80] Hallquist, J.O., LS-DYNA Keyword User's Manual, Livermore Software Technology Corporation, 2001.

APPENDIX A:

File Name	Earthquake Code	Station Code	Waveform Code	Sampling Period [sec]	Record Length [sec]	PGA [g]
48xa.cor	34	13	48	0.01	32.55	0.0306
49xa.cor	34	14	49	0.01	41.31	0.0642
50xa.cor	34	15	50	0.01	37.51	0.0515
62xa.cor	38	24	62	0.01	11.50	0.0433
63xa.cor	38	25	63	0.01	11.68	0.0866
65xa.cor	39	24	65	0.01	9.76	0.0304
66xa.cor	39	25	66	0.01	10.36	0.0471
67xa.cor	40	24	67	0.01	18.09	0.1872
68xa.cor	40	25	68	0.01	16.18	0.0733
70xa.cor	41	24	70	0.01	12.58	0.0704
73xa.cor	42	24	73	0.01	8.55	0.0137
75xa.cor	44	24	75	0.01	13.63	0.0585
76xa.cor	44	28	76	0.01	11.98	0.0373
77xa.cor	45	24	77	0.01	11.62	0.0230
78xa.cor	46	24	78	0.01	8.96	0.0142
79xa.cor	47	24	79	0.01	9.30	0.0257
81xa.cor	48	24	81	0.01	10.00	0.0447

82xa.cor	48	29	82	0.01	9.05	0.0203
83xa.cor	49	24	83	0.01	11.62	0.0735
85xa.cor	49	29	85	0.01	11.39	0.0133
86xa.cor	49	30	86	0.01	11.43	0.0143
87xa.cor	49	28	87	0.01	8.69	0.0300
88xa.cor	50	24	88	0.01	8.92	0.0103
99xa.cor	53	29	99	0.01	9.50	0.0075
91xa.cor	51	29	91	0.01	14.61	0.0183
92xa.cor	51	30	92	0.01	14.64	0.0232
93xa.cor	51	28	93	0.01	12.09	0.0581
94xa.cor	52	24	94	0.01	13.46	0.0442
96xa.cor	52	30	96	0.01	10.28	0.0068
97xa.cor	52	29	97	0.01	13.18	0.0198
99xa.cor	53	29	99	0.01	9.50	0.0075
100xa.cor	53	30	100	0.01	9.60	0.0071
102xa.cor	54	29	102	0.01	9.66	0.0088
103xa.cor	54	30	103	0.01	9.67	0.0114
105xa.cor	56	31	105	0.01	15.85	0.3452
107xa.cor	58	24	107	0.01	12.81	0.0208
109xa.cor	59	24	109	0.01	9.54	0.0289
110xa.cor	59	30	110	0.01	8.58	0.0071
111xa.cor	59	29	111	0.01	8.64	0.0086
113xa.cor	60	35	113	0.01	15.93	0.1356
114xa.cor	60	24	114	0.01	15.08	0.0965

115xa.cor	60	28	115	0.01	10.43	0.0399
119xa.cor	61	15	119	0.01	13.19	0.0134
120xa.cor	61	28	120	0.01	13.03	0.0915
123xa.cor	61	24	123	0.01	18.55	0.1315
125xa.cor	62	24	125	0.01	9.66	0.0260
126xa.cor	63	35	126	0.01	9.98	0.4737
129xa.cor	63	14	129	0.01	30.55	0.0714
130xa.cor	63	15	130	0.01	18.88	0.0132
131xa.cor	63	28	131	0.01	16.40	0.0662
134xa.cor	63	24	134	0.01	22.07	0.2636
135xa.cor	64	35	135	0.01	13.59	0.0617
136xa.cor	64	24	136	0.01	12.15	0.0579
139xa.cor	65	35	139	0.01	25.44	0.1588
142xa.cor	65	14	142	0.01	26.68	0.0454
143xa.cor	65	15	143	0.01	26.03	0.0189
146xa.cor	65	24	146	0.01	24.59	0.3461
147xa.cor	65	28	147	0.01	16.89	0.1411
152xa.cor	66	24	152	0.01	10.49	0.0275
153xa.cor	67	37	153	0.01	28.36	0.0974
157xa.cor	1335	2482	157	0.01	35.98	0.0198
159xa.cor	72	24	159	0.01	21.57	0.2416
160xa.cor	72	28	160	0.01	16.90	0.1016
161xa.cor	73	43	161	0.01	8.11	0.0768

162xa.cor	74	43	162	0.01	6.50	0.2091
171xa.cor	81	47	171	0.01	28.97	0.1522
179xa.cor	87	51	179	0.01	39.46	0.0922
181xa.cor	87	53	181	0.01	34.96	0.1023
183xa.cor	87	55	183	0.01	39.96	0.0923
184xa.cor	87	56	184	0.01	32.98	0.0380
186xa.cor	87	58	186	0.01	39.98	0.0273
187xa.cor	87	59	187	0.01	63.43	0.9259
191xa.cor	91	62	191	0.01	15.00	0.0493
192xa.cor	91	63	192	0.01	18.30	0.0706
196xa.cor	93	62	196	0.01	48.22	0.4536
197xa.cor	93	63	197	0.01	48.21	0.2936
199xa.cor	93	67	199	0.01	47.81	0.3751
202xa.cor	93	70	202	0.01	45.53	0.0418
205xa.cor	94	63	205	0.01	13.02	0.0400
206xa.cor	95	62	206	0.01	18.38	0.0694
207xa.cor	96	67	207	0.01	13.04	0.0812
208xa.cor	97	63	208	0.01	21.86	0.0595
209xa.cor	98	62	209	0.01	28.22	0.0995
210xa.cor	98	63	210	0.01	11.66	0.0540
211xa.cor	98	67	211	0.01	20.74	0.0521
214xa.cor	100	63	214	0.01	14.38	0.0700
215xa.cor	100	67	215	0.01	19.36	0.0505

218xa.cor	101	73	218	0.01	15.10	0.0414
219xa.cor	102	73	219	0.01	12.08	0.0381
220xa.cor	103	73	220	0.01	22.96	0.1448
221xa.cor	103	74	221	0.01	15.52	0.0858
222xa.cor	104	63	222	0.01	15.06	0.0832
227xa.cor	108	63	227	0.01	27.54	0.0340
228xa.cor	108	67	228	0.01	34.34	0.2024
229xa.cor	108	75	229	0.01	25.66	0.1741
230xa.cor	108	73	230	0.01	32.52	0.1195
231xa.cor	108	76	231	0.01	30.08	0.1659
239xa.cor	112	80	239	0.01	7.18	0.2171
244xa.cor	115	83	244	0.01	23.81	0.0393
291xa.cor	146	276	291	0.01	86.05	0.1560
295xa.cor	146	101	295	0.01	48.97	0.0388
336xa.cor	159	123	336	0.01	18.30	0.1427
376xa.cor	175	150	376	0.01	14.92	0.0156
536xa.cor	250	206	536	0.01	21.87	0.0292
584xa.cor	284	217	584	0.01	30.49	0.0394
595xa.cor	290	83	595	0.01	46.32	0.0387
947xa.cor	422	94	947	0.01	38.40	0.0962
001862xa.cor	203	1303	1862	0.01	23.20	0.0595
001863xa.cor	204	1303	1863	0.01	20.37	0.0390
945xa.cor	423	99	945	0.01	30.47	0.0705
232xa.cor	108	77	232	0.01	28.22	0.0571

233xa.cor	108	74	233	0.01	29.54	0.1183
235xa.cor	109	568	235	0.01	9.11	0.0476
237xa.cor	110	63	237	0.01	9.60	0.0460
240xa.cor	113	63	240	0.01	12.66	0.1095
241xa.cor	114	25	241	0.01	10.94	0.0409
247xa.cor	115	279	247	0.01	24.86	0.0427
248xa.cor	115	85	248	0.01	13.28	0.0358
250xa.cor	117	86	250	0.01	12.41	0.0666
252xa.cor	118	86	252	0.01	12.72	0.0183
253xa.cor	119	86	253	0.01	11.33	0.0218
254xa.cor	120	86	254	0.01	10.46	0.0139
255xa.cor	121	86	255	0.01	10.44	0.0159
259xa.cor	124	89	259	0.01	18.22	0.0605
288xa.cor	146	94	288	0.01	30.15	0.2267
289xa.cor	146	95	289	0.01	72.31	0.1078
293xa.cor	146	99	293	0.01	83.92	0.0987
297xa.cor	146	103	297	0.01	59.73	0.0475
300xa.cor	146	106	300	0.01	14.60	0.0249
301xa.cor	146	107	301	0.01	28.98	0.0357
305xa.cor	147	276	305	0.01	24.87	0.0238
307xa.cor	149	111	307	0.01	23.52	0.0500
308xa.cor	150	112	308	0.01	23.57	0.0670
309xa.cor	151	112	309	0.01	40.60	0.0573

310xa.cor	151	111	310	0.01	40.52	0.0622
311xa.cor	152	112	311	0.01	107.96	0.1583
313xa.cor	152	111	313	0.01	67.94	0.0583
314xa.cor	153	114	314	0.01	29.99	0.0684
315xa.cor	153	97	315	0.01	25.21	0.0205
316xa.cor	153	115	316	0.01	33.57	0.1346
317xa.cor	153	116	317	0.01	15.86	0.0764
318xa.cor	153	117	318	0.01	28.06	0.1489
319xa.cor	153	118	319	0.01	18.18	0.1133
320xa.cor	153	119	320	0.01	30.14	0.0567
322xa.cor	153	111	322	0.01	29.57	0.0674
323xa.cor	154	114	323	0.01	22.66	0.0408
324xa.cor	154	115	324	0.01	25.39	0.0505
325xa.cor	154	116	325	0.01	11.46	0.0428
326xa.cor	154	117	326	0.01	21.74	0.1207
327xa.cor	154	119	327	0.01	26.37	0.0243
328xa.cor	155	115	328	0.01	25.26	0.0472
329xa.cor	155	118	329	0.01	9.28	0.0325
330xa.cor	155	112	330	0.01	25.38	0.0510
345xa.cor	165	127	345	0.01	15.79	0.0318
347xa.cor	167	128	347	0.01	20.29	0.0765
351xa.cor	170	130	351	0.01	11.26	0.0181
352xa.cor	170	131	352	0.01	19.20	0.0510

353xa.cor	170	132	353	0.01	9.19	0.0241
354xa.cor	171	133	354	0.01	29.12	0.1263
355xa.cor	172	128	355	0.01	16.62	0.1124
356xa.cor	173	132	356	0.01	7.83	0.2087
366xa.cor	175	141	366	0.01	24.93	0.0704
367xa.cor	175	142	367	0.01	23.40	0.0271
370xa.cor	175	144	370	0.01	15.53	0.0110
381xa.cor	176	141	381	0.01	16.71	0.0267
406xa.cor	186	159	406	0.01	13.70	0.1002
407xa.cor	187	123	407	0.01	11.69	0.0873
409xa.cor	188	160	409	0.01	8.89	0.1089
411xa.cor	190	162	411	0.01	11.26	0.0468
413xa.cor	192	164	413	0.01	25.85	0.2149
414xa.cor	192	163	414	0.01	29.73	0.2399
415xa.cor	193	164	415	0.01	11.24	0.0429
416xa.cor	194	164	416	0.01	11.89	0.0520
417xa.cor	195	164	417	0.01	11.66	0.0458
418xa.cor	196	164	418	0.01	11.68	0.0496
419xa.cor	197	164	419	0.01	20.98	0.3338
420xa.cor	197	163	420	0.01	22.59	0.2401
422xa.cor	198	164	422	0.01	12.25	0.0529
423xa.cor	199	159	423	0.01	13.28	0.0358
424xa.cor	200	166	424	0.01	10.51	0.0275

426xa.cor	201	168	426	0.01	15.71	0.0571
432xa.cor	207	159	432	0.01	13.12	0.0208
433xa.cor	208	159	433	0.01	10.33	0.0260
434xa.cor	209	159	434	0.01	10.62	0.0187
435xa.cor	210	159	435	0.01	30.52	0.0830
436xa.cor	210	171	436	0.01	27.41	0.1508
441xa.cor	215	159	441	0.01	9.70	0.0254
443xa.cor	216	175	443	0.01	6.97	0.0431
446xa.cor	217	178	446	0.01	12.78	0.1111
449xa.cor	218	175	449	0.01	5.95	0.0597
455xa.cor	219	175	455	0.01	6.96	0.1300
459xa.cor	220	175	459	0.01	6.96	0.0743
464xa.cor	221	175	464	0.01	6.97	0.1898
469xa.cor	226	166	469	0.01	16.13	0.1171
474xa.cor	229	123	474	0.01	16.87	0.0346
476xa.cor	230	185	476	0.01	60.42	0.1839
477xa.cor	230	187	477	0.01	9.91	0.0330
478xa.cor	230	186	478	0.01	17.55	0.0113
481xa.cor	230	190	481	0.01	48.87	0.0676
484xa.cor	233	164	484	0.01	12.78	0.0210
485xa.cor	233	192	485	0.01	9.95	0.0291
488xa.cor	235	194	488	0.01	26.61	0.0382
490xa.cor	235	196	490	0.01	31.93	0.0806

491xa.cor	235	197	491	0.01	16.30	0.0069
496xa.cor	236	196	496	0.01	14.34	0.0051
500xa.cor	239	194	500	0.01	29.92	0.0075
502xa.cor	240	200	502	0.01	27.06	0.0229
504xa.cor	240	202	504	0.01	31.97	0.0782
506xa.cor	241	200	506	0.01	26.20	0.0192
508xa.cor	241	202	508	0.01	25.75	0.0432
511xa.cor	242	204	511	0.01	22.37	0.0613
514xa.cor	243	200	514	0.01	20.61	0.0522
516xa.cor	243	204	516	0.01	25.93	0.0284
517xa.cor	244	200	517	0.01	19.73	0.0962
518xa.cor	244	202	518	0.01	20.56	0.0674
519xa.cor	244	204	519	0.01	18.73	0.0077
521xa.cor	245	200	521	0.01	22.28	0.0273
523xa.cor	245	202	523	0.01	22.98	0.0410
524xa.cor	245	204	524	0.01	30.73	0.1663
525xa.cor	246	164	525	0.01	11.07	0.0140
527xa.cor	247	202	527	0.01	16.22	0.0378
528xa.cor	247	204	528	0.01	20.14	0.0120
530xa.cor	248	200	530	0.01	44.01	0.1118
532xa.cor	248	202	532	0.01	38.25	0.0718
533xa.cor	248	204	533	0.01	47.37	0.0571
535xa.cor	250	205	535	0.01	21.27	0.3888
537xa.cor	250	207	537	0.01	22.77	0.0705

538xa.cor	251	205	538	0.01	33.14	0.0324
545xa.cor	258	159	545	0.01	20.22	0.0267
547xa.cor	259	210	547	0.01	12.44	0.0288
548xa.cor	259	43	548	0.01	19.88	0.0288
549xa.cor	259	162	549	0.01	23.60	0.0665
550xa.cor	260	166	550	0.01	15.53	0.0378
552xa.cor	261	178	552	0.01	10.63	0.0248
556xa.cor	265	159	556	0.01	14.23	0.0306
557xa.cor	266	159	557	0.01	14.81	0.0448
559xa.cor	267	159	559	0.01	23.94	0.1143
560xa.cor	268	159	560	0.01	13.67	0.0349
561xa.cor	269	159	561	0.01	13.25	0.0388
562xa.cor	270	159	562	0.01	9.46	0.0126
563xa.cor	271	159	563	0.01	9.24	0.0059
564xa.cor	272	159	564	0.01	14.52	0.0244
565xa.cor	273	164	565	0.01	10.17	0.0143
567xa.cor	274	123	567	0.01	10.09	0.0186
568xa.cor	275	159	568	0.01	16.33	0.0510
569xa.cor	276	166	569	0.01	16.71	0.0340
570xa.cor	276	159	570	0.01	9.62	0.0194
572xa.cor	276	178	572	0.01	18.83	0.0506
892xa.cor	379	86	892	0.01	22.79	0.0261
577xa.cor	280	166	577	0.01	11.36	0.0274

578xa.cor	280	178	578	0.01	13.93	0.0686
893xa.cor	380	86	893	0.01	21.00	0.0345
582xa.cor	282	123	582	0.01	21.53	0.0331
586xa.cor	287	221	586	0.01	12.99	0.1157
588xa.cor	288	221	588	0.01	24.46	0.0666
590xa.cor	289	221	590	0.01	8.74	0.0449
591xa.cor	290	221	591	0.01	44.44	0.3447
592xa.cor	286	221	592	0.01	48.51	0.1989
596xa.cor	286	83	596	0.01	50.50	0.0788
601xa.cor	290	224	601	0.01	28.49	0.0461
602xa.cor	286	224	602	0.01	29.03	0.1166
619xa.cor	286	231	619	0.01	27.00	0.0461
620xa.cor	291	83	620	0.01	28.93	0.0365
622xa.cor	291	221	622	0.01	28.24	0.1309
627xa.cor	291	86	627	0.01	28.00	0.0331
640xa.cor	292	86	640	0.01	39.12	0.0979
643xa.cor	292	224	643	0.01	27.32	0.0257
645xa.cor	292	83	645	0.01	40.36	0.0448
648xa.cor	292	221	648	0.01	41.86	0.0920
658xa.cor	558	714	658	0.01	3.19	0.6830
659xa.cor	488	714	659	0.01	204.67	0.0063
699xa.cor	300	250	699	0.01	22.19	0.1440
700xa.cor	303	250	700	0.01	16.22	0.0410

701xa.cor	304	250	701	0.01	17.97	0.0364
774xa.cor	350	83	774	0.01	22.99	0.0199
776xa.cor	350	221	776	0.01	19.17	0.0807
777xa.cor	351	221	777	0.01	15.90	0.0240
778xa.cor	352	221	778	0.01	13.44	0.0234
790xa.cor	355	86	790	0.01	15.20	0.0383
792xa.cor	355	221	792	0.01	13.28	0.0461
795xa.cor	356	86	795	0.01	14.15	0.1465
802xa.cor	357	221	802	0.01	12.67	0.0406
806xa.cor	358	221	806	0.01	11.72	0.0670
807xa.cor	359	221	807	0.01	10.39	0.0225
808xa.cor	360	221	808	0.01	9.29	0.0226
809xa.cor	359	86	809	0.01	10.63	0.0227
810xa.cor	360	86	810	0.01	12.93	0.0646
841xa.cor	361	221	841	0.01	9.78	0.0156
860xa.cor	362	86	860	0.01	17.21	0.0173
864xa.cor	363	83	864	0.01	18.15	0.0174
866xa.cor	363	221	866	0.01	17.69	0.0159
867xa.cor	363	224	867	0.01	20.96	0.0391
871xa.cor	364	224	871	0.01	20.99	0.0288
875xa.cor	364	83	875	0.01	12.86	0.0236
876xa.cor	365	83	876	0.01	8.64	0.0093
885xa.cor	373	86	885	0.01	13.24	0.0503

887xa.cor	375	273	887	0.01	17.61	0.1286
888xa.cor	376	86	888	0.01	15.54	0.0616
889xa.cor	377	86	889	0.01	19.97	0.0612
779xa.cor	353	221	779	0.01	13.88	0.0339
48ya.cor	34	13	48	0.01	32.39	0.0272
49ya.cor	34	14	49	0.01	41.32	0.0877
50ya.cor	34	15	50	0.01	37.46	0.0726
62ya.cor	38	24	62	0.01	11.38	0.0360
63ya.cor	38	25	63	0.01	11.70	0.0464
65ya.cor	39	24	65	0.01	9.68	0.0292
66ya.cor	39	25	66	0.01	10.43	0.0362
67ya.cor	40	24	67	0.01	18.13	0.3059
68ya.cor	40	25	68	0.01	16.19	0.0794
70ya.cor	41	24	70	0.01	12.57	0.0666
73ya.cor	42	24	73	0.01	8.59	0.0262
75ya.cor	44	24	75	0.01	13.63	0.0618
76ya.cor	44	28	76	0.01	11.92	0.0445
77ya.cor	45	24	77	0.01	11.60	0.0237
78ya.cor	46	24	78	0.01	8.95	0.0089
79ya.cor	47	24	79	0.01	6.80	0.0205
81ya.cor	48	24	81	0.01	10.03	0.0441
82ya.cor	48	29	82	0.01	9.06	0.0107
83ya.cor	49	24	83	0.01	11.80	0.0541

85ya.cor	49	29	85	0.01	11.42	0.0086
86ya.cor	49	30	86	0.01	11.44	0.0123
87ya.cor	49	28	87	0.01	8.77	0.0371
88ya.cor	50	24	88	0.01	8.90	0.0086
99ya.cor	53	29	99	0.01	9.52	0.0062
91ya.cor	51	29	91	0.01	14.52	0.0132
92ya.cor	51	30	92	0.01	14.59	0.0173
93ya.cor	51	28	93	0.01	11.66	0.0301
94ya.cor	52	24	94	0.01	13.65	0.0543
96ya.cor	52	30	96	0.01	10.28	0.0175
97ya.cor	52	29	97	0.01	13.16	0.0142
99ya.cor	53	29	99	0.01	9.52	0.0062
100ya.cor	53	30	100	0.01	9.62	0.0099
102ya.cor	54	29	102	0.01	9.64	0.0099
103ya.cor	54	30	103	0.01	9.65	0.0081
105ya.cor	56	31	105	0.01	18.18	0.2607
107ya.cor	58	24	107	0.01	12.80	0.0216
109ya.cor	59	24	109	0.01	9.89	0.0184
110ya.cor	59	30	110	0.01	8.59	0.0092
111ya.cor	59	29	111	0.01	8.62	0.0083
113ya.cor	60	35	113	0.01	20.41	0.1733
114ya.cor	60	24	114	0.01	15.12	0.1096
115ya.cor	60	28	115	0.01	10.55	0.0698

119ya.cor	61	15	119	0.01	13.15	0.0115
120ya.cor	61	28	120	0.01	13.00	0.0885
123ya.cor	61	24	123	0.01	18.58	0.2314
125ya.cor	62	24	125	0.01	9.66	0.0153
126ya.cor	63	35	126	0.01	9.98	0.5052
129ya.cor	63	14	129	0.01	30.45	0.0201
130ya.cor	63	15	130	0.01	18.81	0.0212
131ya.cor	63	28	131	0.01	16.13	0.1226
134ya.cor	63	24	134	0.01	21.99	0.2177
135ya.cor	64	35	135	0.01	13.58	0.0721
136ya.cor	64	24	136	0.01	12.30	0.0516
139ya.cor	65	35	139	0.01	25.43	0.4216
142ya.cor	65	14	142	0.01	26.65	0.0378
143ya.cor	65	15	143	0.01	26.04	0.0284
146ya.cor	65	24	146	0.01	24.57	0.3360
147ya.cor	65	28	147	0.01	16.75	0.2364
152ya.cor	66	24	152	0.01	10.49	0.0403
153ya.cor	67	37	153	0.01	28.20	0.0639
157ya.cor	1335	2482	157	0.01	35.98	0.0708
159ya.cor	72	24	159	0.01	21.46	0.1927
160ya.cor	72	28	160	0.01	16.91	0.0900
161ya.cor	73	43	161	0.01	5.13	0.1295
162ya.cor	74	43	162	0.01	3.63	0.0660

171ya.cor	81	47	171	0.01	28.98	0.1312
179ya.cor	87	51	179	0.01	39.52	0.1894
181ya.cor	87	53	181	0.01	34.96	0.0869
183ya.cor	87	55	183	0.01	39.96	0.1021
184ya.cor	87	56	184	0.01	32.98	0.0382
186ya.cor	87	58	186	0.01	39.98	0.0265
187ya.cor	87	59	187	0.01	63.41	1.1014
191ya.cor	91	62	191	0.01	15.00	0.0347
192ya.cor	91	63	192	0.01	18.30	0.0648
196ya.cor	93	62	196	0.01	48.22	0.3058
197ya.cor	93	63	197	0.01	48.16	0.2406
199ya.cor	93	67	199	0.01	47.81	0.3626
202ya.cor	93	70	202	0.01	45.53	0.0583
205ya.cor	94	63	205	0.01	13.02	0.0529
206ya.cor	95	62	206	0.01	18.38	0.0382
207ya.cor	96	67	207	0.01	13.04	0.1197
208ya.cor	97	63	208	0.01	21.86	0.0504
209ya.cor	98	62	209	0.01	28.22	0.0890
210ya.cor	98	63	210	0.01	11.66	0.0342
211ya.cor	98	67	211	0.01	20.74	0.0829
214ya.cor	100	63	214	0.01	14.38	0.1305
215ya.cor	100	67	215	0.01	19.36	0.0440
218ya.cor	101	73	218	0.01	15.10	0.0464

219ya.cor	102	73	219	0.01	12.08	0.0745
220ya.cor	103	73	220	0.01	22.96	0.1351
221ya.cor	103	74	221	0.01	15.52	0.0578
222ya.cor	104	63	222	0.01	15.06	0.0587
227ya.cor	108	63	227	0.01	27.54	0.0309
228ya.cor	108	67	228	0.01	34.34	0.2704
229ya.cor	108	75	229	0.01	25.66	0.2755
230ya.cor	108	73	230	0.01	32.52	0.2675
231ya.cor	108	76	231	0.01	30.08	0.1329
239ya.cor	112	80	239	0.01	9.92	0.2875
244ya.cor	115	83	244	0.01	23.84	0.0234
291ya.cor	146	276	291	0.01	86.03	0.1753
295ya.cor	146	101	295	0.01	48.94	0.0542
336ya.cor	159	123	336	0.01	18.32	0.1356
376ya.cor	175	150	376	0.01	14.91	0.0174
536ya.cor	250	206	536	0.01	21.41	0.0303
584ya.cor	284	217	584	0.01	30.50	0.0576
595ya.cor	290	83	595	0.01	46.32	0.0529
947ya.cor	422	94	947	0.01	38.37	0.0803
001862ya.cor	203	1303	1862	0.01	23.20	0.0438
001863ya.cor	204	1303	1863	0.01	20.37	0.0327
945ya.cor	423	99	945	0.01	30.47	0.0384
232ya.cor	108	77	232	0.01	28.22	0.0553

233ya.cor	108	74	233	0.01	29.54	0.1515
235ya.cor	109	568	235	0.01	4.97	0.0402
237ya.cor	110	63	237	0.01	9.60	0.1000
240ya.cor	113	63	240	0.01	12.66	0.1415
241ya.cor	114	25	241	0.01	10.90	0.0413
247ya.cor	115	279	247	0.01	24.84	0.0391
248ya.cor	115	85	248	0.01	13.29	0.0374
250ya.cor	117	86	250	0.01	12.39	0.1039
252ya.cor	118	86	252	0.01	12.71	0.0192
253ya.cor	119	86	253	0.01	11.34	0.0320
254ya.cor	120	86	254	0.01	10.46	0.0234
255ya.cor	121	86	255	0.01	10.43	0.0299
259ya.cor	124	89	259	0.01	18.25	0.0355
288ya.cor	146	94	288	0.01	73.20	0.1738
289ya.cor	146	95	289	0.01	72.33	0.1389
293ya.cor	146	99	293	0.01	83.94	0.0994
297ya.cor	146	103	297	0.01	59.71	0.0349
300ya.cor	146	106	300	0.01	14.60	0.0210
301ya.cor	146	107	301	0.01	28.97	0.0302
305ya.cor	147	276	305	0.01	24.86	0.0387
307ya.cor	149	111	307	0.01	23.38	0.0390
308ya.cor	150	112	308	0.01	23.53	0.0551
309ya.cor	151	112	309	0.01	40.60	0.0370

310ya.cor	151	111	310	0.01	40.49	0.0517
311ya.cor	152	112	311	0.01	107.92	0.1475
313ya.cor	152	111	313	0.01	67.92	0.0797
314ya.cor	153	114	314	0.01	29.98	0.0981
315ya.cor	153	97	315	0.01	25.20	0.0197
316ya.cor	153	115	316	0.01	33.59	0.1692
317ya.cor	153	116	317	0.01	15.86	0.0882
318ya.cor	153	117	318	0.01	28.06	0.1551
319ya.cor	153	118	319	0.01	18.17	0.1528
320ya.cor	153	119	320	0.01	30.12	0.0719
322ya.cor	153	111	322	0.01	29.57	0.1078
323ya.cor	154	114	323	0.01	22.66	0.0273
324ya.cor	154	115	324	0.01	25.43	0.0645
325ya.cor	154	116	325	0.01	11.45	0.0286
326ya.cor	154	117	326	0.01	21.73	0.0481
327ya.cor	154	119	327	0.01	26.36	0.0449
328ya.cor	155	115	328	0.01	25.29	0.0521
329ya.cor	155	118	329	0.01	9.34	0.0437
330ya.cor	155	112	330	0.01	25.37	0.0481
345ya.cor	165	127	345	0.01	15.80	0.0518
347ya.cor	167	128	347	0.01	20.30	0.1817
351ya.cor	170	130	351	0.01	11.13	0.0265
352ya.cor	170	131	352	0.01	18.59	0.0442

353ya.cor	170	132	353	0.01	9.17	0.0152
354ya.cor	171	133	354	0.01	28.01	0.1606
355ya.cor	172	128	355	0.01	16.62	0.2066
356ya.cor	173	132	356	0.01	6.57	0.1251
366ya.cor	175	141	366	0.01	24.90	0.0659
367ya.cor	175	142	367	0.01	23.40	0.0288
370ya.cor	175	144	370	0.01	15.53	0.0167
381ya.cor	176	141	381	0.01	16.69	0.0217
406ya.cor	186	159	406	0.01	13.69	0.0572
407ya.cor	187	123	407	0.01	11.67	0.0468
409ya.cor	188	160	409	0.01	8.81	0.1785
411ya.cor	190	162	411	0.01	11.23	0.0856
413ya.cor	192	164	413	0.01	25.88	0.2966
414ya.cor	192	163	414	0.01	29.86	0.2722
415ya.cor	193	164	415	0.01	11.16	0.0356
416ya.cor	194	164	416	0.01	11.91	0.0429
417ya.cor	195	164	417	0.01	11.68	0.0261
418ya.cor	196	164	418	0.01	7.59	0.0267
419ya.cor	197	164	419	0.01	21.04	0.1590
420ya.cor	197	163	420	0.01	22.58	0.1407
422ya.cor	198	164	422	0.01	12.39	0.0376
423ya.cor	199	159	423	0.01	13.28	0.0299
424ya.cor	200	166	424	0.01	10.48	0.0376

426ya.cor	201	168	426	0.01	15.72	0.0535
432ya.cor	207	159	432	0.01	13.10	0.0181
433ya.cor	208	159	433	0.01	10.31	0.0112
434ya.cor	209	159	434	0.01	10.59	0.0235
435ya.cor	210	159	435	0.01	30.51	0.1561
436ya.cor	210	171	436	0.01	27.82	0.1461
441ya.cor	215	159	441	0.01	9.77	0.0223
443ya.cor	216	175	443	0.01	6.99	0.0316
446ya.cor	217	178	446	0.01	12.76	0.1011
449ya.cor	218	175	449	0.01	5.96	0.0711
455ya.cor	219	175	455	0.01	6.95	0.1227
459ya.cor	220	175	459	0.01	6.96	0.0532
464ya.cor	221	175	464	0.01	6.94	0.2059
469ya.cor	226	166	469	0.01	16.13	0.1990
474ya.cor	229	123	474	0.01	16.87	0.0345
476ya.cor	230	185	476	0.01	60.41	0.1307
477ya.cor	230	187	477	0.01	9.91	0.0292
478ya.cor	230	186	478	0.01	17.55	0.0128
481ya.cor	230	190	481	0.01	48.88	0.1052
484ya.cor	233	164	484	0.01	12.78	0.0219
485ya.cor	233	192	485	0.01	9.95	0.0326
488ya.cor	235	194	488	0.01	26.61	0.0405
490ya.cor	235	196	490	0.01	31.93	0.1176

491ya.cor	235	197	491	0.01	16.30	0.0073
496ya.cor	236	196	496	0.01	14.34	0.0064
500ya.cor	239	194	500	0.01	29.92	0.0085
502ya.cor	240	200	502	0.01	27.06	0.0250
504ya.cor	240	202	504	0.01	31.97	0.0772
506ya.cor	241	200	506	0.01	26.20	0.0173
508ya.cor	241	202	508	0.01	25.75	0.0490
511ya.cor	242	204	511	0.01	22.37	0.0664
514ya.cor	243	200	514	0.01	20.61	0.0375
516ya.cor	243	204	516	0.01	25.93	0.0230
517ya.cor	244	200	517	0.01	19.73	0.1124
518ya.cor	244	202	518	0.01	20.56	0.0470
519ya.cor	244	204	519	0.01	18.73	0.0086
521ya.cor	245	200	521	0.01	22.28	0.0434
523ya.cor	245	202	523	0.01	22.98	0.0563
524ya.cor	245	204	524	0.01	30.73	0.1251
525ya.cor	246	164	525	0.01	11.06	0.0114
527ya.cor	247	202	527	0.01	16.22	0.0513
528ya.cor	247	204	528	0.01	20.14	0.0094
530ya.cor	248	200	530	0.01	44.01	0.1052
532ya.cor	248	202	532	0.01	38.25	0.0431
533ya.cor	248	204	533	0.01	47.37	0.0613
535ya.cor	250	205	535	0.01	20.74	0.5125

537ya.cor	250	207	537	0.01	23.31	0.0692
538ya.cor	251	205	538	0.01	33.14	0.0389
545ya.cor	258	159	545	0.01	20.22	0.0209
547ya.cor	259	210	547	0.01	11.81	0.0287
548ya.cor	259	43	548	0.01	19.64	0.0392
549ya.cor	259	162	549	0.01	23.90	0.0816
550ya.cor	260	166	550	0.01	15.51	0.0280
552ya.cor	261	178	552	0.01	10.63	0.0461
556ya.cor	265	159	556	0.01	14.22	0.0561
557ya.cor	266	159	557	0.01	14.80	0.0478
559ya.cor	267	159	559	0.01	23.94	0.0903
560ya.cor	268	159	560	0.01	13.66	0.0240
561ya.cor	269	159	561	0.01	13.24	0.0666
562ya.cor	270	159	562	0.01	9.44	0.0267
563ya.cor	271	159	563	0.01	9.23	0.0134
564ya.cor	272	159	564	0.01	14.51	0.0424
565ya.cor	273	164	565	0.01	10.16	0.0104
567ya.cor	274	123	567	0.01	10.09	0.0155
568ya.cor	275	159	568	0.01	16.31	0.0761
569ya.cor	276	166	569	0.01	16.70	0.0519
570ya.cor	276	159	570	0.01	9.58	0.0255
572ya.cor	276	178	572	0.01	18.83	0.0431
892ya.cor	379	86	892	0.01	22.78	0.0352

577ya.cor	280	166	577	0.01	11.34	0.0265
578ya.cor	280	178	578	0.01	13.90	0.1040
893ya.cor	380	86	893	0.01	20.99	0.0582
582ya.cor	282	123	582	0.01	21.50	0.0346
586ya.cor	287	221	586	0.01	12.99	0.0653
588ya.cor	288	221	588	0.01	24.46	0.0740
590ya.cor	289	221	590	0.01	8.74	0.0187
591ya.cor	290	221	591	0.01	44.44	0.2608
592ya.cor	286	221	592	0.01	48.51	0.2226
596ya.cor	286	83	596	0.01	50.50	0.0756
601ya.cor	290	224	601	0.01	28.49	0.0488
602ya.cor	286	224	602	0.01	29.03	0.1087
619ya.cor	286	231	619	0.01	27.00	0.0322
620ya.cor	291	83	620	0.01	28.93	0.0516
622ya.cor	291	221	622	0.01	28.24	0.1081
627ya.cor	291	86	627	0.01	28.00	0.0229
640ya.cor	292	86	640	0.01	39.12	0.1341
643ya.cor	292	224	643	0.01	27.32	0.0188
645ya.cor	292	83	645	0.01	40.36	0.0369
648ya.cor	292	221	648	0.01	41.86	0.0680
658ya.cor	558	714	658	0.01	3.19	0.3749
659ya.cor	488	714	659	0.01	204.67	0.0063
699ya.cor	300	250	699	0.01	22.19	0.1384

700ya.cor	303	250	700	0.01	16.22	0.0510
701ya.cor	304	250	701	0.01	17.97	0.0476
774ya.cor	350	83	774	0.01	22.99	0.0228
776ya.cor	350	221	776	0.01	19.17	0.1261
777ya.cor	351	221	777	0.01	15.90	0.0174
778ya.cor	352	221	778	0.01	13.44	0.0247
790ya.cor	355	86	790	0.01	15.20	0.0685
792ya.cor	355	221	792	0.01	13.28	0.0321
795ya.cor	356	86	795	0.01	14.15	0.0970
802ya.cor	357	221	802	0.01	12.67	0.0338
806ya.cor	358	221	806	0.01	11.72	0.0440
807ya.cor	359	221	807	0.01	10.39	0.0114
808ya.cor	360	221	808	0.01	9.29	0.0187
809ya.cor	359	86	809	0.01	10.63	0.0267
810ya.cor	360	86	810	0.01	12.93	0.0677
841ya.cor	361	221	841	0.01	9.78	0.0125
860ya.cor	362	86	860	0.01	17.21	0.0112
864ya.cor	363	83	864	0.01	18.15	0.0183
866ya.cor	363	221	866	0.01	17.69	0.0173
867ya.cor	363	224	867	0.01	20.96	0.0270
871ya.cor	364	224	871	0.01	20.99	0.0312
875ya.cor	364	83	875	0.01	12.86	0.0273
876ya.cor	365	83	876	0.01	8.64	0.0133

885ya.cor	373	86	885	0.01	13.23	0.0504
887ya.cor	375	273	887	0.01	17.59	0.1671
888ya.cor	376	86	888	0.01	15.54	0.0712
889ya.cor	377	86	889	0.01	20.25	0.2331
779ya.cor	353	221	779	0.01	13.88	0.0337